TEMPORAL AND SPATIAL PATTERNS AT ALPINE TREELINE IN THE SIERRA NEVADA USA: IMPLICATIONS FOR GLOBAL CHANGE

by

Andrew Godard Bunn

A dissertation submitted in partial fulfillment

of the requirements for the degree

of

Doctor of Philosophy

in

Land Resources and Environmental Sciences

MONTANA STATE UNIVERSITY

Bozeman, Montana

June 2004

APPROVAL

of a dissertation submitted by

Andrew Godard Bunn

This dissertation has been read by each member of the dissertation committee and has been found to be satisfactory regarding content, English usage, format, citations, bibliographic style, and consistency, and is ready for submission to the College of Graduate Studies.

Dr. Lisa J. Graumlich

Approved for the Department of Land Resources and Environmental Sciences

Dr. Jon M. Wraith

Approved for the College of Graduate Studies

Dr. Bruce R. McLeod

STATEMENT OF PERMISSION TO USE

In presenting this dissertation in partial fulfillment of the requirements for a doctoral degree at Montana State University, I agree that the Library shall make it available to borrowers under rules of the Library. I further agree that copying of this dissertation is allowable only for scholarly purposes, consistent with "fair use" as prescribed in the U.S. Copyright Law. Requests for extensive copying or reproduction of this dissertation should be referred to Bell and Howell Information and Learning, 300 North Zeeb Road, Ann Arbor, Michigan 48106, to whom I have granted "the exclusive right to reproduce and distribute my dissertation in and from microform along with the non-exclusive right to reproduce and distribute my abstract in any format in whole or in part."

Andrew G. Bunn

June 8, 2004

ACKNOWLEDGEMENTS

I extend thanks to Lisa Graumlich who has provided excellent advising. Dean Urban has been a stalwart professional advisor and has graciously furnished his time and the resources of the Landscape Ecology Lab at Duke University to me several times during the course of this work. The quality of the research was thoroughly improved by the exacting editing of Rick Lawrence and the insightful comments of Cathy Zabinski. Gabe Bellante, Greg Buppert, Chris Caruso, Jeanette Goodwin, Steve Gray, Sean Hill, Jeremy Littell, Greg Pederson, Brian Peters, Mike Pisaric, Todd Kipfer, and Andra Toivola (among others) provided help in the field, lab, or office. I extend special thanks to the Canon National Parks Science Scholars Program, and its director Dr. Gary Machlis, which has generously supported me during this research. Most importantly I thank Rebecca for patience and flexibility and Samuel Bunn for the witty discourse that only a two year old can provide.

TABLE OF CONTENTS

TABLE OF CONTENTS – CONTINUED

TABLE OF CONTENTS - CONTINUED

LIST OF TABLES

LIST OF FIGURES

LIST OF FIGURES – CONTINUED

LIST OF FIGURES – CONTINUED

ABSTRACT

This work focuses on developing understanding of the role of climate variability in shaping montane landscapes. Due to the temperature-related stresses on treeline populations it is thought that change at treeline is an indicator of global warming. Interpretation of treeline changes has been hampered by issues of scale and the paucity of landscape-scale data. The application of remotely sensed imagery and computer-based mapping programs has filled this gap with datasets that have large extents and fine spatial grain. I used geospatial information about treeline in concert with population and paleoecological data to answer questions on ecological patterns and processes. My research focused on the treeline tree communities in the southern Sierra Nevada. There, on the eastern crest of the Sierra Nevada foxtail pine (*Pinus balfouriana*) forms an abrupt treeline in the vicinity of Sequoia National Park which gives way to a less well defined treeline of whitebark pine (*P. albicaulis*), limber pine (*P. flexilis*), and lodgepole pine (*P. contorta*) north to Yosemite National Park. By analyzing treeline growth patterns and spatial composition at the level of the region (10^9 m^2), stand (10^3 m^2), and organism (10^{-1} m^2) I was able to make inference about the interactions of autecology, biophysical setting, and climate variability in shaping these subalpine forests over the last millennium. At the regional scale I improved paleoclimatic understanding derived from long chronologies of tree rings by relating species-specific differences in the climate-growth relationship over time to the realized niche space of each species in geographic space. At the level of the stand I was able to show how decadal versus centennial modes of growth and stand density vary with biophysical setting related to drought stress. At the level of the organism I was able to show that differences in tree growth and seedling patterns are related to fine scale physical variations in surrounding each tree as well as tree autecology. Over the course of my dissertation, I developed fresh insights into the complex interactions that govern the growth and structure of forests and improved the state-of-science for monitoring treeline as a critical indicator of global change.

CHAPTER 1

DISSERTATION OVERVIEW

Introduction

There is widespread consensus that global temperatures during the 20th century have increased (IPCC 2001) representing significant departures from the long-term mean (Mann et al. 1998; 1999). Interactions between multidecadal-scale (e.g., the Atlantic Multidecadal Oscillation) decadal-scale (e.g., the Pacific Decadal Oscillation) and climate forcing and inter-annual climate events such as ENSO (El Niño/Southern Oscillation) add regional and global complexity that is only beginning to be understood (Mantua et al. 1997; Gray et al. 2002; McCabe et al. 2004). Convincing documentation now exists that 20th-century climate change has affected biota in terms of physiology, productivity, and growth as well as altering the distributions and ranges of many species (Parmesan and Yohe 2003; Root et al. 2003).

The focus of this work is alpine treeline, the boundary between forest and tundra on high mountains. Ecotones, where the abiotic environment exerts ultimate control over ecological processes, are ideal for observing patterns of plant response to climate (Hansen and di Castri 1992; Risser 1995). The alpine treeline ecotone is a particularly rich system to investigate due to the abundance of high-resolution paleoecological records that allow current trends in tree growth to be interpreted climatically and ecologically in a long-term context. The temporal datasets associated with subalpine

forest dynamics are widespread spatially, climatically sensitive, and annually resolved (Graumlich et al. 2004). Documenting and understanding changes at treeline are particularly interesting because, if projections of future global warming are correct, treeline is likely to be one of the first natural ecosystems to register the change in climate (Körner 1999). Previous research has largely focused on using paleoecological records to understand where and when climatic variation alters high elevation forests (e.g., LaMarche 1974; Brubaker 1986; Lloyd and Graumlich 1997). This research has shown that at time scales of decades to centuries and spatial scales of regions to continents, temperature and precipitation interact strongly in controlling treeline growth and position.

Montane landscapes with complex topography comprise a substantial portion of the western United States (Schimel et al. 2002), and many of the United State's National Park Units are dominated by high mountain systems. While they are a unique network of protected areas and provide an unparalleled laboratory for leveraging landscape-scale perspective on global climate-change science, they are also real landscapes with varying degrees of management needs (Seastedt et al. 2004). Spatially explicit understanding and mapping response of subalpine forests to climate change is important to Park managers from hydrologic, habitat, and visitor perspectives.

My research addressed several issues relating to developing further temporal and spatial understanding of ecological patterns at alpine treeline in the southern Sierra Nevada and five research chapters follows this introductory chapter. The results are synthesized in the seventh chapter. In this work, I addressed an important issue involving the appropriate methods for the obligatory detrending of individual tree-ring series for

use in a mean value chronology of tree growth. I then used regional subalpine forest tree growth measured with a multi-species network at 13 sites in the Sierra Nevada, and adjacent White Mountains, to make inferences about twentieth century growth trends in the context of the last millennium. I then looked at how growth patterns changed with biophysical setting in the rugged topography of two sites in Sequoia National Park. I looked at how the rugged topography interacts with species autecology at alpine treeline at the scale of the organism in Sequoia National Park and near Yosemite National Park. Finally, I merged these temporal studies with spatial data of treeline forest species composition and density at two spatial scales and propose a system for establishing monitoring protocols for this important global change resource. Over the course of the dissertation, I developed fresh insights into the complex interactions that govern the growth and structure of forests and improve the state-of-science for monitoring treeline as a critical indicator of global change.

References

Brubaker L.B. (1986) Responses of tree populations to climatic change. *Vegetatio* 67, 119-130

Graumlich L.J., Waggoner L.A. and Bunn A.G. (2004) Detecting global change at alpine treeline: coupling paleoecology with contemporary studies. In: *Global Change and Mountain Regions: a State of Knowledge Overview* (eds Huber U., Bugmann H. and Reasoner M.), pp. 1-13. Kluwer Academic Publishers, The Netherlands

Gray S.T., Betancourt J.L., Fastie C.L. and Jackson S.T. (2003) Patterns and sources of multidecadal oscillations in drought-senitive tree-ring records from the central and southern Rocky Mountains. *Geophysical Research Letters* 30, 1316

Hansen A.J. and di Castri F. (1992) *Landscape boundaries: consequences for ecological flows*. Springer-Verlag, New York City, NY

IPCC (2001) Contribution of working group I to the third assessment report of the intergovernmental panel on climate change. In: *Climate Change 2001: The Scientific Basis* (eds Houghton J.T., Ding Y., Griggs D.J., Noguer M., van der Linden P.J. and Xiaosu D.) Cambridge University Press, Cambridge, UK

Körner C. (1999) *Alpine plant life: Functional plant ecology of high mountain ecosystems*. Springer, Berlin

LaMarche V.C.Jr. (1974) Paleoclimatic inferences from long tree-ring records. *Science* 183, 1043-1048

Lloyd A.H. and Graumlich L.J. (1997) Holocene dynamics of treeline forests in the Sierra Nevada. *Ecology* 78, 1199-1210

Mann M.E., Bradley R.S. and Hughes M.K. (1999) Northern hemisphere temperatures during the past millennium: inferences, uncertainties, and limitations. *Geophysical Research Letters* 26, 759-762

Mann M.E., Bradley R.S. and Hughes M.K. (1998) Global-scale temperature patterns and climate forcing over the past six centuries. *Nature* 392, 779-787

Mantua N.J., Hare S.R., Zhang Y., Wallace J.M. and Fancis R.C. (1997) A Pacific interdecadal climate oscillation with impacts on salmon production. *Bulletin of the American Meteorological Society* 78, 1069-1079

McCabe G.J., Palecki M.A. and Betancourt J.L. (2004) Pacific and Atlantic Ocean influences on multidecadal drought frequency in the United States. *Proceedings of the National Academy of Sciences USA* 101, 4136-4141

Parmesan C. and Yohe G. (2003) A globally coherent fingerprint of climate change impacts across natural systems. *Nature* 421, 37-42

Risser P.G. (1995) The status of the science examining ecotones. *BioScience* 45, 318-325

Root T.L., Price J.T., Hall K.R., Schnieder S.H., Rosenweig C. and Pounds J.A. (2003) Fingerprints of global warming on wild animals and plants. *Nature* 421, 57-60

Schimel D., Kittel T.G.F., Running S., Monson R., Turnipseed A. and Anderson D. (2002) Carbon sequestration studied in western U.S. mountains. *EOS, Transactions, American Geophysical Union* 83, 445-456

Seastedt T.R., Bowman W.D., Caine T.N., Mcknight D., Townsend A. and Williams M.W. (2004) The landscape continuum: a model for high-elevation ecosystems. *Bioscience* 54, 111-121

CHAPTER 2

USING A SIMULATION MODEL TO COMPARE METHODS OF TREE-RING DETRENDING AND TO INVESTIGATE THE DETECTABILITY OF LOW FREQUENCY SIGNALS

Introduction

Despite the importance of tree-ring chronologies as annually resolved quantitative paleoclimate proxies, consensus does not exist among dendrochronologists regarding the best methods for transforming many individual increment cores into mean-value chronologies of the sort used in countless studies. The method by which tree-ring series are processed has a tremendous impact on the mean value chronology of growth (Cook and Kairiukstis 1990). An area of active research in the global change community is identifying the scales and amplitudes of low-frequency variations in temperature in which tree-ring data play a pivotal role (Jones et al. 1998). This is despite claims that tree-ring records cannot provide accurate data on systematic trends in the environment lasting multiple centuries (Broecker 2001). Were one method of tree-ring processing able to preserve true exogenous low-frequency forcings, say as the result from climate change, then it would logically become the preferred method for working with long-lived climate sensitive trees.

A recent report by Esper, Cook, and Schweingruber (hereafter referred to as ECS) documents a new record of extratropical Northern Hemisphere temperature variability with substantially higher multi-centennial variability than previously shown (Esper et al. 2002). The tree-ring based reconstruction of ECS has been compared to the widely cited multi-proxy Northern Hemisphere temperature reconstruction by Mann, Bradley, and Hughes (hereafter referred to as MBH, Mann et al. 1998; 1999). The ECS record shows greater low-frequency variability than the MBH record resulting in discrepancies regarding the magnitude of warming seen about 1000 A.D. during the so-called "Medieval Warm Period" (Lamb 1965; Hughes and Diaz 1994).

The ECS reconstruction partially attributes its low-frequency variation to the method used to standardize the raw ring-width series. The detrending of tree-ring series, i.e., the removal of the natural decrease in ring-widths as the tree ages, is an essential part of dendrochronology and is required in virtually all dendroclimatic studies (Fritts 1976). Traditionally, if a series shows a non-linear juvenile growth curve, it is removed via negative exponential curve standardization (NECS) whereby a negative exponential curve is fit to each series and the departures from that fit are retained, in some manner or another (Fritts 1976; and see Cook and Peters 1997 for more information). The ECS reconstruction revives and greatly enhances an old detrending technique now called Regional Curve Standardization (RCS) that aligns all the samples to be included in the chronology by cambial age and developing the detrending curve by averaging their values (Esper et al. 2002). Then departures from that fit are then taken from the regional curve for each series (see Methods).

There is circularity in asserting which detrending method better reproduces a low-frequency climate signal given that sample series are used to infer the absolute true signal. Given that dilemma, we developed a simple statistical model of tree growth with known systematic and random noise and simulated "climate regimes" with known statistical properties. Since the systematic signals are removed from any proximate climate forcing, we prefer to call them "growth regimes." We used a simulation framework to build thousands of chronologies under different climatic forcings and two different detrending methods. Our objectives were to compare the efficacy of NECS and RCS in retaining the input signals and to explore what combination of growth forcings lead to the detectability of multi-centennial signals in the simulated trees.

Methods

We developed a simulation model to test detrending efficacy and explore issues surrounding low-frequency variability based on known growth parameters for foxtail pine (*Pinus balfouriana* Grev. et Balf.). Foxtail pine is a high elevation, temperature-sensitive species from the Sierra Nevada, USA that has been critical in many paleoclimatic studies and has shown substantial low-frequency variation (Graumlich 1991; Graumlich 1993; Scuderi 1993; Lloyd and Graumlich 1997). All growth and chronology parameters for the model were built using existing foxtail pine cores from Graumlich's unpublished data.

A statistical simulation model (RingSim) was developed in the R statistical programming language and environment (Ihaka and Gentleman 1996). All analysis was done in R using the core functions plus the Rwave contributed package (Carmona et al.

1998). We generated tree-ring like series, with specified features of tree growth, added systematic climatic effects to them, then detrended the series by RCS and NECS. We iterated these steps with random selections of parameters and computed bootstrapped confidence intervals of statistical comparisons of the detrending methods. These steps are described in detail below and a sample run is shown in figures 2.1-2.3.

Generating the Samples

For each model run, trees were grown in an empty chronology space spanning 2000 years. The ages of the trees ranged from 300 to 1700 years, with a mean age of 550 years and a standard deviation of 250 years fit from a normal distribution. Constraining tree ages in this manner fits with existing datasets and produces a positively skewed age class distribution. Given that long tree-ring chronologies are composed of living and dead trees, one third of the trees floated in the chronology space similar to incorporation of snags and subfossil wood via cross-dating. The dead trees were fit into the chronology space randomly while the live trees died in the 2000^{th} year and were germinated (plus years to breast height) in the year that corresponded to 2000 minus their age. A 350 year-old live tree, therefore, lived in the chronology space from 1650 to 2000 while a 350 year-old dead tree could float in the chronology space anywhere that its age permitted (e.g., from 200 to 1550). The age class structure and floating series plots from a single iteration are detailed in Figure 2.1.

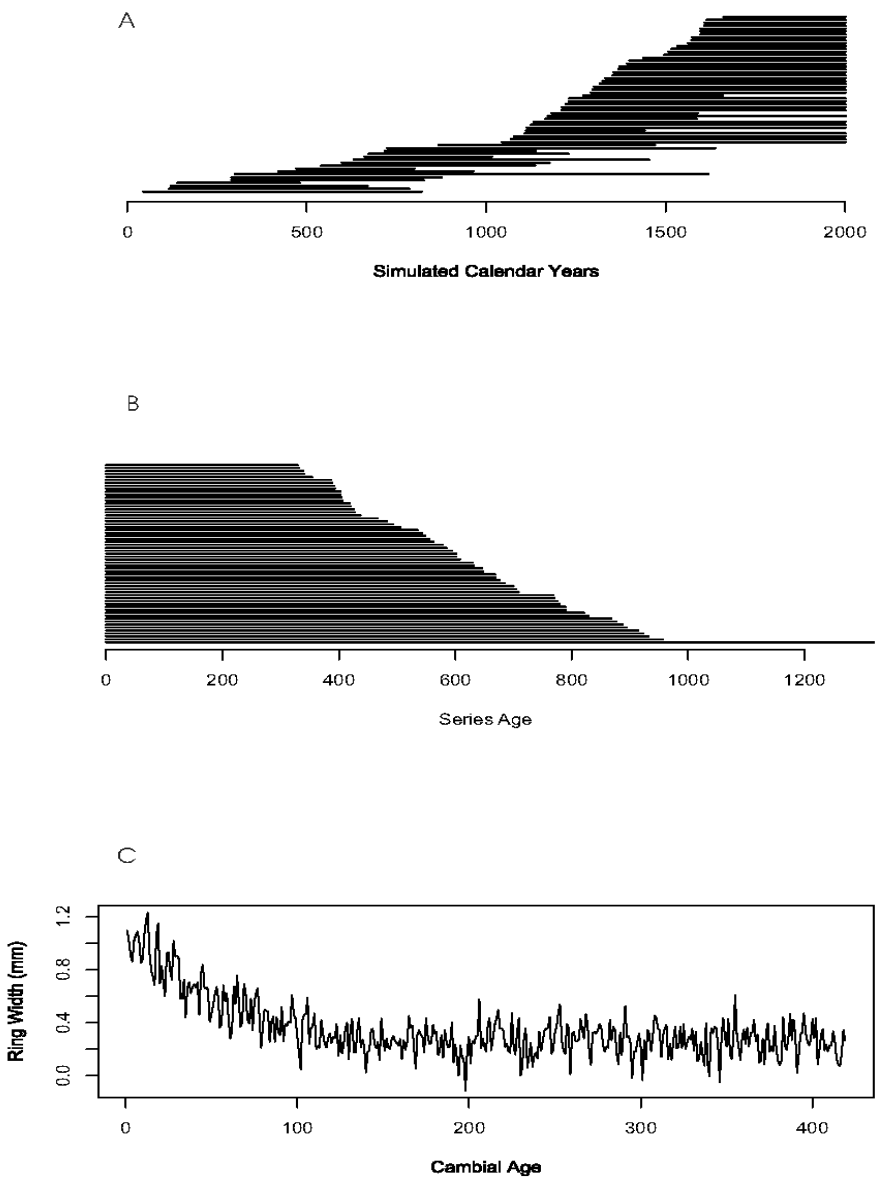

Fig. 2.1. A single run from RingSim has been extracted at random. This model run contains 61 series. It has a multi-centennial period of 229 years, a decadal period of 27 years, and an annual period of 6 years. The amplitudes of the signals are 1.336, 1.027, and 1.911 respectively. The location of each of the 61 series in the simulated space are shown (A) and reordered in an age class plot (B). One of the series has been plotted at random in the bottom panel (C).

Parameters for a juvenile growth curve for the simulated series were generated from 53 foxtail pine cores where the pith was clearly visible using cores from Graumlich's lab. The growth curve was estimated using a negative exponential growth equation $RW_t = Ae^{-Bt} + K$ where RW_t was the expected growth at time t, A was the initial year, $-B$ was the slope of the decrease in growth of the ring-widths, t was time in years, and K was the sequential growth per year after the initial growth spurt. Parameters A, $-B$ and K were drawn from a random uniform distribution following the range observed from the cores. Once the growth curve had been created, a simulation from an ARMA model with standard deviations ranging from 0.025 to 0.075 mm was used to create individual variation in growth with a lag of one year such as those seen from internal gap dynamics [AR1 = 0.2]. The curve and the temporally autocorrelated noise represented the base growth pattern for each individual series (a single series chosen from a random model run is shown in Fig. 2.1C). For each model run, the number of trees generated ranged uniformly from 15 to 100. This ensured that we had many model runs with a low number of trees in the chronology population and many runs with a high number of trees.

Adding the Effects of Climate and Weather

Two perturbations were created in the chronology space that were added to each individual series. The first was random noise common to all trees – not unlike the effects of interannual weather. Since trees experience weather events slightly differently, a small random scalar was added to the "weather noise" when it was applied to each series. This

feature was also an AR1 process at 0.2 and simulated as above to mimic climatic influences, such as temperature variability, which show interannual persistence.

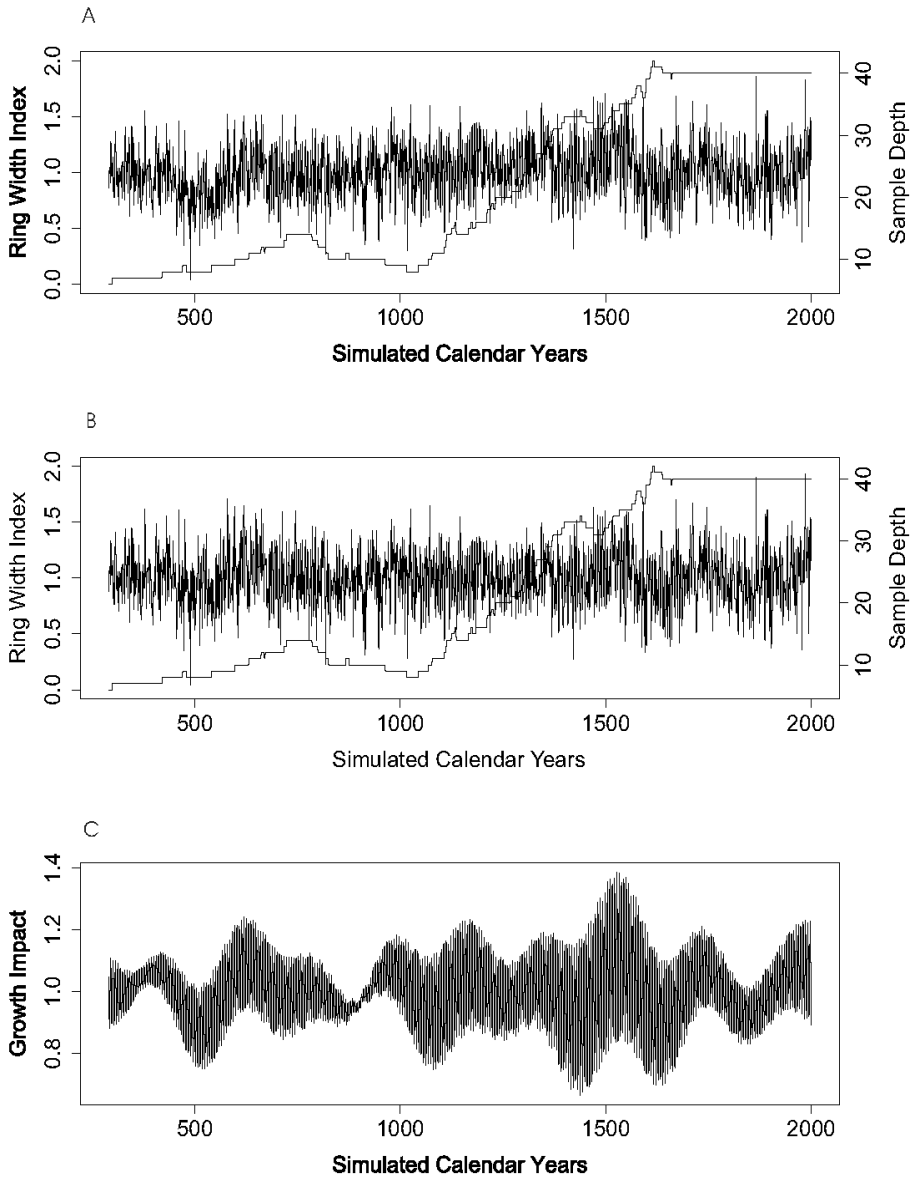

Fig. 2.2. The RCS (A) and NECS (B) chronologies are shown along with the growth regime (C) from the run depicted in Fig. 1. The sample depth is plotted alongside the chronologies (A and B).

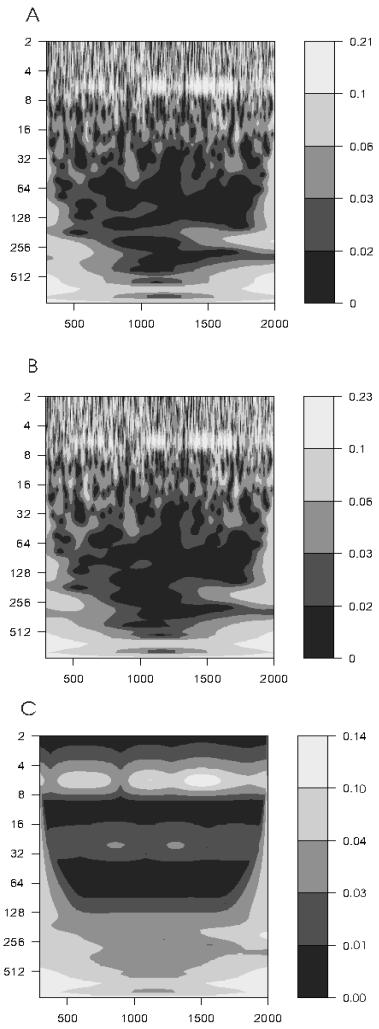

Fig. 2.3. Continuous wavelet power spectra density estimates for the RCS (A) and NECS (B) chronologies and the growth regime (C) are shown. The gray-scaled contour intervals show 0-25%, 25-50%, 50-95%, 75-95%, and 95-100% of the wavelet power. There are few differences between the chronologies and their coherence with the growth regime.

The major feature generated in the chronology space corresponded to long-term climate. Since our objectives were to probe the nature of low frequency signals, the

climate regimes generated all contained quasi-oscillatory signals with greater than 200 year periods. Due to the possible interaction of multiple scales of climate forcing, we added two more types of signal at the lower orders of magnitude: years and decades. The multi-centennial forcing ranged from 200-1000, the multi-decadal forcing ranged from 20 – 60 years, and the annual forcing ranged from 2-10 years (Table 2.1). Magnitudes for observed and modeled forcings were much scarcer in the literature (particularly for the lower-frequency forcings), and we set their sum influence on the series to range uniformly from zero to two (removing to doubling the growth for year *t*). That is, each forcing was a scalar that ranged from a minimum of 0.66 to a maximum of 1.33 so that the sum of all the forcings could double or negate the growth for any year *t* if the waves were all at the extent of their range and in phase.

The growth forcing was generated using an inverse Fourier transform. For each run, a Fourier Space was generated for 2000 years (the maximum length of the chronologies). Three spaces in the Fourier space corresponding to the frequencies drawn for the model run were filled with random normal numbers with a mean of zero and a standard deviation equal to the amplitudes drawn for the corresponding frequency. Finally, this complex vector was transformed out of Fourier space. The result was an oscillating wave with known periods and amplitudes (see Fig. 2.2C). Each series was multiplied by this wave and therefore incorporated this systematic noise.

Table 2.1. Variables used in the 10,000 random model runs. Random numbers for each run were drawn from a random uniform distribution.

Variable	Abbreviation	Range
Initial Ring-Width (mm)	A	0.4 to 1
Decay Coefficient	negB	-0.041 to -0.017
Mean Growth at Asymptote	K	0.1 to 0.9
Number of Trees	nTrees	15 to 99
Multi-centennial Period	Period.MC	200 to 1000
Decadal Period	Period.Dec	10 to 60
Annual Period	Period.An	2 to 10
Multi-centennial Amplitude	Amp.MC	1 to 1.333
Decadal Amplitude	Amp.Dec	1 to 1.333
Annual Amplitude	Amp.An	1 to 1.333

Detrending and Chronology Construction

ECS built two chronologies with RCS – one with the series demonstrating non-linear trends and one with series demonstrating linear trends and observed only slight differences between them. Non-linear series are the biological expectation and more challenging to detrend than linear series. Our simulated data, therefore, were exclusively non-linear (Table 2.1) so as to provide a more conservative test of the detrending methods. We followed the methods of Esper et al. (2003) in developing the regional curve. The regional curve was calculated by aligning each series by cambial age and taking the bi-weight robust mean for a given age (Cook 1985). A cubic spline was fit to the mean values with a 50% frequency cut-off width equal to 10% of the length (Cook and Peters 1981; and see Cook and Kairiukstis 1990 for more information on smoothing splines). A ring-width index (RWI) measured departures from the regional curve and was calculated as ratios (Fritts 1976). We also explored the use of residuals and residuals with a power transformation (Cook and Peters 1997). As noted by Esper et al. (2003) neither

residuals nor ratios can be universally recommended for millennial-length chronologies. We found that the results were often, but not always, similar with all three methods and plan to systematically explore the differences in future work. A chronology of all the series was built by taking the average for each year. The minimum number of series typically used in chronologies depends on the strength of the expressed climate signal across cores, their fractional variance terms, and the desired accuracy level (Wigley et al. 1984). We arbitrarily truncated our chronologies to a sample depth of five series to be consistent with the biology of the species we are simulating based on previous experience with the sub sample signal strength and expressed population signal of foxtail pine (e.g., Graumlich 1991; 1993).

To perform the NECS we used non-linear regression to fit a curve to each series. A negative exponential model was fit to each series. The model was used to predict a growth curve for each series and each series was detrended using the ratio method as above. A chronology was also built as above (e.g., Fig. 2.2 A and 2.2 B). A continuous wavelet transform showed that both methods faithfully captured most of the true power spectrum for this example as with other model runs (Fig. 2.3).

The additional power generated by the AR functions was in the wavelet spectra in the highest frequencies. The comparison provided in figure 2.3 is also useful for seeing the abundance and diversity of structures that exist in the simulated tree-ring chronologies that are common to both detrending techniques and do not exist in the growth forcing.

Assessing Standardization Efficacy with Model Runs

With a chronology built using RCS and NECS the model was then able to compare each chronology to the systematic growth input. The RCS chronology, the NECS chronology, and the systematic growth inputs were combined into a multivariate time series and run through a spectral analysis. Standardization efficacy was assessed using the squared coherency of the time series. Coherency analysis evaluates the correlation of multiple time series at all frequencies and is reported in terms of magnitude-squared coherence, the values of which range from zero to one. We judged how well the chronologies captured the growth signal by looking at the squared coherency of between the input growth signal and the two types of chronology at the exact frequencies used to generate the growth signal.

We ran the model 10,000 times. At each iteration, there were randomly assigned values for growth-regime periods, growth-regime amplitudes, biological growth factors, number of trees per chronology, and random noise as described above. The number of trees used in the simulation, the growth-regime periods and amplitudes, and the coherencies between the growth-regime forcings and each type of chronology for the three time scales examined were saved (e.g., Table 2.2 contains an example of two iterations of model output). Because the coherency output from the model is not normally distributed, we used a non-parametric bootstrap test to compare the difference in the means of the coherencies for RCS minus NECS (i.e., $\left(\sum_{i=i}^{n} CohRCS_i \Big/ n\right) - \left(\sum_{i=i}^{n} CohNECS_i \Big/ n\right)$ where *CohRCS* is the squared coherency for the RCS chronology, *CohNECS* is the squared coherency for the RCS chronology at run *i*, and *n* is the 10,000 model runs – see Davison and Hinkley 1997 and Venables and Ripley 1999 for more information).

Table 2.2 Example output for two of 10,000 model runs. The number of trees simulated is followed by the inputs for the growth forcings. The squared coherency between each standardized chronology and the climate disturbance is shown for each time scale examined. nTrees = Number of Trees; MC = Multi-centennial; Dec = Decadal; An = Annual.

		Periods			Amplitudes			Coherency for RCS			Coherency for NECS		
ID	nTrees	MC	Dec	An	MC	Dec	An	MC	Dec	An	MC	Dec	An
1	39	836	25	7	1.128	1.106	1.256	0.894	0.820	0.995	0.814	0.780	0.995
2	56	536	28	3	1.183	1.061	1.139	0.982	0.643	0.992	0.949	0.693	0.990

Results

The RCS method showed significantly greater ability to retain low frequency information as compared to the NECS method (Table 2.3). The difference in the means of the multi-centennial coherencies for RCS and NECS was 0.048. Studentized 95% confidence intervals from 1000 bootstrap replicates with 100 internal bootstrap replications were 0.042 and 0.054. Because the 95% CIs did not span zero, the null hypothesis that there was no difference between the means was rejected and therefore the difference between RCS and NECS in retaining low frequency signals was statistically significant (bootstrapped p-value ≤ 0.001). The differences in the means between the RCS method and the NECS method in retaining higher frequency signals corresponding to decadal and annual periodicities were not significantly greater than zero (Table 2.3).

Table 2.3. The mean coherency between the standardization methods (RCS and NECS) and the systematic noise are shown for each time scale. The differences in the means values of RCS and NECS are significant from zero under a studentized bootstrapped resampling test, with 1000 bootstrap replicates and 100 predictions made at each bootstrap replicate, for the multi-centennial periods only.

Temporal Scale	RCS Coherency	NECS Coherency	mean(RCS) – mean(NECS)	95% CI
Multi Centennial	0.848	0.800	0.048 (p value ≤ 0.001)	0.042 –0.054
Decadal	0.895	0.902	-0.007 (p value = 0.1495)	-0.013 –0.003
Annual	0.908	0.914	-0.006 (p value = 0.1188)	-0.011 –0.002

The ability to detect systematic signals in the chronologies can be seen as a function of the input signal's amplitude. Signals less 1.06 were difficult to detect, regardless of period (Fig. 2.4). Furthermore, at amplitudes greater than 1.13 the RCS

chronologies were more coherent with the input than the NECS chronologies at the multi-centennial time scale (Fig. 2.4, top). When decomposed by period and amplitude of the input signal, RCS began to outperform NECS at periods greater than 450 years (Fig. 2.5 vs. Fig. 2.6). The differences between RCS and NECS were not detectable at decadal or annual time scales.

The RCS method was sensitive to the number of series used to generate the regional curve (Fig. 2.7). If the model runs containing 15 trees were subset (115 of the 10,000 models runs), then the mean coherency between the input signals and the RCS chronology for the multi-centennial time scales was 0.76. The mean coherency between the input signals and the NECS chronology for the multi-centennial time scales was 0.79 for the same data. This is contrary to the entire dataset where RCS coherency was greater than NCS at multi-centennial time scales. The difference in the means of the squared coherencies (RCS minus NECS) for the subset containing 15 trees, however, was not significantly different than zero under the same bootstrap procedure described above (95% CI were -0.052 to 0.015 and the bootstrapped p-value = 0.1980). This failed to reject the null hypothesis that there was no difference between the means of the squared coherency for RCS and NECS for model runs containing 15 trees. The general relationship held at the other end of the spectrum. If the model runs containing 99 trees (117 of the 10,000 models runs) were subset, then the mean coherency between the input signals and the RCS chronology for the multi-centennial time scales was 0.90. The mean coherency between the input signals and the NECS chronology for the multi-centennial time scales was 0.81 for the same data. This difference was significantly different than

zero under the bootstrap procedures described above (95% CI are 0.0124 to 0.1378 and the bootstrapped p-value = 0.0099).

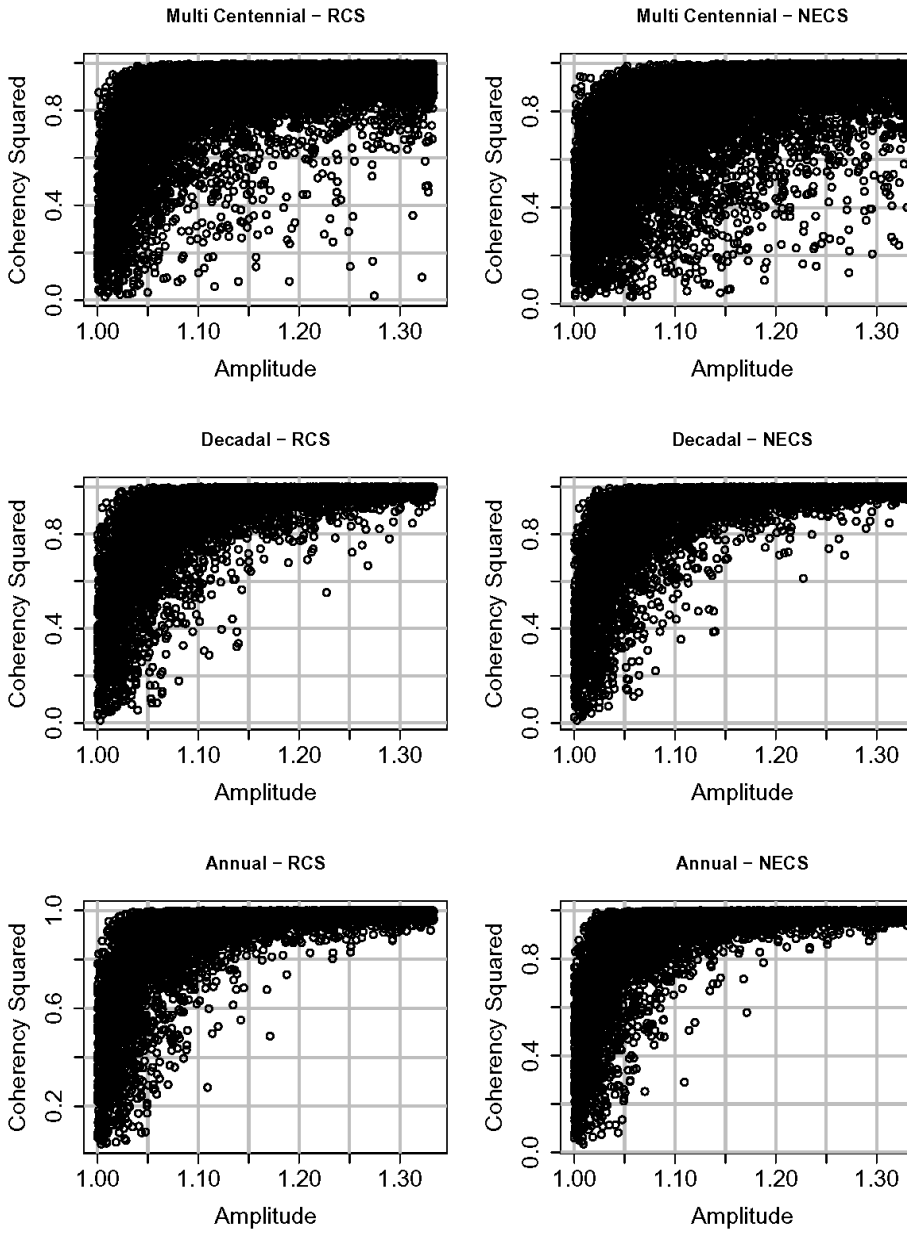

Fig. 2.4. Coherency squared between the growth regime and chronology is shown as a function of signal amplitude for RCS and NECS chronologies (columns) for the three time scales examined (rows). The only noticeable difference between the methods is at the multi-centennial time scale (compare to Table 3).

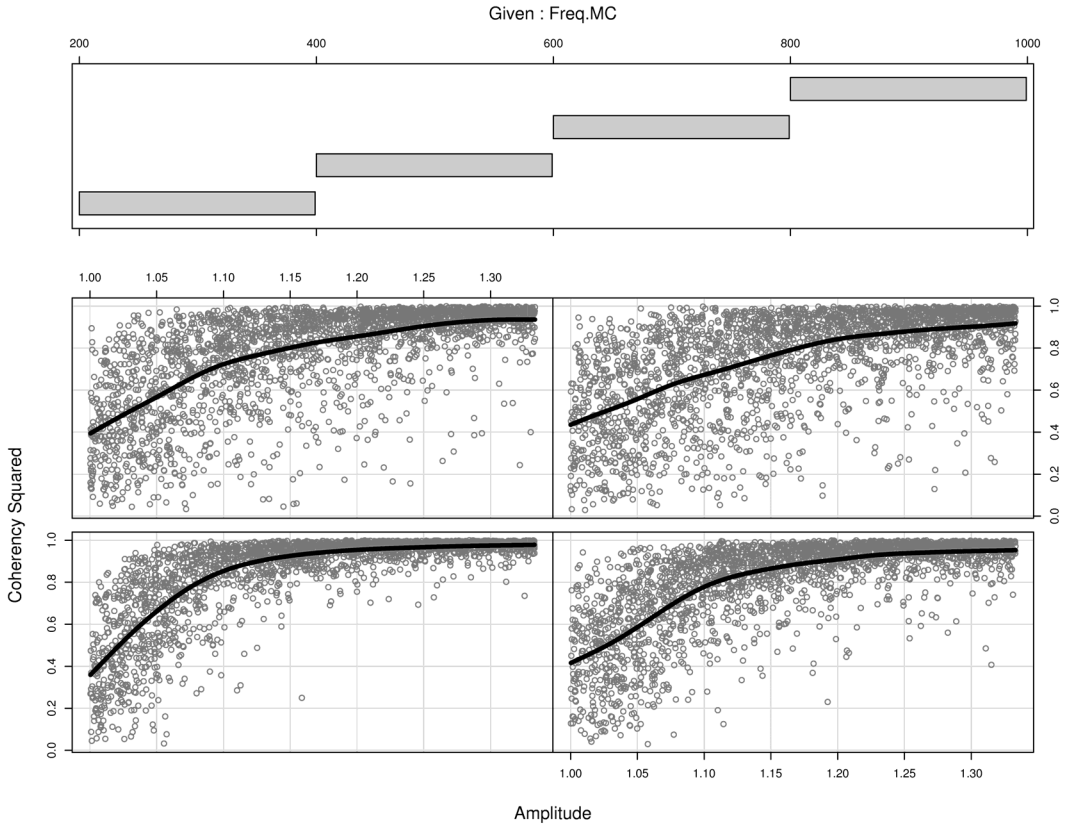

Fig. 2.5. A conditioning plot shows the coherency squared between the growth regime and the RCS chronology as a function of signal amplitude conditioned by the multi-centennial period. The bottom left panel (A) subsets model runs with periods between 200 and 400 years while the top right panel (D) subsets model runs with periods from 800 to 1000 years. There is minimal loss of coherency at longer wavelengths. The black lines are stiff cubic splines to highlight trends in the data.

Discussion

Regional curve standardization outperformed negative exponential decay standardization for maintaining low-frequency variability in our simulated tree-ring chronologies but did not preserve decadal or annual periods with greater efficacy. This supports previous claims regarding the power of RCS in maintaining low-frequency

variability (Briffa et al. 1992; Briffa et al. 1996; Esper et al. 2002; 2003). This study contributed a methodological basis to the body of literature in refuting the idea that tree-ring chronologies cannot preserve low-frequency signals (e.g., Esper et al. 2002). Despite these results, we concur with Briffa et al. (1996) who state, "The RCS approach is far from being a general panacea for the loss of long-timescale information in dendroclimatology," and discuss the results and caveats in our model.

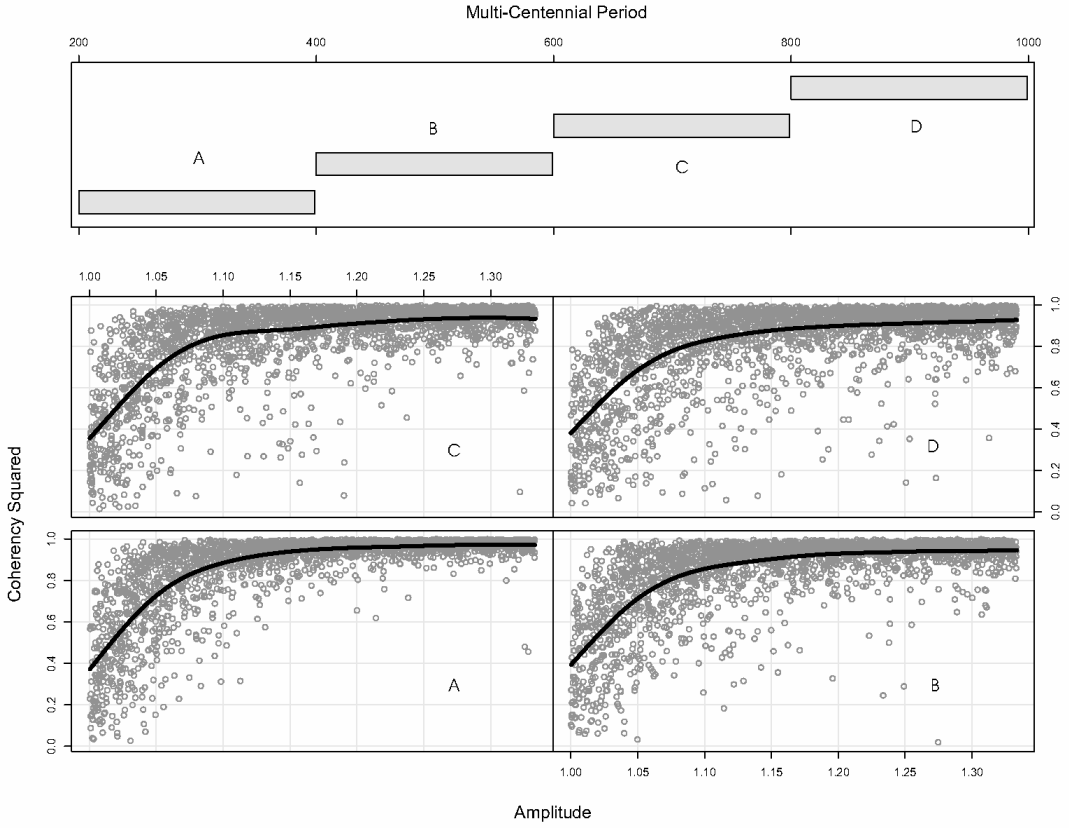

Fig. 2.6. A conditioning plot shows the coherency squared between the growth regime and the NECS chronology as a function of signal amplitude conditioned by the multi-centennial period. As above, the bottom left panel (A) subsets model runs with periods between 200 and 400 years while the top right panel (D) subsets model runs with periods from 800 to 1000 years. Unlike the RCS chronologies, the NECS shows substantial degradation of coherency at the lowest frequencies even at the strongest amplitudes.

There are enormous advantages to using a simulation model to explore questions of standardization and low-frequency signals. All the advantages correspond to the natural variation in the parameters examined: tree-ring series show variation in juvenile growth curves; tree-ring chronologies have variation in sample depth; climate periods vary at multiple scales. Even for a model as simple as this one, the parameter-space for these questions was enormous (Table 2.1). The simulation framework allowed us to explore the response variable, coherency of a chronology to a known growth modifier, with well-enumerated predictors (e.g., the number of trees simulated). The advantage of establishing this model with minimal assumptions (e.g., using uniform distributions for selecting parameters) will allow us to perform uncertainty and sensitivity analysis in future work.

Our tree growth simulation model is statistical, meaning that model parameters for growth and forcings are not directly derived from the proximate causes of those variables. Biologically, the width of the initial ring of a foxtail pine core is a function of air and soil temperatures and soil water content for periods of the tree's growing season, among other factors. In our model runs, the width of the initial ring of a series was drawn from a random distribution of observed initial widths. Similarly, the periods of growth-regime variability were drawn from observed periodicities and removed from first-order calculations of sea surface temperatures, orbital parameters, etc. These gross generalizations allowed us to explore the association between signal duration and strength from theory without becoming mired in the contentious and highly technical aspects of climate forcings and climate-growth relationships over time.

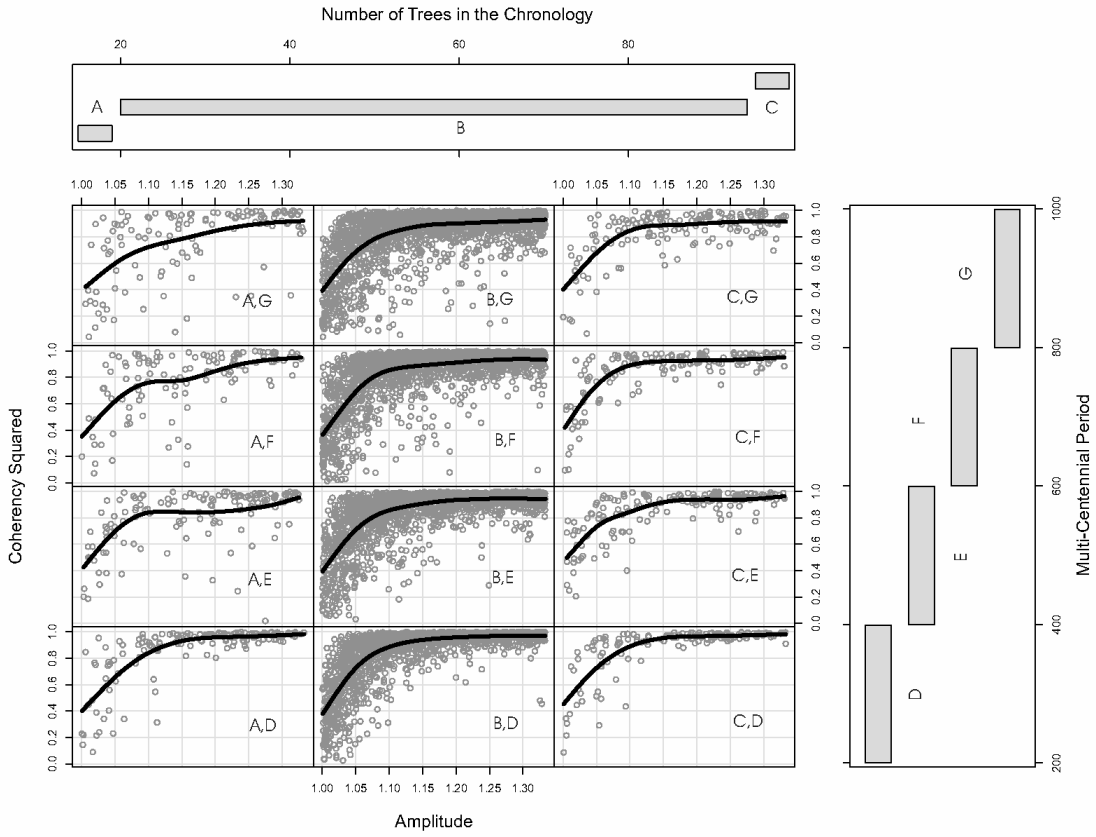

Fig. 2.7. A double conditioning plot shows the coherency squared between the growth regime and the RCS chronology as a function of signal amplitude conditioned by the multi-centennial period (rows) and the number of trees used in the chronology (columns). For instance, the top left panel (A, G) subsets model runs with 15 to 20 trees and periods from 800 to 1000 years. The bottom right panel (C, D) subsets model runs with 95 to 99 trees and periods from 200 to 400 years. This shows the effect of the number of trees on the detectability of multi-centennial periods where the longest periods are easiest to detect with the highest number of trees. However, at high enough amplitudes signals are generally detectable regardless of period or the number of trees. The NECS method is not shown because the difference between the numbers of trees was not as striking.

In the model runs, trees were grown following a negative exponential curve that varied with parameters observed in cores from foxtail pines. Tree growth was idealized using a negative exponential curve with three parameters: the initial width of the first ring, the mean growth after the juvenile period and a coefficient that determined the rate

of decay from the initial width to the mean adult width. To avoid circularity when the series were detrended, these parameters were estimated without the aid of a mathematical model. Some circularity was introduced, however, when the series were generated in the model which necessitated using a negative exponential function. As NECS had an innate advantage in this comparison (the growth curves were generated with a negative exponential), it is noteworthy that the RCS detrending method was better at extracting the low frequency signal.

The RCS method is an appealing theoretical framework for removing low-frequency signals from tree-ring series that are much shorter than the periods being sought. The reasons for this have been well-covered elsewhere (Briffa et al. 1996; Esper et al. 2003) and will not be discussed here beyond pointing out that negative exponential curves are extremely sensitive to the first decades of growth. For instance, if a series originates during a period of high growth (e.g., favorable climate) the curve fit to that via NECS will dampen that signal by misfitting the initial growth parameter and decay coefficient. The RCS method guards against this if the series are distributed across a variety of growth periods (i.e., some series originate in periods of favorable growth and some periods initiate in periods of restricted growth).

Our model results indicate that having series distributed across a range of growth conditions was necessary but not sufficient in developing an accurate regional curve. Our model results also indicated that RCS was sensitive to the number of series used to develop the regional curve. The general relationship for all model runs was for RCS to be more coherent with low-frequency signals (Table 2.3). That relationship did not hold

when the number of trees in the chronologies ranges equaled 15. In those cases, NECS and RCS were statistically equivalent. Although our results indicated that there was no statistical difference between RCS and NECS for a chronology with 15 trees, we are reluctant to give a recommendation on the number of series needed for an accurate regional curve given the tendency of dendrochronologists to use multiple series from a single tree and the difficulties associated with aligning real tree-ring series by cambial age. Constructing a regional curve requires the analyst to know the correct cambial age of the series. In a simulation model, this is known. In ancient tree-ring series and sub-fossil wood samples, the pith is often missing due to rot, requiring the application of pith offsetting to estimate cambial age. Although Esper et al. (2003) expended considerable energy exploring regional curves where the pith of some series was estimated and reported good results, caution is still warranted. The construction of a good tree-ring chronology requires the analyst to make judgments about which cores (or portions of a core) to include. This is especially true with very long, temperature-sensitive chronologies. We do not want a researcher to work towards a threshold of samples that are indicated by this model but instead urge the careful consideration of each sample and the exploration of both detrending methods.

RCS showed improvement over NECS at multi-centennial scales only (Table 2.3, Fig. 2.4). At the multi-centennial scale, RCS showed the greatest improvement at the longest wavelengths (Figs. 2.5 and 2.6). These wavelengths are thought to be expressed in temperature variability (e.g., Jones et al. 1998; Mann and Jones 2003) indicating that when low-frequency temperature variability is being investigated, and when the data

support the construction of an accurate regional curve, RCS is to be preferred over NECS. The analyst should also consider using multiple methods of detrending. In real tree-ring series, for instance, high frequency signals tend to be local compared to multi-decadal or centennial signals (Jones et al. 1998). In those cases, a NECS chronology could be used to display and interpret high-frequency features in a chronology while RCS could be used to emphasize low-frequency features. As is common in science, one method will rarely accomplish all the research goals.

The retrieval of an input signal was highly dependent on its amplitude. Signals were difficult when the scalar applied was less than 1.06. This occurs when the signal falls below the background noise simulated in the chronology. The amount of noise from day to day weather and stand dynamics was known in these simulated chronologies. In real tree-ring data the level of background noise (red or white) is troublesome to remove without affecting the true signals being sought. Dendroclimatic research therefore seeks systems where the interference of non-climatic signals can be minimized (e.g., latitudinal and alpine treeline). A significant challenge to the global change community is to quantify unbiased estimates of the amplitude of the climate signal to tree-growth (transfer function) as well as the amount of background noise inherited by each series. If that becomes possible, estimates about the relative detectability of low-frequency climate signals can be drastically improved.

Conclusions

Of the more than 2400 entities in the International Tree-Ring Database, roughly 5% are greater than 800 years in length. Only a fraction of these chronologies are of

interest to researchers extracting low-frequency variation related to climate. According to our model results, low frequency variability, of the sort seen in the ECS reconstruction of extra-tropical tree-rings, is better preserved using RCS if an accurate regional curve can be constructed. Despite the statistical significance described above, we saw only a 4.8% increase between RCS and NECS in 10,000 model runs. Accordingly and not surprisingly, we could not visually detect differences between the RCS and NECS chronologies. Therefore, this study in no way diminishes the multi-proxy MBH reconstruction but rather points to the need to further understand the spatial scale of the expression of low-frequency variation. Most importantly, it shows that low frequency variation can be preserved in tree chronologies. Given the paucity of very long tree-ring chronologies, proper processing techniques are critical, and the RCS method shows tremendous promise.

References

Briffa K.R., Jones P.D., Bartholin T.S., Eckstein D., Schweingruber F.H., Karlen W., Zetteberg P. and Eronen M. (1992) Fennoscandian summers from A.D. 500: Temperature changes on short and long time scales. *Climate Dynamics* 7, 111-119

Briffa K.R., Jones P.D., Schweingruber F.H., Karlén W. and Shiyatov S.G. (1996) Tree-ring variables as proxy-climate indicators: problems with low-frequency signals. In: *Climatic Variations and Forcing Mechanisms of the Last 2000 Years* (eds Jones P.D., Bradley R.S. and Jouzel J.), NATO ASI Series edn, pp. 9-41. Springer-Verlag, Berlin

Broecker W.S. (2001) Was the medieval warm period global? *Science* 291, 1497-1499

Carmona R., Hwang W.L. and Torresani B. (1998) Practical TimeFrequency Analysis: Gabor and Wavelet Transforms with an Implementation in S. Academic Press, San Diego, CA

Cook, E.R. (85) A time-series analysis approach to tree-ring standardization. PhD dissertation, University of Arizona. Tucson, AZ

Cook E.R. and Kairiukstis L.A.e. (1990) *Methods of dendrochronology - applications in the environmental sciences*. Kluwer Academic Publishers and International Institute for Applied Systems Analysis., Dordrecht, The Netherlands

Cook E.R. and Peters K. (1981) The smoothing spline: A new approach to standardizing forest interior tree-ring width series for dendroclimatic studies. *Tree-Ring Bulletin* 41, 45-53

Cook E.R. and Peters K. (1997) Calculating unbiased tree-ring indices for the study of climatic and environmental change. *The Holocene* 7, 361-370

Davison A.C. and Hinkley D.V. (1997) *Bootstrap Methods and Their Application*. Cambridge University Press, Cambridge, UK

Esper J., Cook E.R., Krusic P.J., Peters K. and Schweingruber F.H. (2004) Tests of the RCS method for preserving low-frequency variability in long tree-ring chronologies. *Tree-Ring Research* 59, 81-98

Esper J., Cook E.R. and Schweingruber F.H. (2002) Low-frequency signals in long tree-ring chronologies for reconstructing past temperature variability. *Science* 295, 2250-2253

Fritts H.C. (1976) *Tree rings and climate*. Academic Press, London, New York

Graumlich L.J. (1991) Subalpine tree growth, climate, and increasing CO2: An assessment of recent growth trends. *Ecology* 72, 1-11

Graumlich L.J. (1993) A 1000-year record of temperature and precipitation in the Sierra Nevada. *Quaternary Research* 39, 249-255

Hughes M.K. and Diaz H.F. (1994) Was there a 'Medieval Warm Period' and if so, where and when? *Climatic Change* 26, 109-142

Ihaka R. and Gentleman R. (1996) R: A language for data analysis and graphics. *Journal of Computational and Graphical Statistics* 5, 299-314

Jones P.D., Briffa K.R., Barnett T.P. and Tett S.F.B. (1998) High-resolution palaeoclmatic records for the last millennium: interprettion, integration and

comparison with General Circulation Model control-run temperatures. *The Holocene* 8, 455-471

Jones P.D., Osborn T.J. and Briffa K.R. (1997) Estimating sampling errors in large-scale temperature averages. *Journal of Climate* 10, 2548-2568

Lamb H.H. (1965) The early medieval warm epoch and its sequel. *Palaeogeography, Palaeoclimatology, Palaeoecology* 1, 13-37

Lloyd A.H. and Graumlich L.J. (1997) Holocene dynamics of treeline forests in the Sierra Nevada. *Ecology* 78, 1199-1210

Mann M.E., Bradley R.S. and Hughes M.K. (1999) Northern hemisphere temperatures during the past millennium: inferences, uncertainties, and limitations. *Geophysical Research Letters* 26, 759-762

Mann M.E., Bradley R.S. and Hughes M.K. (1998) Global-scale temperature patterns and climate forcing over the past six centuries. *Nature* 392, 779-787

Mann M.E. and Jones P.D. (2003) Global surface temperatures over the past two millenia. *Geophysical Research Letters* 30, 1820-1824

Scuderi L.A. (1993) A 2000-year tree ring record of annual temperatures in the Sierra Nevada Mountains. *Science* 259, 1433-1436

Venables W.N. and Ripley B.D. (1999) *Modern Applied Statistics with S-PLUS. Third Edition*. Springer, New York

Wigley T.M.L., Briffa K.R. and Jones P.D. (1984) On the average value of correlated time series, with applications in dendroclimatology and hydrometeorology. *Journal of Climate and Applied Meteorology* 23, 201-21

CHAPTER 3

TRENDS IN TWENTIETH-CENTURY TREE GROWTH AT HIGH ELEVATIONS IN THE SIERRA NEVADA AND WHITE MOUNTAINS, USA

Introduction

Networks of long, annually-resolved proxies of past climate derived from tree rings, ice cores, and historical records play a pivotal role in assessing the degree of greenhouse warming in current Northern Hemisphere climate trends (LaMarche 1974; Williams and Wigley 1983; Graumlich 1993; Bradley and Jones 1992; Scuderi 1993; Stine 1994; Briffa et al. 1992; Mann et al. 1998; 1999; Barber et al. 2000; Crowley 2000; Stahle et al. 2000). Arguably some of the most critical data in the analyses are tree-ring records from high elevation conifers in western North America. The Sierra Nevada and White Mountains of California provide a rich opportunity for paleoclimatic research due to an unusually high concentration of long-lived tree species in conjunction with preservation of subfossil wood in a cold dry setting (Graumlich 1993; Scuderi 1993; Hughes and Graumlich 1996). Since the 1960s, tree-ring chronologies from this region have informed our concepts regarding the nature of climate change, especially with regard to temperature variability.

Inferring past climate from trees growing near their temperature limit in a semi-arid setting, however, is challenging because of the strong potential for interactions between growing season temperature and soil moisture in controlling growth (Graumlich

1993). In this paper, we exploited inter-species and inter-site variations in the growth pattern of 13 millennial-length subalpine chronologies and assessed the climate response in a two-dimensional reduction of the data. We were able to address the relative contributions of species and site in understanding climate-growth relationships by using five species from two genera over a relatively small, but rugged geographic area. The opportunity for exploiting species and site differences among temperature-sensitive tree-ring records is rare. Our network stands in stark contrast to the to the relatively low diversity of temperature sensitive tree species worldwide: of the 33 chronologies found above 60 N in Canada on the International Tree-Ring Database, for example, 28 are *Picea glauca,* four are *Picea mariana*, and one chronology is mixture of both species. We used the high regional diversity of tree species to increase the ties between paleoclimatic inference and tree autecology.

Specifically, in this paper we compared the growth patterns to instrumental records of temperature and precipitation and assessed the patterns of growth in the twentieth century to those of the preceding 900 years. We exploited inter-species and inter-site variations in climate response by describing the contributions of each species and site to the ordination, especially regarding the role of precipitation. Unlike some dendroclimatic results (Briffa and Osborne 1999; Barber et al. 2000), we saw no evidence for a reduced or altered sensitivity to climate in the most recent decades. The multivariate growth trend of the last century showed no analog in the past millennium, providing strong evidence of substantial climate change.

Methods

Tree cores from living trees and cross-sections from subfossil wood were collected by Graumlich or others in the tree-ring community (Fig. 3.1, Table 3.1). All of the series total-ring widths were cross-dated and measured using standard methods (Stokes and Smiley 1968; Fritts 1976). Age-related trends (i.e., the natural reduction in growth as a tree ages) were removed by fitting conservative, negative exponential curves to each series (Fritts 1976). All the chronologies had segment lengths in the constituent series of adequate length to interpret multi-decadal trends in growth. A chronology for each site was calculated as a mean-value function of the series using the ring-width index that is dimensionless, has a mean of one, and a stable variance (Fritts 1976) (Fig. 3.2). The chronologies spanned the years from AD 1000 to approximately 1990 (Table 3.1). The data were arranged in a single matrix of 991 rows (years) by 13 columns (sites/species). Missing values (< 0.15% of the matrix) were filled with a 25-yr running average.

Our objective in analyzing the dataset was to identify inter- and intra-specific differences in tree-ring growth in response to synoptic-scale climatic variation. We used a data reduction technique that minimizes assumptions regarding linearity and uniformity of response over time in light of concerns regarding the stationarity of climate-growth responses (Briffa et al. 1992; Barber et al. 2000; Briffa and Osborne 1999). We used nonmetric multidimensional scaling (NMS) to ordinate sample years based on their similarity in ring-width indices among sites. NMS ordinates the data by projecting the dataset into a reduced space so that distances between samples (years) in ordination space reflect dissimilarities in the original 13-dimensional site data space of ring-width indices

(Kruskal 1964; Kruskal and Wish 1978). NMS is a powerful data compression technique that makes no assumptions about the underlying structure of the data (see Clarke 1993 for summary). NMS has been successfully employed with climatically sensitive tree-ring data (Oberhuber and Kofler 2000).

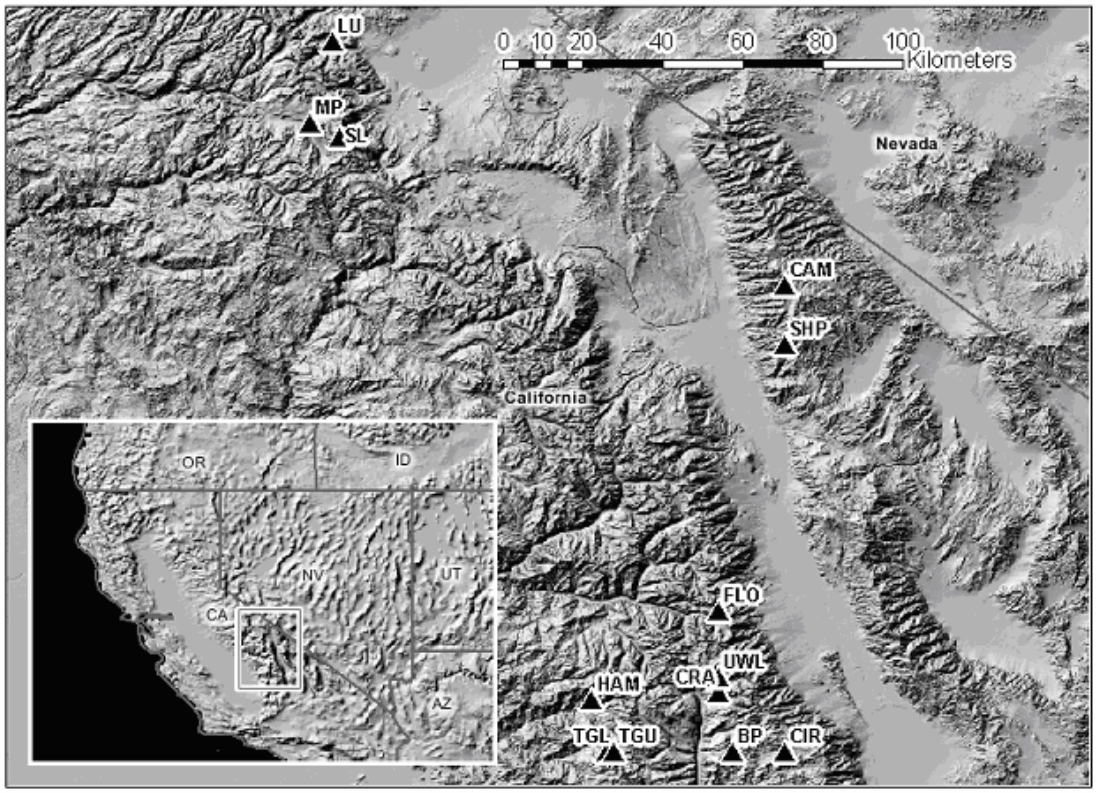

Fig. 3.1. Location of tree-ring sites in the Sierra Nevada and White Mountains of California. Each triangle marks a site with an approximately 1000 year long tree-ring chronology. Sites are abbreviated according to entries in table 3.1 which gives species

Table 3.1. Sources for tree-ring data include the authors' data archives (#1, #3-5, #9, #10-11) and the International Tree Ring Data Bank (#2, #6-8, #12-13). All of the authors' data will be made available online via the International Tree Ring Data Bank (http://www.ngdc.noaa.gov/paleo/treering.html).

ID	Code	Site	Species	Lat. (N)	Long. (W)	Elev (m)	Chronology	Strip-bark morphology?
1	BP	Boreal Plateau	*Pinus balfouriana*	36.45	118.33	3420	1000 - 1992	N
2	CIR	Cirque Peak	*Pinus balfouriana*	36.45	118.22	3505	1000 - 1987	N
3	HAM	Hamilton	*Juniperus occidentalis*	36.57	118.65	2630	1000 - 1988	N
4	CRA	Crabtree	*Pinus balfouriana*	36.58	118.37	3378	1000 - 1996	N
5	UWL	Upper Wright Lakes	*Pinus balfouriana*	36.62	118.37	3510	1000 - 1992	N
6	FLO	Flower Lake	*Pinus balfouriana*	36.77	118.37	3291	1000 - 1987	Y
7	SHP	Sheep Mtn	*Pinus longaeva*	37.37	118.22	3475	1000 - 1990	Y
8	CAM	Campito	*Pinus longaeva*	37.50	118.22	3400	1000 - 1983	Y
9	SL	Spillway Lake	*Pinus albicaulis*	37.83	119.22	3305	1000 - 1996	N
10	MP	Mammoth Peak	*Pinus albicaulis*	37.87	119.28	3350	1000 - 1996	N
11	LU	Lundy Lake	*Pinus flexilis*	38.05	119.23	2925	1000 - 1994	Y
12	TGL	Timber Gap Lower	*Pinus balfouriana*	36.45	118.62	3017	1050 - 1987	Y
13	TGU	Timber Gap Upper	*Pinus balfouriana*	36.45	118.60	3216	1000 - 1987	Y

2 = Graybill (1987a); 6 = Graybill(1987b); 7 = Graybill (1990); 8 = Graybill and LaMarche (1983); 12 = Graybill (1987c); 13 = Graybill (1987d).

We used the software package PC-ORD to perform the ordination (McCune and Mefford 1999). The basis of the dissimilarity matrix used was a 13x13 Euclidean distance matrix, measured as the 13-dimensional version of the Pythagorean theorem. The index is metric so there can be a direct mapping of ecological distance into ordination space (Legendre and Legendre 1998). To determine the best number of axes in which to project the data swarm, we conducted NMS in a step-down fashion where solutions of varying dimensionality (from six to one) were compared for their ability to minimize a goodness of fit metric (stress) in the ordination space and accurately compress the data. A scree plot suggested that a two-dimensional solution (stress=16.2%) was appropriate (not shown). This solution had significantly lower stress than randomized runs of the data (p-

value < 0.001). The final result of the NMS procedure was a reduction of the 13 chronologies over 991 years into two ordination scores for each year in the data set. We performed a varimax rotation in order to align the axes in a more intuitive way (Kaiser 1958).

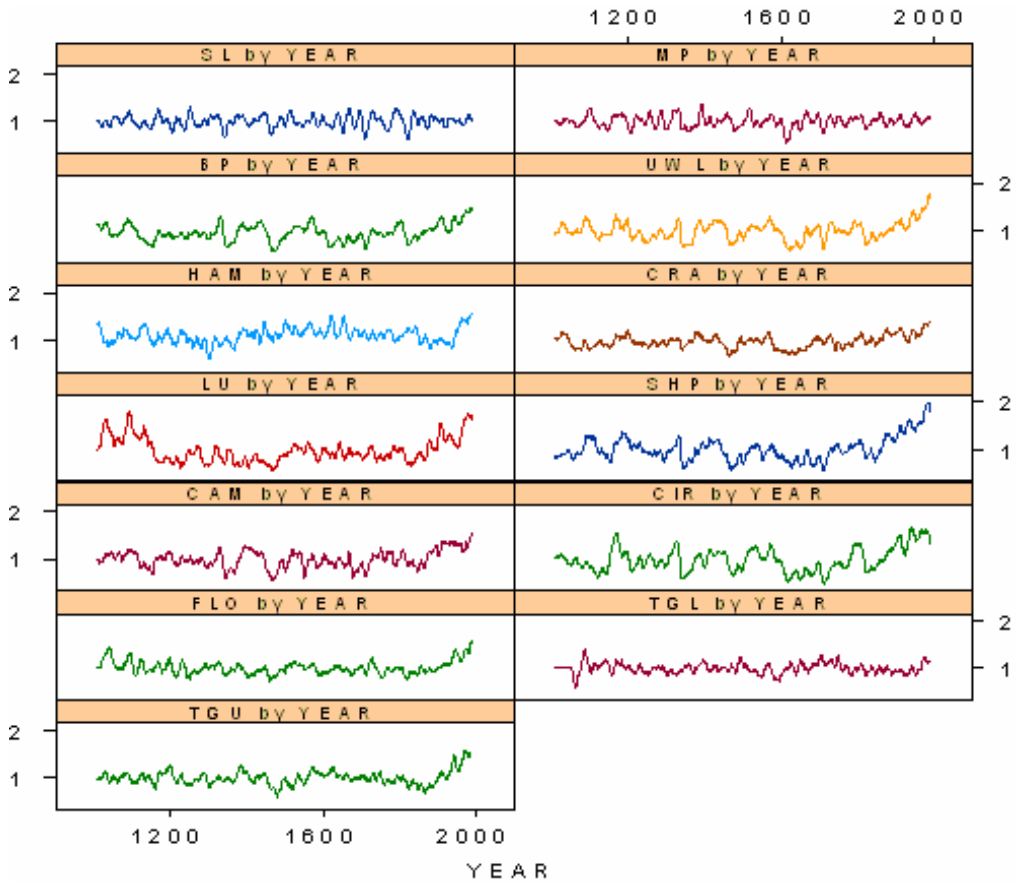

Fig. 3.2. Time series plots of the tree-ring data with a 25-year running average. The tree-chronologies are indexed with a ring width index that has a mean value of one. Compare to table 3.1 and figure 3.1 for species and geographic context.

The trees in this study are known to be sensitive recorders of precipitation and temperature variability (LaMarche 1974; Graumlich 1993; Hughes and Graumlich 1996). Tree growth at these cold and dry high elevations sites is limited both by cold

temperatures and low soil water content (Graumlich 1993). We used mean daily summer temperature as a surrogate for growing season length and previous winter's precipitation as a surrogate for growing season moisture. Long instrumental records of climate in the region of interest are available from Yosemite National Park (1907 to present; 1209 m; western slope of Sierra Nevada) and Independence, California (1894 to present; 1204 m; eastern slope of Sierra Nevada; Fig. 3.1). Daily precipitation and temperature data from the Yosemite and Independence stations showed strong linear correlations (r^2 = 0.72 and 0.70 respectively). We elected to use the Yosemite station for our analysis due to its more complete record and the relatively high coherencency between the records. We compared the ordination scores from 1907 to 1990 to the climate variables and plotted them in the ordination space as a biplot (Gabriel 1971).

In an effort to identify discrete climate episodes as revealed by tree growth trends, the samples were organized into clusters using hierarchical agglomerative classification (Legendre and Legendre 1998). This was accomplished by establishing a joining algorithm that unites individual samples into similar groups based on pairwise dissimilarity or distance. Again, we used Euclidean distance to form the dissimilarity matrix and Ward's (1963) minimum variance method as a joining rule. This linkage method produced tight clusters with low chaining (22%). As the same dissimilarity matrix was used for clustering and ordination, the results can be viewed in the same space.

We used multi-response permutation procedures (MRPP) to test whether the samples within the same group are more similar than samples in different groups (Mielke

et al. 1981; Mielke 1991). MRPP contrasts among- to within-group variability in the data and uses permutation to test the null hypothesis that groups are not clustered in dissimilarity space. There were at least 15 statistically separable groups (p-value < 0.001).We determined the best number of clusters to represent this data by comparing the within-group homogeneity to a random expectation because many more groups are statistically separable than are ecologically interpretable (Legendre and Legendre 1998; McCune and Mefford 1999). By definition, the number of clusters and the within-group homogeneity increases simultaneously. The relationship of chance-correlated within-group agreement as a function of number of groups indicated that five clusters, while somewhat subjective, offered the best trade-off between group fidelity and interpretability.

The 13 individual tree ring sites can be added to the ordination as indicator scores by weighted averaging (Whittaker 1967). Indicator scores as derived from weighted averaging have long been used in plant ecology as a means of environmental assessment (see Jongman et al. 1995 for review). The idea underlying a weighted average as an indicator score is to devise a single scalar for each ordination axis that represents the site. Here, we calculated ordination scores for the sites using sample unit scores to find the position of each site along each ordination axis, averaged over time. The sites can then be plotted into the ordination.

Finally, we employed a signal detection method on the ordination scores to assess the strength and frequency of any periodicity in the ordination through time. We used the multitaper spectral estimation (MTM) and robust noise level determination (Mann and

Lees 1996). This method allowed detection of harmonic and broader-band signals buried in climatic noise. This analysis gave us a further way to describe the ordination axes and their relationship to climate.

Results

The result of the NMS procedure was a reduction of the 13 chronologies over 991 years into two ordination scores for each year in the data. The two axes of the ordination captured 89% of the variation in the original 13-dimensional space, with 77% loading on axis one. The axes were over 99% orthogonal. Due to the high inter-annual variability of tree-ring data, the ordination scores are shown as 25-year moving averages in subsequent figures.

Summer temperature (May to September calculated as mean daily temperature) and previous winter's precipitation (November through March calculated as total daily precipitation) was significantly correlated to axis one (p-value < 0.001) and previous winter's precipitation was also significantly correlated to axis two (p-value < 0.001). Summer temperature was correlated with axis one ($r = 0.46$) and slightly negatively with axis two ($r = -0.02$). Previous winter's precipitation correlated positively for axis one ($r = 0.42$) and axis two ($r = 0.41$). As the correlations were based on a subset of ordination scores that were obtained from the entire data set, the interpretation applied to the entire ordination space. The climate correlates were plotted in the ordination space as vectors (Fig. 3.3a). Overlaying deviation ellipsoids onto the smoothed ordination scores showed the degree of variation in the ordination space (Fig. 3.4).

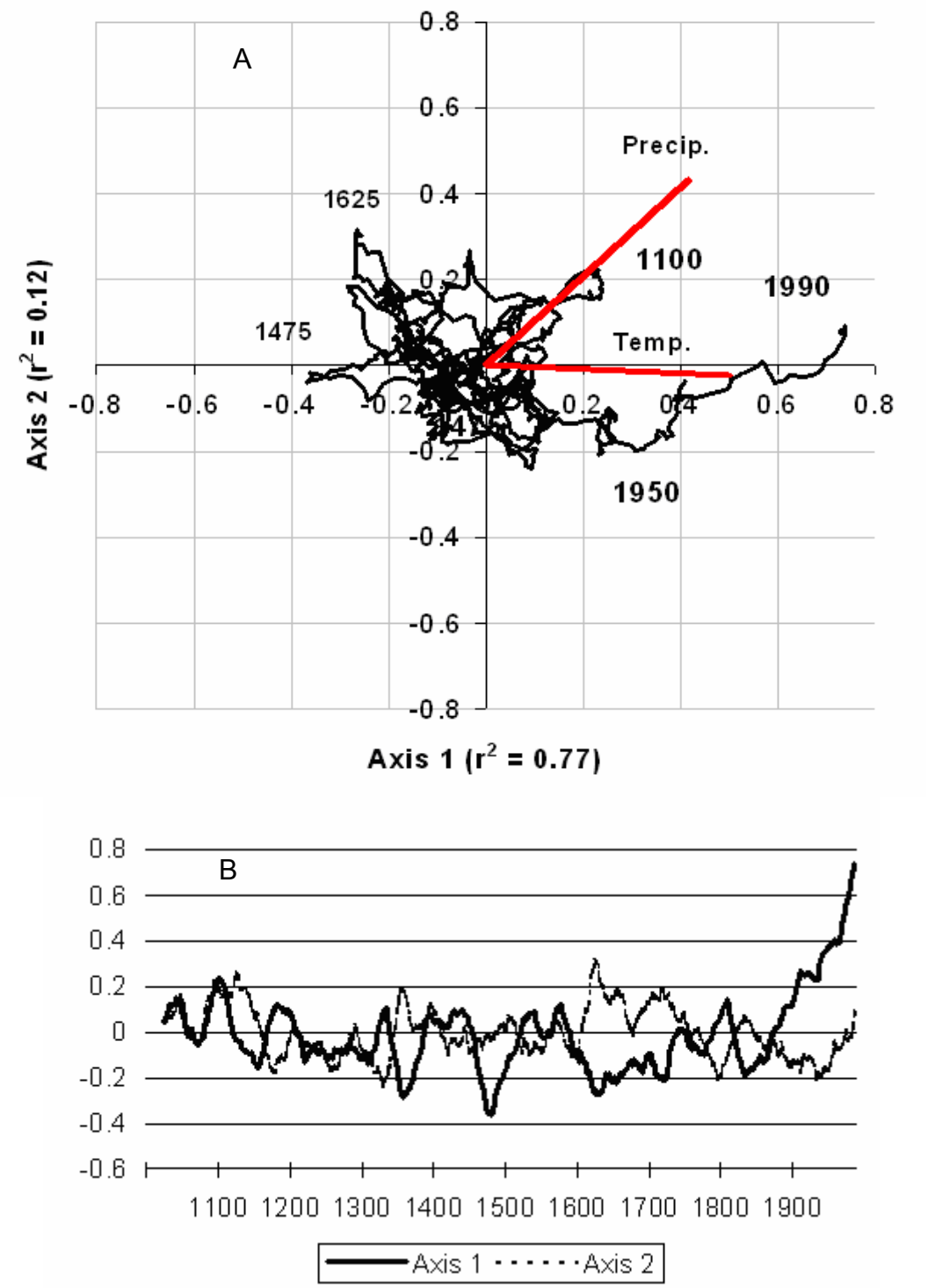

Fig. 3.3. A) Temporal vector of smoothed ordination scores (25-year running average) mapped onto ordination space. Labels have been inserted at several points. Temperature vectors are summer temperature and previous winter's precipitation derived from instrumental data. B) Time series plot of smoothed ordination scores (25-year running average).

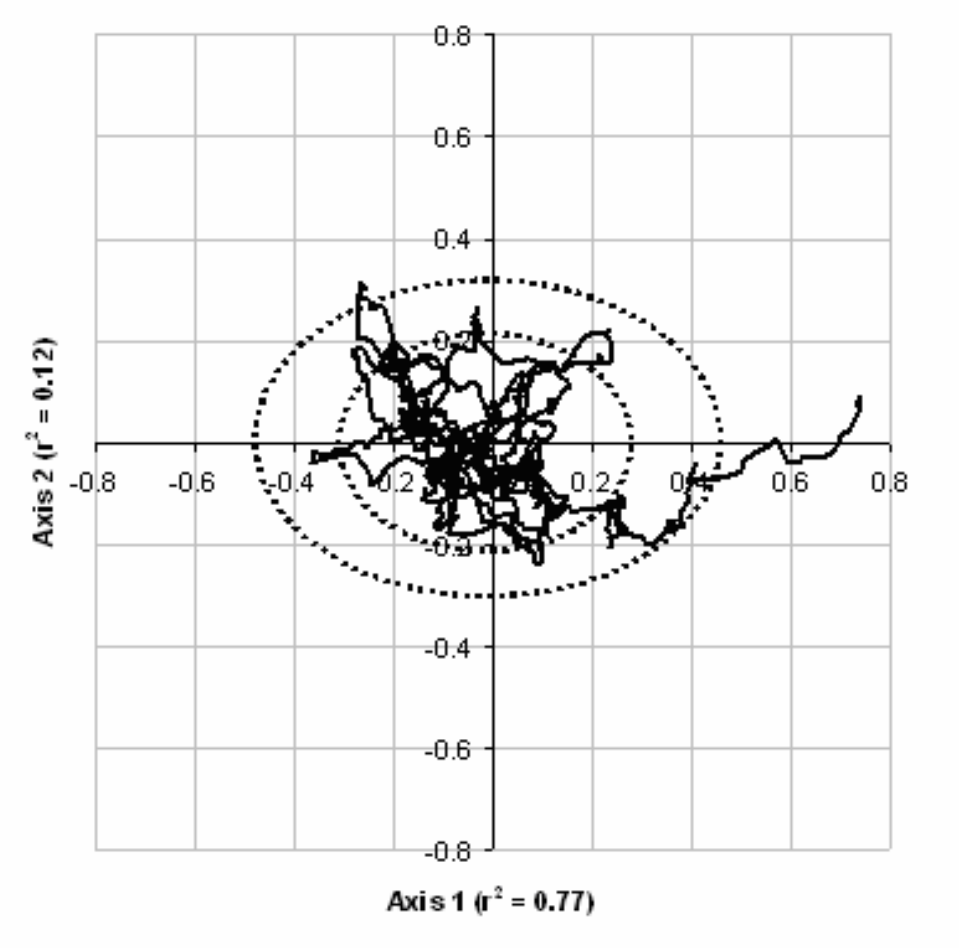

Fig. 3.4. Confidence ellipsoids of two and three standard deviations are superimposed onto the temporal vector of smoothed ordination scores shown in Figure 3.3.

We used cluster analysis to assess the degree to which multivariate patterns in tree growth define climate episodes. Five clusters were chosen that have not only distinctive patterns within the ordination space but also distinctive mean growth index values (Fig. 3.5). The period from AD 1050 to 1150 was defined by positive values on both axes, mapping into Cluster one (Fig. 3.5) and is characterized by growth rates slightly higher than average. We interpret this period as slightly warmer than the long-term average and analogous to the Medieval Climatic Anomaly (MCA) recognized in the Sierra Nevada

(Graumlich 1993; Stine 1994) and elsewhere (Briffa et al. 1992; Williams and Wigley 1983). A period from 1900-1950 is also mapped into this period. The next distinct period of anomalous growth extended from AD 1425 to 1500 and was defined by negative values on axis one. This period mapped into Cluster five with growth values below average. The period from AD 1600 to 1750 was defined by negative values on axis one and positive values of axis two and maps onto Cluster three with growth slightly below average. We interpret this period as colder and wetter relative to the long-term average, coincident with the initial phase of the Little Ice Age (LIA), as defined by widespread glacial advances (Grove 1988; Bradley and Jones 1992). While the MCA and LIA periods are known in many records (Mann et al. 1998; Bradley and Jones 1992; Lamb 1965; Hughes and Diaz 1994), the synchronicity and climatic interpretation of these periods is open to debate (Hughes and Diaz 1994). Finally, the second half of the twentieth century was also robustly indicated in ordination space with positive scores on axis one and mapping onto Cluster four with growth rates above the long-term average. This is the most easily interpretable period, mapping directly onto the temperature vector. Cluster two is located near the centroid of the ordination and shows growth rates near the average.

The weighted-averaging procedure allowed the different sites to be mapped into the ordination space (Fig. 3.6). The sites congregated very near the center of the space (as opposed to the edges), indicating that the multivariate signal shown in the ordination space was robust to site- and species-level differences. The fine-scale variation, however, showed the separation of sites based on species and relative landscape position. For

instance, bristlecone and the highest-elevation foxtail pine sites clustered along the positive segment of the first axis, indicating relative sensitivity to temperature. The site comprised of western juniper aligned on the precipitation vector along with a relatively low-elevation foxtail pine site (Timber Gap Lower). Timber Gap Lower and Hamilton are relatively more mesic sites than the others.

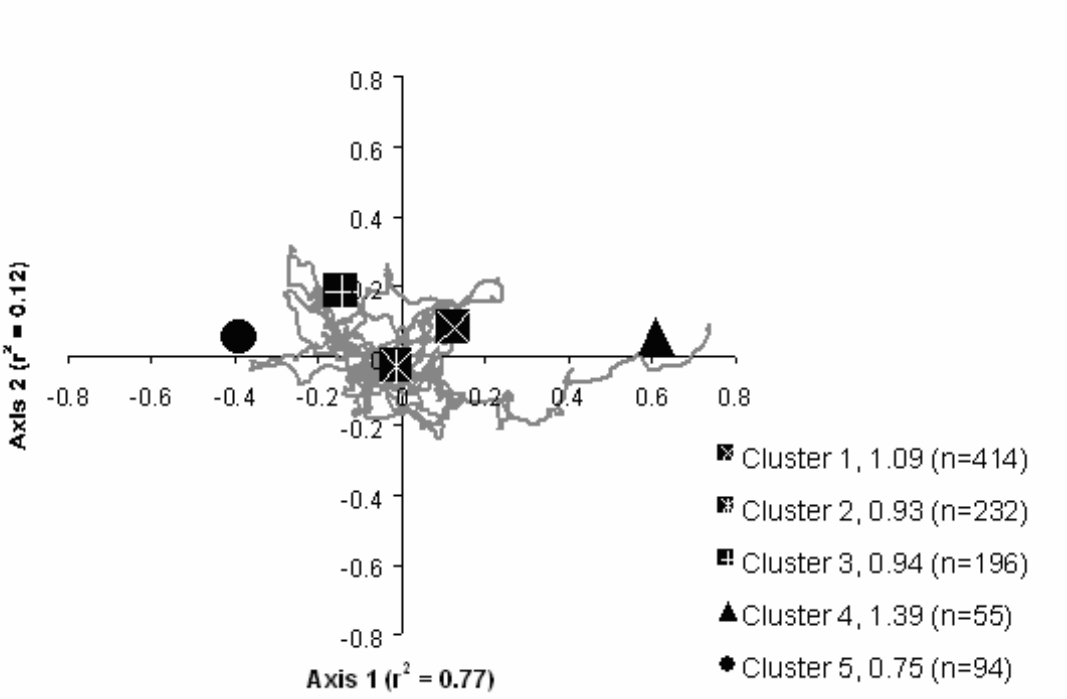

Fig. 3.5. Cluster centroids plotted in ordination space. The data were hierarchically assembled into five clusters and are outlined in ordination space in Fig. 3. The legend gives the cluster id, the mean growth index values, and the number of years in the cluster.

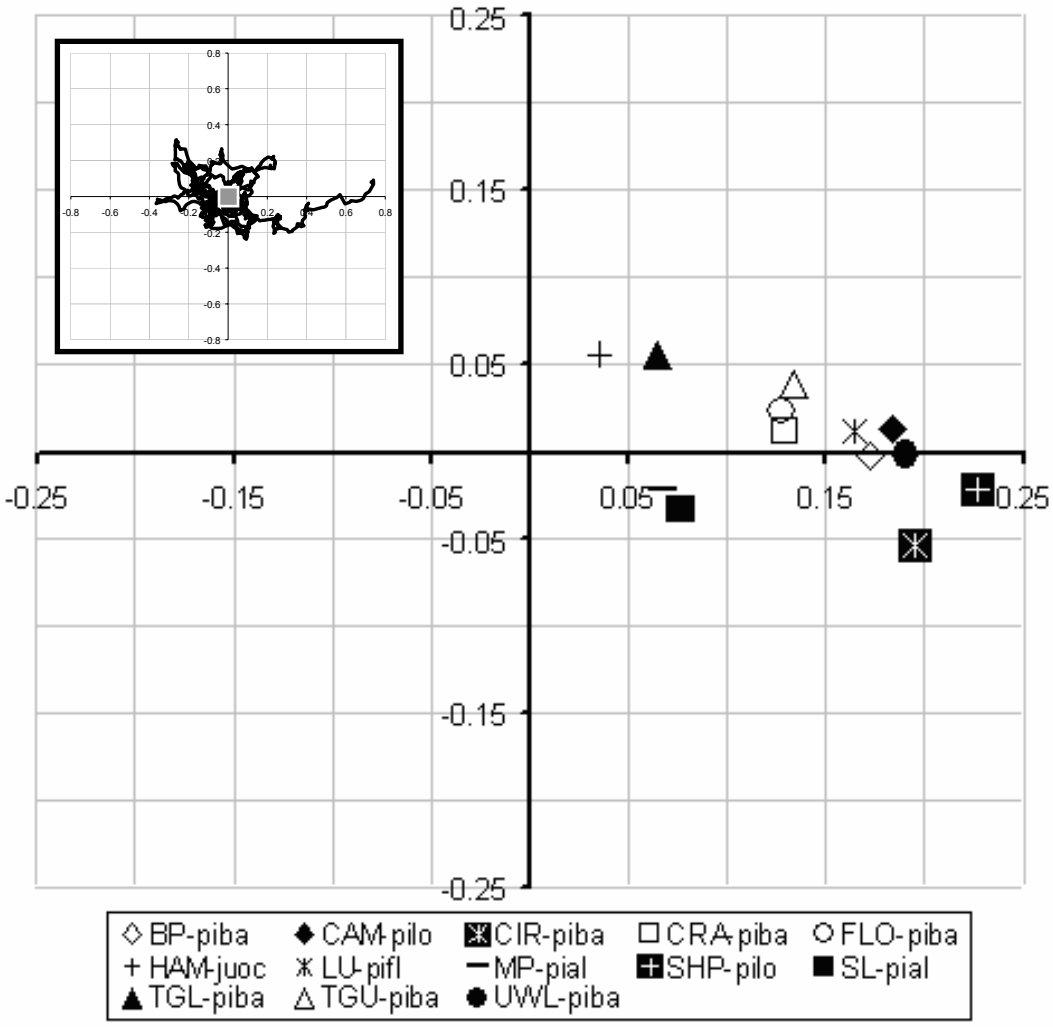

Fig. 3.6. Weighted average indicator scores for all 13 sites are plotted into the ordination space (The severe change in the scaling of the axis should be noted).

When the ordination scores were plotted as power spectra over frequency, two interesting patterns emerged (Fig. 3.7). The MTM spectrum for axis one showed significant variation from a red noise background at several time scales. The most striking was a long-term, secular trend. Significant signals on decadal and inter-annual El Nino-Southern Oscillation (ENSO) timescales were also present. The MTM spectrum for

axis two showed significant variation from a red noise background at several time scales. Again there was a long-term, secular trend although not as pronounced as in axis one. There were also significant signals on decadal and inter-annual ENSO-like timescales.

Discussion

Our 13 sites and five species significantly augment the existing North American tree-ring proxy indicator series (Mann et al. 1998; Mann et al. 1999) in two ways that enhance the interpretation of the record. First, our high elevation chronologies include three species not represented in previous work. In addition to foxtail pine (*Pinus balfouriana*) and bristlecone pine (*P. longaeva*), we contributed western juniper (*Juniperus occidentalis*), limber pine (*P. flexilis*), and whitebark pine (*P. albicaulis*). In cold and dry environments, multi-species networks can help decipher complex climate-growth relationships due to the tendency for species to respond to different climate variables (Graumlich 1993). For instance, junipers and foxtail pines have different water requirements and tolerate droughts differently (Stephenson 1990).

Second, the trees sampled by Graumlich do not exhibit strip-bark form (i.e., partial cambial dieback). Twentieth-century growth trends in strip-bark trees growing in moisture-stressed environments have been linked to a potential CO_2 fertilization effect, while entire-bark trees in similar sites do not exhibit anomalous trends (Graumlich 1991; Graybill and Idso 1993; Jacoby and D'Arrigo 1997; Bunn et al. 2003). Investigation of the multivariate signal with and without strip-bark trees showed no substantial differences between the chronologies (see below).

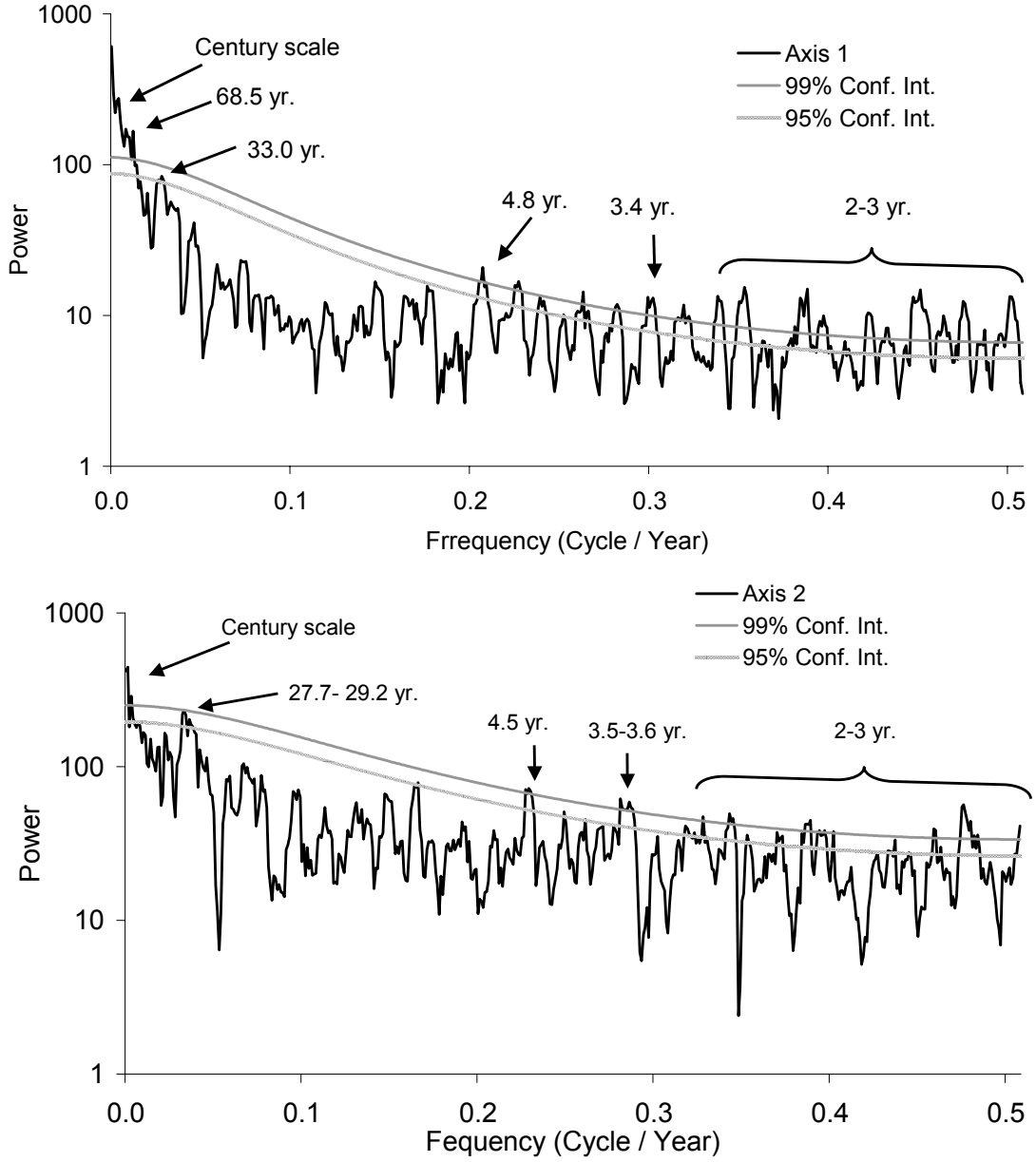

Fig. 3.7. Multitaper spectrum of signal for axis one and axis two plus 95% and 99% confidence intervals based on a robust estimate of a red noise background. Significant peaks are labeled by periodicity in years.

The complex inter-annual and decadal variability in tree-ring data makes visualizing simultaneous temporal trends difficult. By computing a running 25-year average of ordination scores, however, the temporal trends in ordination space could be readily interpreted (Fig. 3.3). Smoothing the data decreased the magnitude of the averaged ordination scores; they converged toward the centroid (Smith and Urban 1988). Nevertheless, the temporal variability was highly structured with distinct multi-decadal deviations from the centroid that have no analog in the record (Fig. 3.3). The ordination scores were not significantly different from a normal distribution. By plotting confidence ellipsoids, it could be seen that the growth rates of the last 50 years were more than three standard deviations higher than the mean over the last 1000 (Fig. 3.4).

The sites, shown as indicator scores in figure 3.6, were largely clumped in the center of the ordination space showing the overall coherence of the ordination. Differences among sites were slight, but ecologically interesting. Most obviously, the sites keyed on species, with the whitebark pine sites separating most distinctly. The bristlecone, limber, and foxtail pines (with the exception of TGL) grouped together in the ordination space despite significant geographic distances and whether the chronologies contained strip-barked trees. The Hamilton and lower Timber Gap sites grouped together despite being comprised of different species. We attributed this to the relatively low elevation of the TGL site. The low landscape position of this foxtail pine site indicated that it is likely more sensitive to precipitation variability (drought tolerance) and responds to climate more like the junipers at the Hamilton site (Graumlich 1993). Their position in ordination space aligned with the precipitation vector and provided more evidence of

similar sensitivities. The lack of clustering by the strip-bark chronologies implied that they are not showing a substantially different growth patterns than the entire-bark chronologies. This might suggest that chronologies built and standardized with some representation of strip-bark trees do not show CO_2 fertilization effects over chronologies without strip-bark trees. However, counter evidence for an enhanced growth response in individual strip bark trees has been shown (Tang et al. 2002; Bunn et al. 2003). Strip bark tree responses remain enigmatic and might depend on soil moisture in some microtopographic exposures (Bunn et al. 2003). Chronologies comprised of many trees cored at different locations are not likely to be affected by local extremes in physical setting because tree-ring chronologies give a mean growth response. It is also possible that variance associated with strip-bark tree growth was discarded in the ordination, which necessarily compresses information.

Axis one of the ordination was correlated to temperature. The MTM spectrum for axis one was consistent with a secular warming trend (Mann and Lees 1996). The long-term warming trend seen in this study is consistent with climate model predictions of the response to anthropogenic forcing of climate (Kuo and Thomson 1990; Mann et al. 1999). There were also some significant quasi-oscillatory components superimposed. The nature of these oscillations is consistent with internal dynamics of the climate system (Schlesinger and Ramankutty 1994; Mann and Lees 1996). Precipitation was correlated to axes one and two equally. The MTM spectrum for axis two was also consistent with a secular warming trend and showed some of the same periodicity of the MTM spectrum for axis one (Fig. 3.7). Particularly noticeable in light of axis two's correlation with

precipitation were the significant quasi-oscillatory components at ~28 years and the clear inter-annual ENSO-type variation. These periodicities are consistent with our current understanding of precipitation variability (e.g., Cayan et al. 1998; McCabe and Dettinger 1999; Dettinger et al. 1998; Biondi et al. 2001; Gedalof and Smith 2001).

The possibility that tree growth (e.g., annual rings) in natural environments has been fertilized by elevated atmospheric CO_2 in the last several decades of the twentieth century has been discussed in several dendroecological studies (e.g. LaMarche et al. 1984; Graumlich 1991; Briffa 1992; Graybill and Idso 1993; Nicolussi et al. 1995; Knapp et al. 2001). Most studies to date have been based on small networks of tree-ring sites. The most compelling evidence for CO_2 enhancement points to differential increases in water-use efficiency in strip-bark trees (Bunn et al. 2003) and in severely drought-stressed trees (Knapp et al. 2001). There is no consensus, however, on the presence or impact of CO_2 on growth; a review article on the subject states that there is inconclusive evidence to support CO_2 enhancement on tree growth in natural environments (Jacoby and D'Arrigo 1997). Given the potential for multiple interpretation of the growth signal in this dataset, however, we feel compelled to address this issue further.

The dramatic trend that is seen in the late twentieth century growth rates of the trees in this study is similar to that seen in other paleoclimate research, particularly the Mann-Bradley-Hughes (MBH) multiproxy reconstruction of northern hemisphere annual temperatures (Mann et al. 1998; 1999). By combining instrumental temperature data with multiple temperature-sensitive proxy records, the MBH reconstruction indicated that the 20th-century warming is abrupt and truly exceptional in the context of the last

millennium. Due to concerns about CO_2 fertilization effects, the reconstruction was rebuilt with a sparser dataset without tree-ring data (instead relying on historical instrumental, coral, and ice core records), and the authors verified that there was no bias due to non-climatic influences on their tree-ring datasets (Mann et al. 2000). Comprised mostly of high elevation tree-ring data, the MBH tree-ring data is similar to the data used in this study. As the MBH data shows no evidence of CO_2 fertilization in their high elevation tree growth data, we have no reason to suspect that the growth trends seen in this work are related to atmospheric CO_2 fertilization. Instead, it is our contention that the signals seen in this data are the result of climatic influence.

Our results support the emerging paradigm that the climate of the twentieth century was highly variable as compared to the last millennium. While our results strongly underscore our notions of how variable climate has been in the past, we also see clear evidence for a current trend that will exceed twentieth century variability. Specifically, our results indicated that these high-elevation conifers consistently demonstrated that modern growth trends had no analog in the last millennium and showed a correlation with increasing temperatures. This distinctive biological signature of unprecedented warming in the last millennium is important on two counts. First, it contributes further evidence to the growing body of data that indicate that physical systems (e.g., cryosphere) and ecosystems are changing in response to recent climate forcing and that our scientific challenges are shifting from detection to impact assessment. Second, our results support the long-held notion that high elevation ecosystems are likely to be among the first systems to register the impacts of global

climate change (e.g., Vale 1987; Henry and Molau 1997; Hansen et al. 2001) and, as such, offer particularly important opportunities for understanding the complexity of biotic response to climate change.

References

Barber V.A., Juday G.P. and Finney B.P. (2000) Reduced growth of Alaskan white spruce in the twentieth century from temperature-induced drought stress. *Nature* 405, 668-673

Biondi F., Cayan D.R. and Gershunov A. (2001) North pacific decadal climate variability since 1661. *Bulletin of the American Meteorology Society* 14, 5-9

Bradley R.S. and Jones P.D. (1992) *Climate since A.D. 1500*. Routledge, London, New York

Briffa K.R., Jones P.D., Bartholin T.S., Eckstein D., Schweingruber F.H., Karlen W., Zetteberg P. and Eronen M. (1992) Fennoscandian summers from A.D. 500: Temperature changes on short and long time scales. *Climate Dynamics* 7, 111-119

Briffa K.R. and Osborn T.J. (1999) Seeing the wood from the trees. *Science* 284, 926-927

Briffa, K.R. (1992) Increasing productivity of "natural growth"'conifers in Europe over the last century. Tree Rings And Eenvironment, Proceedings of the International Dendochronological Symposium, Ystad, South Sweden

Bunn A.G., Lawrence R.L., Bellante G.J., Waggoner L.A. and Graumlich L.J. (2003) Spatial variation in distribution and growth patterns of old growth strip-bark pines. *Arctic, Antarctic, and Alpine Research* 35, 323-330

Cayan D.R., Dettinger M.D., Diaz H.F. and Graham N.E. (1998) Decadal variability of precipitation over western North America. *Jounal of Climate* 11, 3148-3166

Clarke K.R. (1993) Non-parametric multivariate analyses of changes in community structure. *Australian Journal of Ecology* 18, 117-143

Crowley T.J. (2000) Causes of climate change over the past 1,000 years. Science 289, 270-277

Dettinger M.D., Cayan D.R., Diaz H.F. and Meko D. (1998) North-south precipitation patterns in western North America on interannual-to-decadal timescales. Journal of Climate 11, 3095-3111

Fritts H.C. (1976) Tree rings and climate. Academic Press, London, New York

Gabriel K.R. (1971) The biplot graphic display of matrices with application to principal component analysis. Biometrika 58, 453-467

Gedalof Z. and Smith D.J. (2001) Interdecadal climate variability and regime-scale shifts in Pacific North America. Geophysical Research Letters 28, 1515-1518

Graumlich L.J. (1991) Subalpine tree growth, climate, and increasing CO2: An assessment of recent growth trends. Ecology 72, 1-11

Graumlich L.J. (1993) A 1000-year record of temperature and precipitation in the Sierra Nevada. Quaternary Research 39, 249-255

Graybill, D.A. (1987) Cirque Peak tree-ring chronology, data contribution series CPF729. Holdings of the International Tree-Ring Data Bank. IGBP PAGES/World Data Center for Paleoclimatology, NOAA/NGDC Paleoclimatology Program, Boulder, CO

Graybill, D.A. (1987) Flower Lake tree-ring chronology, data contribution series FLF729. Holdings of the International Tree-Ring Data Bank. IGBP

PAGES/World Data Center for Paleoclimatology, NOAA/NGDC Paleoclimatology Program, Boulder, CO

Graybill, D.A. (1987) Timber Gap lower tree-ring chronology, data contribution series TGL729. Holdings of the International Tree-Ring Data Bank. IGBP PAGES/World Data Center for Paleoclimatology, NOAA/NGDC Paleoclimatology Program, Boulder, CO

Graybill, D.A. (1987) Timber Gap upper tree-ring chronology, data contribution series TGU729. Holdings of the International Tree-Ring Data Bank. IGBP PAGES/World Data Center for Paleoclimatology, NOAA/NGDC Paleoclimatology Program, Boulder, CO

Graybill, D.A. (1990) Sheep Mountain tree-ring chronology, data contribution series SHP519. Holdings of the International Tree-Ring Data Bank. IGBP PAGES/World Data Center for Paleoclimatology, NOAA/NGDC Paleoclimatology Program, Boulder, CO

Graybill D.A. and Idso S.B. (1993) Detecting the aerial fertilization effect of atmospheric CO2 enrichment in tree-ring chronologies. Global Biogeochemical Cycles 7, 81-95

Graybill, D.A. and LaMarche Jr., V.C. (1983) Campito Mountain tree-ring chronology, data contribution series CAM519. Holdings of the International Tree-Ring Data Bank. IGBP PAGES/World Data Center for Paleoclimatology, NOAA/NGDC Paleoclimatology Program, Boulder, CO

Grove J.M. (1988) The Little Ice Age. Methuen, London, New York

Hansen A.J., Neilson R.R., Dale V.H., Flather C.H., Iverson L.R., Currie D.J., Shafer S., Cook R. and Bartlein P.J. (2001) Global change in forests: Responses of species, communities, and biomes. Bioscience 51, 765-779

Henry G.H.R. and Molau U. (1997) Tundra plants and climate change: the International Tundra Experiment (ITEX). Global Change Biology 3 (Supplement 1), 1-10

Hughes M.K. and Diaz H.F. (1994) Was there a 'Medieval Warm Period' and if so, where and when? Climatic Change 26, 109-142

Hughes M.K. and Graumlich L.J. (1996) Multimillennial dendroclimatic studies from the western United States. In: Climatic Variations and Forcing Mechanisms of the Last 2000 Years (eds Jones P.D., Bradley R.S. and Jouzel J.), pp. 109-124. Springer-Verlag, Berlin

Jacoby G.C. and D'Arrigo R.D. Tree rings, carbon dioxide, and climatic change. Proceedings of the National Academy of Sciences 94, 8350-8353. 1997.

Jongman R.H.G., ter Braak C.J.F. and van Tongeren O.F.R. (1995) Data analysis in community and landscape ecology. Cambridge University Press, Cambridge

Kaiser H.F. (1958) The varimax criterion for analytic rotation in factor analysis. Psychometrika 23, 187-200

Knapp P.A., Soule P.T. and Grissino-Mayer H.D. (2001) Detecting potential regional effects of increased atmospheric CO2 on growth rates of western juniper. Global Change Biology 7, 903-917

Kruskal J.B. (1964) Multidimensional scaling by optimizing goodness of fit to a nonmetric hypothesis. Psychrometrika 28, 1-27

Kruskal J.B. and Wish M. (1978) Multidimensional Scaling. Sage Publications, Beverly Hills

Kuo C., Lindberg C. and Thomson D.J. (1990) Coherence established between atmospheric carbon dioxide and global temperature. Nature 343, 709-713

LaMarche Jr.V.C. (1974) Paleoclimatic inferences from long tree-ring records. Science 183, 1043-1048

LaMarche Jr.V.C., Graybill D.A., Fritts H.C. and Rose M.R. (1984) Increasing atmospheric carbon dioxide: tree ring evidence for growth enhancement in natural vegetation. Science 225, 1019-1021

Lamb H.H. (1965) The early medieval warm epoch and its sequel. Palaeogeography, Palaeoclimatology, Palaeoecology 1, 13-37

Legendre P. and Legendre L. (1998) Numerical ecology, 2nd edn. Elsevier, Amsterdam, New York

Mann M.E., Bradley R.S. and Hughes M.K. (1999) Northern hemisphere temperatures during the past millennium: inferences, uncertainties, and limitations. Geophysical Research Letters 26, 759-762

Mann M.E., Gille E., Bradley R.S., Hughes M.K., Overpeck J.T., Keimig F.T. and Gross W. (2000) Global temperature patterns in past centuries: An interactive presentation. Earth Interactions 4, 1-29

Mann M.E., Bradley R.S. and Hughes M.K. (1998) Global-scale temperature patterns and climate forcing over the past six centuries. Nature 392, 779-787

Mann M.E. and Lees J.M. (1996) Robust estimation of background noise and signal detection in climatic time series. Climatic Change 33, 409-445

McCabe G.J. and Dettinger M.D. (1999) Decadal variations in the strength of ENSO teleconnections with precipitation in the western United States. International Journal of Climatology 19, 1399-1410

McCune B. and Mfford M.J. (1999) PC-ORD: Multivariate analysis of ecological data. MjM Software Design, Gleneden Beach, Oregon

Mielke P.W. (1991) The application of multivariate permutation methods based on distance functions in the earth sciences. Earth-Science Reviews 31, 55-71

Nicolussi K., Bortenschlager S. and Körner C. (1995) Increase in tree-ring width in subalpine Pinus cembra from the central Alps that may be CO2-related. Trees 9,

Oberhuber W. and Kofler W. (2000) Topographic influences on radial growth of Scots pine (Pinus sylvestris L.) at small spatial scales. Plant Ecology 146, 231-240

Schlesinger M.E. and Ramankutty N. An oscillation in the global climate system of period 65-70 years. Nature 367, 723-726. 1994.

Scuderi L.A. (1993) A 2000-year tree ring record of annual temperatures in the Sierra Nevada Mountains. Science 259, 1433-1436

Smith T. and Urban D.L. Scale and resolution of forest structural pattern. Vegetatio 74, 143-150

Stahle D.W., Cook E.R., Cleaveland M.K., Therrell M.D., Meko D.M., Grissino-Mayer H.D., Watson E. and Luckman B.H. (2000) Tree-ring data document 16th century

megadrought over North America. EOS, Transactions, American Geophysical Union 81, 121-125

Stephenson N.L. (1990) Climatic control of vegetation distribution: The role of the water balance. The American Naturalist 135, 649-670

Stine S. (1994) Extreme and persistent drought in California and Patagonia during Medieval time. Nature 369, 546-549

Stokes M.A. and Smiley T.L. (1968) An Introduction to Tree Ring Dating. The University of Chicago Press, Chicago

Tang K., Feng X. and Funkhouser G. (1999) The □13C of tree rings in full-bark and strip-bark bristlecone pine trees in the White Mountains of California. Global Change Biology 5, 33-40

Vale T.R. (1987) Vegetation change and park purposes in the high elevations of Yosemite National Park, California. Annals of the Association of American Geographers 77, 1-18

Ward J.H. (1963) Hierarchical grouping to optimize an objective function. Journal of the American Statistical Association 58, 236-244

Whittaker R.H. (1967) Gradient analysis of vegetation. Biological Review 49, 207-264

Williams L.D. and Wigley T.M.L. (1983) A comparison of evidence for late Holocene summer temperature variations in the Northern Hemisphere. Quaternary Research 20, 286-307

CHAPTER 4

TOPOGRAPHIC MEDIATION OF GROWTH OF SUBALPINE FORESTS IN THE SIERRA NEVADA, USA

Introduction

Observational and paleoclimatological studies of the earth's climate indicate that the Northern Hemisphere warmed substantially during the 20th century (Mann et al. 1998; 1999; IPCC 2001), and there is scientific consensus that recent warming is anthropogenic in nature. Changes in precipitation during the 20th century and its impacts on ecosystems remain more uncertain (Walsh et al., 1998; Kattsov and Walsh 2000; IPCC, 2001). It is evident, however, that precipitation is an important mediator of forest dynamics not only in deserts but also in cold, semi-arid environments (Barber et al., 2000). Given the impact of slowly evolving ocean-atmosphere interactions in governing precipitation at decadal and longer time scales (Latif and Barnett, 1994; Mantua et al., 1997; Minobe, 1997; 1999; Zhang et al., 1997; Bond and Harrison, 2000), there is a clear need to develop long-term (i.e., multi-century) ecological records that can disaggregate the interactions between temperature and precipitation in governing ecosystem processes. Interest in disentangling the role of temperature and precipitation in the context of forest dynamics is also driven by questions that arise in tracking the carbon cycle as evidence accumulates that 20th century carbon accumulation in dry montane forests has profound implications for local to global carbon calculations (Schimel et al., 2002).

We addressed these issues by developing long-term records of tree growth and stem recruitment from alpine treeline environments in the Sierra Nevada, USA. Our focus on alpine treeline reflects, in part, the traditional notion that alpine and arctic ecosystems will be critical ecosystems for detecting and characterizing climate change (Billings and Bliss, 1959; Walker et al., 1993; 1994; Henry and Molau, 1997). Further, alpine treeline is a particularly rich system to investigate long-term dynamics due to the abundance of high-resolution paleoecological records. Long-duration time series associated with subalpine forest, particularly in western North America, are widespread spatially, climatically sensitive, and annually resolved (Graumlich et al., 2004). While tree growth at alpine treeline is primarily temperature limited (Wardle, 1971; Wardle, 1974), precipitation plays a strong role in patterning alpine treeline (Lloyd and Graumlich, 1997). Changes in temperature and the length of the growing season, in concert with precipitation variability are predicted to have substantial impacts on growth and forest pattern (Scuderi, 1993; Cairns, 1998). Furthermore, chronologies of tree-rings from long-lived conifers at or near alpine treeline in western North America have greatly informed the state-of-knowledge of natural and anthropogenic climate change over the last millennium (LaMarche, 1974; Scuderi, 1993; Mann et al., 1998; 1999; Crowley, 2000). The combination of a rich paleoclimatic record with a dynamic ecosystem has made alpine treeline an attractive system to monitor for assessing the impacts of global climate change and an important area for natural resource management (Vale, 1987).

The Sierra Nevada is typical of alpine environments in that rugged topography creates steep ecological gradients (Urban et al., 2000). We focused on the physical abiotic

template as a mediator of subalpine forest structure in this paper. Although alpine trees are generally considered limited by climate and therefore good recorders of past climate (Graumlich et al., 2004), there is not a body of literature that incorporates the effect of biophysical setting at the scale of relatively small plots (< 1 ha) in determining treeline forest structure, ring-width patterns, and subsequent climate inference. A notable exception is Villalba et al. (1994), who showed the importance of topography in understanding species-specific response to climate in the Colorado Front Range.

Foxtail pine presents a rare opportunity to further understanding of the effects of rugged topographic for a single species. Foxtail pine is a rare plant that occurs in two disjunct areas, one in the Sierra Nevada near Sequoia National Park and another about 500 km to the north in the Klamath mountains (Mastroguiseppe and Mastroguiseppe, 1980). Geographically separated in the early Pleistocene (Bailey, 1970), foxtail pine inhabits a very narrow biogeographic niche near alpine treeline where growth and reproduction are ostensibly limited by growing season temperature. Borrowing techniques and understanding from landscape ecology, we hypothesized that the physical template of the landscape ameliorates forest structure and annual growth (i.e., tree-ring) pattern in two sites in the southern range of the species. Examining the associations between proxies for soil moisture and radiation and age class, seedling recruitment, and ring-width patterns in foxtail pine forests allowed us to demonstrate the impact of topography in growth and recruitment. We paid particular attention to the potential for temperature induced water stress to limit the tree growth and affect demography in especially dry locations. This study provides a glimpse into the spatial heterogeneity of

treeline forests in the Sierra Nevada and shows the need to account for the physical template, as well as demonstrating methods to wed a priori geographic information system (GIS) modeling to sampling schemes, monitoring protocols, and process modeling as a way of detecting and understanding change.

Methods

With elevations above 3000 m a.s.l. and slope gradients routinely in excess of 20%, the treeline ecotone of the eastern Sierra Nevada crest is both remote and extremely rugged. Given the difficulties of logistics and expense involved in transporting personnel and equipment to these backcountry field sites, we partitioned the treeline ecosystem in Sequoia National Park into manageable study units using GIS models (Urban, 2000). These models were based on topographic features most likely to influence tree growth: radiation and soil moisture. This allowed the sampling of eight plots at two sites to be done over the course of the summer field season in 2001, providing data in disparate biophysical settings.

Study Area

The study was conducted on the eastern crest of the Sierra Nevada in Sequoia National Park at the alpine treeline (elev. ca. 3300 m a.s.l.). Two study areas dominated by foxtail pine (Pinus balfouriana Grev. et Balf.) were chosen in the vicinity of Rock Creek and Mt. Tyndall (Fig. 4.1). The regional distribution of subalpine forests is variable with trees absent from cooler microsites, some valley bottoms, and extremely steep slopes. Foxtail pine does not grow in a dwarfed krummholz form and therefore

treeline tends to be an abrupt transition from forest to non-forest, making sampling of this treeline forest straightforward. Foxtail pine is an extremely long-lived species (a 1200-year old specimen was found in this study) and the pattern of its annual growth rings has been found to be sensitive to climate and used in numerous paleoclimatic studies (Scuderi, 1987; Graumlich, 1991; Caprio and Baisan, 1992; Graumlich, 1993; Scuderi, 1993; Lloyd and Graumlich, 1997).

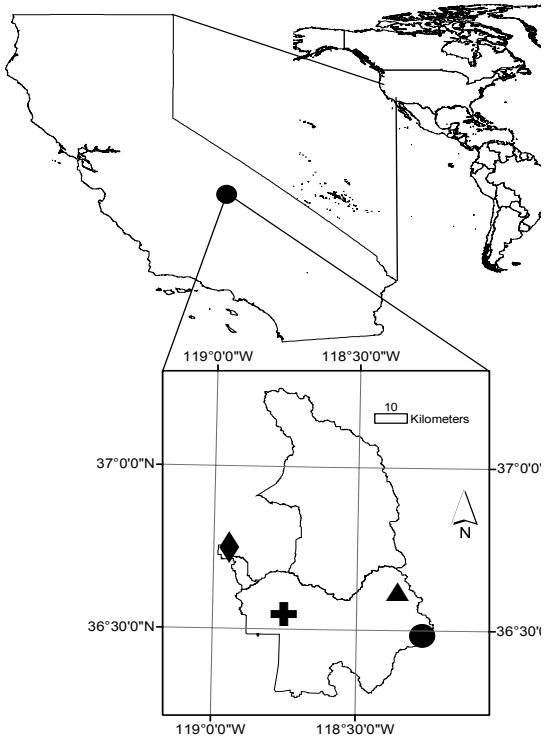

Fig. 4.1. Study areas in Sequoia and Kings Canyon National Parks, California USA are shown with a circle (Rock Creek) and a triangle (Mt. Tyndall). Weather stations used for climate growth correlations are shown with a cross (Giant Forest) and a diamond (Grant Grove).

Site Selection

A 10 m digital elevation model (DEM) was obtained from the National Park Service for Sequoia National Park (http://www.nps.gov/gis). Spurious sinks were filled to remove data anomalies according to standard GIS procedures (Jenson and Domingue, 1988) using ArcInfo 8.2 (ESRI, 2002). Topographic convergence and potential relative radiation were calculated from the DEM. Topographic convergence index (TCI), a function of upslope contributing area and local slope, measured the tendency of water to collect on the landscape (Moore et al., 1991; Urban et al., 2000; Bunn et al., 2003). The index has high values in coves or streambeds and lower values on drained areas such as ridge tops. The potential relative radiation (PRR) index utilizes measurements of the sun position over the course of a year and a shading function common to most GIS packages to measure the relative amount of sunlight that a particular raster element received given the shading that its neighborhood provided (Bunn et al., 2003).

The top and bottom quartile for each index was calculated. Combining them pairwise resulted in 10 m cells that have high radiation and high convergence, high radiation and low convergence, low radiation and high convergence, or low radiation and low convergence. A map was produced of these cells and overlaid onto 1 m color infrared digital orthophotos where treeline was easily discernable. The Rock Creek (3300 m a.s.l.) and Mt. Tyndall (3390 m a.s.l.) areas were chosen for previous dendroclimatological research done in the area (Graumlich, 1991; Graumlich, 1993; Lloyd and Graumlich, 1997) and proximity to trail heads (~10 km and 25 km, respectively). Study plots were randomly placed within the domain of possible sites using this map and the Global

Positioning System. Four plots 90 m by 90 m were chosen at each site at treeline that were high radiation and high convergence, high radiation and low convergence, low radiation and high convergence, and low radiation and low convergence. Plots were divided into nine, 30 m by 30 m subplots to facilitate data collection and analyses.

Forest Demographic and Time Series Data

In each of the eight plots (four plots at two sites) every stem was tallied. This allowed direct comparison of stem density to biophysical setting. An increment core was taken at breast height for trees with diameters at breast height (DBH = 1.37 m) > 2 cm to explore the temporal pattern of stem establishment as well as growth-climate relationships. Cores were taken parallel to the slope contour to minimize the effects of slope pressure on wood formation. All smaller stems were tallied, and for the purposes of this study stems with diameters < 2 cm at breast height were designated as immature stems. Although these forests are almost entirely foxtail pine stands, a small proportion (<10%) of the trees on the plots were either lodgeople pine (Pinus contorta Dougl. ex Loud) or whitebark pine (Pinus albicaulis Engelm.). These trees tended to be at the lowest elevation of the plots. There was no relationship between species composition and plot type and the small proportion of these trees precluded dendrochronological analysis. They were therefore omitted from all analysis.

The cores were mounted, sanded, and measured using standard dendrochronological procedures (Stokes and Smiley, 1968). Samples were cross-dated using with the program COHECHA (Holmes, 1983) and through visual examination of the rings to assign an exact calendar date to each ring. Existing foxtail pine chronologies

developed at near-by sites were utilized to assist in cross dating (Graumlich, unpublished data). The chronologies were created by standardizing ring-width measurements by fitting negative exponential curves or horizontal lines to the ring-width measurements. The standardized ring-width indices were then averaged to obtain mean chronologies at each site (Fritts, 1976). Although all foxtail pine stems > 2 cm DBH were cored to examine age class distribution, only series greater than one hundred years in length were included in the eight chronologies.

To study climate-growth patterns, monthly temperature and precipitation measurements from 1927 to 2000 were obtained by updating the composite data used by Graumlich (1993) from Giant Forest (1927-1968, 36° 34′ N, 118° 46′ W, 1940 m a.s.l.) and Grant Grove (1944-2000, 36° 46′ N, 118° 58′ W, 2005 m a.s.l.). We created two seasonal variables: summer temperature (mean June–August) and growing year precipitation (total of prior September– current August). Because all of the chronologies had highly significant first-order autocorrelation, climate-growth analyses were conducted for the calendar year prior to the growing season (i.e., a lag of one year). We used Pearson's product-moment correlation coefficients to describe the relationship between tree growth and climate by subsetting the chronologies to the period of instrumental climate.

The temporal variance structure of the chronologies was evaluated with wavelet analysis. Wavelets are versatile tools of harmonic analysis that partition time series data into frequency components and then characterize the variance in each component with a resolution matched to its scale. They have advantages over traditional signal detection

methods (e.g., Fourier and spectral analyses) in analyzing data where the signal contains sharp spikes (Torrence and Compo, 1998). We performed a continuous wavelet transformation of the tree-ring chronologies using the non-orthogonal Morlet wavelet. The Morlet wavelet has been used successfully with tree-ring data to detect periodic patterns that might be driven by climate oscillations (Gray et al., 2003). Transforms were done in the statistical software package R (Ihaka and Gentleman 1996) with the Rwave contributed package (Carmona et al., 1998; Carmona and Whitcher, 2002). Peaks in the wavelet power spectra were tested against a red-noise background assumption (a univariate lag-1 autoregressive AR [1] model of 0.70) using the methods of Torrence and Compo (1998). The hypothesis was that peaks in the tree-ring wavelet power spectra that were significantly above the background spectrum were true features (Torrence and Compo, 1998).

Results

The temporal pattern of stem recruitment, as reflected in the age-class structure of the plots, varied between sites and with biophysical setting (Table 4.1, Fig. 4.2). The high convergence, high radiation (bright and wet) sites showed a higher proportion of successful recruitment events after 1900 that was significantly greater than proportions of a bootstrapped uniform age-class distribution (*p-value* ≤ 0.0001). The dark and dry sites, conversely, showed the lowest proportion of recruitment events after 1900 that was significantly less than proportions of a bootstrapped uniform age-class distribution ($p = 0.0047$ and $p = 0.0437$ for Rock Creek and Mt. Tyndall, respectively). With the exception

that the dark and dry sites had fewer stems than the other plots, neither the number of adult stems (Fig. 4.2) nor the number of immature stems per ha (Table 4.2) showed a coherent pattern between sites.

Annual tree growth, as reflected in the chronologies, showed patterns of within site variability and between site coherence that reflected topographic mediation of synoptic-scale climate forcings (Fig. 4.3). Still, there were obvious temporal differences within the sites. The high radiation and high convergence plot at Rock Creek, for instance, showed less variation in year to year growth than the dark and dry site (Fig. 4.3). There was a similar pattern for Mt. Tyndall. The differences between sites were further reflected in their correlations with instrumental climate (Table 4.3). Specifically, the high convergence sites had stronger correlation with temperature while the low convergence sites had stronger correlation with precipitation.

Table 4.1. The percentage of stems successfully recruited after 1900 is greatest in the bright and wet plots and lowest in the dark and dry plots. This pattern is evident at both sites and significantly different than a random expectation using 10,000 bootstrapped replications of a random age-class distribution (compare to Fig. 4.2).

	Percentage of Stems Recruited After 1900 A.D.	
	Rock Creek	Mt. Tyndall
High Radiation, High Convergence	59% (n = 64) *$p < 0.0001$*	56% (n = 55) *$p < 0.0001$*
High Radiation, Low Convergence	10% (n = 72) *NS*	22% (n = 69) *NS*
Low Radiation, High Convergence	12% (n = 41) *NS*	17% (n = 48) *NS*
Low Radiation, Low Convergence	6% (n = 63) *$p = 0.0047$*	10% (n = 78) *$p = 0.0434$*

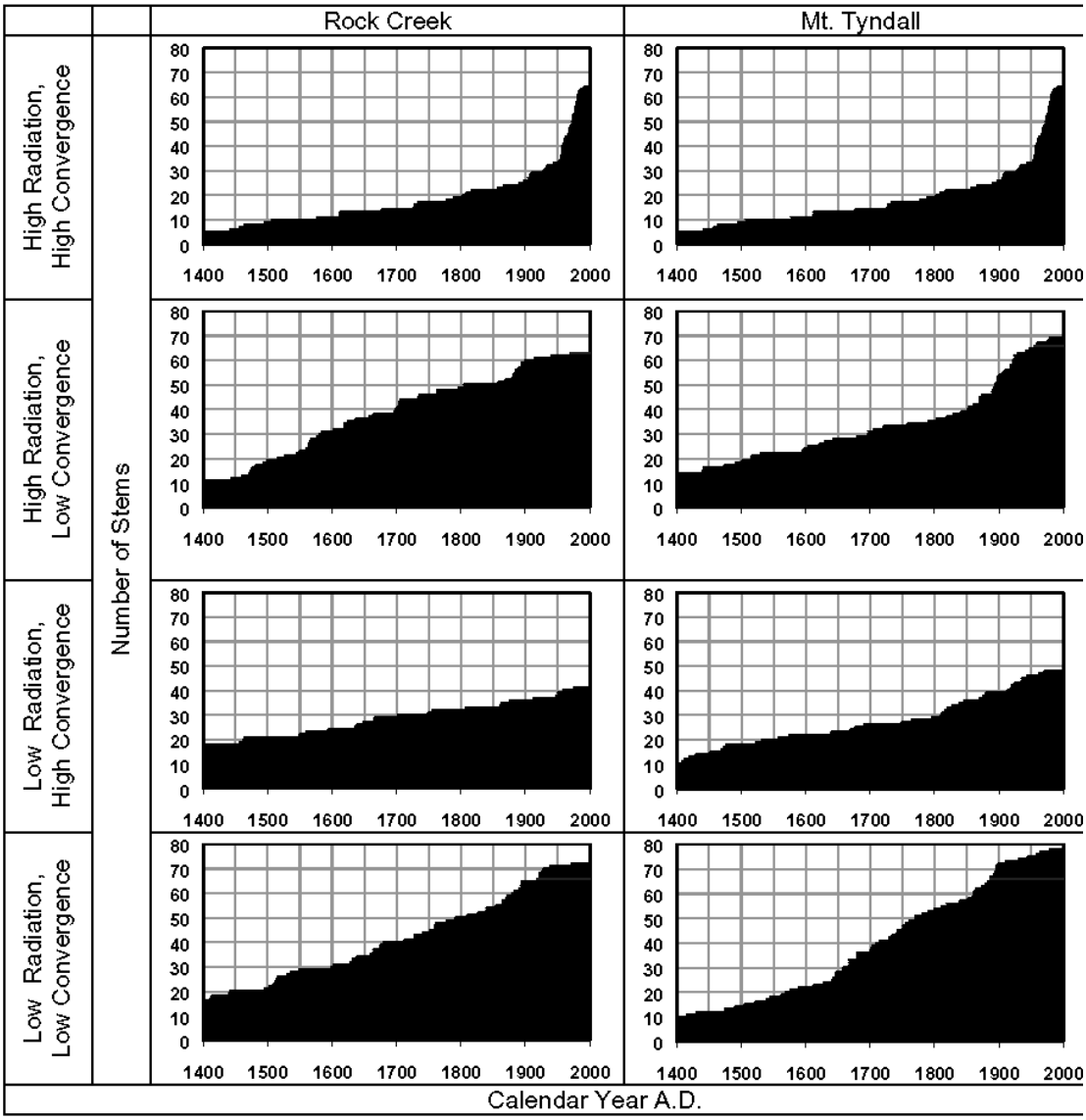

Fig. 4.2. The age-class structure for all eight plots shows similarities between sites. The most obvious similarity is between the high radiation and high convergence sites which show a high proportion of stems successfully recruited after 1900 A.D. The low radiation and low convergence site show the lowest percentage of recruitment after 1900 A.D. (compare to Table 1).

The modes of variability embedded in the chronologies similarly showed within and between site variability (Fig. 4.4). While all eight sites showed secular (i.e., series length) and high frequency (i.e., 2-4 year) periodicities, only the low convergence sites

showed significant variation at the scale of multiple decades. These periodicities were statistically significant as compared to a red-noise background.

Table 4.2. The number of immature stems per ha in the plots does not show coherence within or between sites. One standard error of the sample is shown in parenthesis.

	Immature stems per ha	
	Rock Creek	Mt. Tyndall
High Radiation, High Convergence	67 (20)	78 (16)
High Radiation, Low Convergence	65 (70)	42 (15)
Low Radiation, High Convergence	27 (20)	241 (51)
Low Radiation, Low Convergence	289 (61)	102 (46)

Discussion

Paleoecological research has demonstrated the interaction of multiple climate factors on vegetation dynamics at times scales from years to centuries (Brubaker, 1986; Delcourt and Delcourt, 1987; Graumlich, 1993; Lloyd and Fastie, 2002). Similarly, gradient analysis (the study of species or ecosystems along continua of physical conditions) has a long and influential history from Merriam (1898) to the classic studies by Whittaker (1956; 1967), and Peet (1978), and has demonstrated the importance of multiple limiting factors on community development (Urban et al., 2002). Finally, the influence of spatial scale on observed pattern is increasingly well understood (Urban et al., 1987; Levin,

1992; Turner et al., 2001). Our results emphasized these three ecological tenets for a single species of tree in the Sierra Nevada of California. Specifically, we found that biophysical position of ~1 ha stands of foxtail pine dictated the age-class structure of the stand and the climate-growth relationship. The effect of the topographic position in tree response to climate has been documented elsewhere (Villalba et al., 1994) and is supported by these results.

Our study comprised four types of biophysical setting at two sites. The expense of collecting and analyzing the data in this study was not trivial. We would need many more replicates to make strong statistical inference about the consistency of the patterns we noticed among and between sites. Although we were unable to make strong deductive inference about these results because of the low sample size, we are gratified to see similar qualitative patterns between the sites.

In this study, we attempted to parcel out the variance in two of the most critical abiotic influences on plant growth, soil moisture and radiation, across a rugged alpine landscape. Soil moisture, as represented by topographic convergence, was the most critical variable for determining fine-scale patterns in climate-growth relations, while the role of the radiation index was less clear. Using temperature loggers and soil moisture probes, PRR and TCI predictions can improve estimates of soil water supply/demand (Lookingbill and Urban, 2003; Lookingbill and Urban, 2004) and the ability to account for species distribution (Stephenson, 1990; Urban et al., 2000), but these results were not as obviously expressed in our data.

Table 4.3. Correlations between the chronologies with instrumental climate records from Sequoia National Park (1908-2000) show coherence between and among sites. Temperature is mean previous summer (June through August) temperature and precipitation is the total precipitation from the previous year (September–August).

		Temperature	Site Rank	Precipitation	Site Rank
Rock Creek	High Radiation, High Convergence	0.326	1	0.334	4
	High Radiation, Low Convergence	0.208	4	0.534	2
	Low Radiation, High Convergence	0.311	2	0.480	3
	Low Radiation, Low Convergence	0.254	3	0.552	1
Mt. Tyndall	High Radiation, High Convergence	0.480	1	0.440	4
	High Radiation, Low Convergence	0.238	3	0.564	2
	Low Radiation, High Convergence	0.359	2	0.503	3
	Low Radiation, Low Convergence	0.190	4	0.602	1

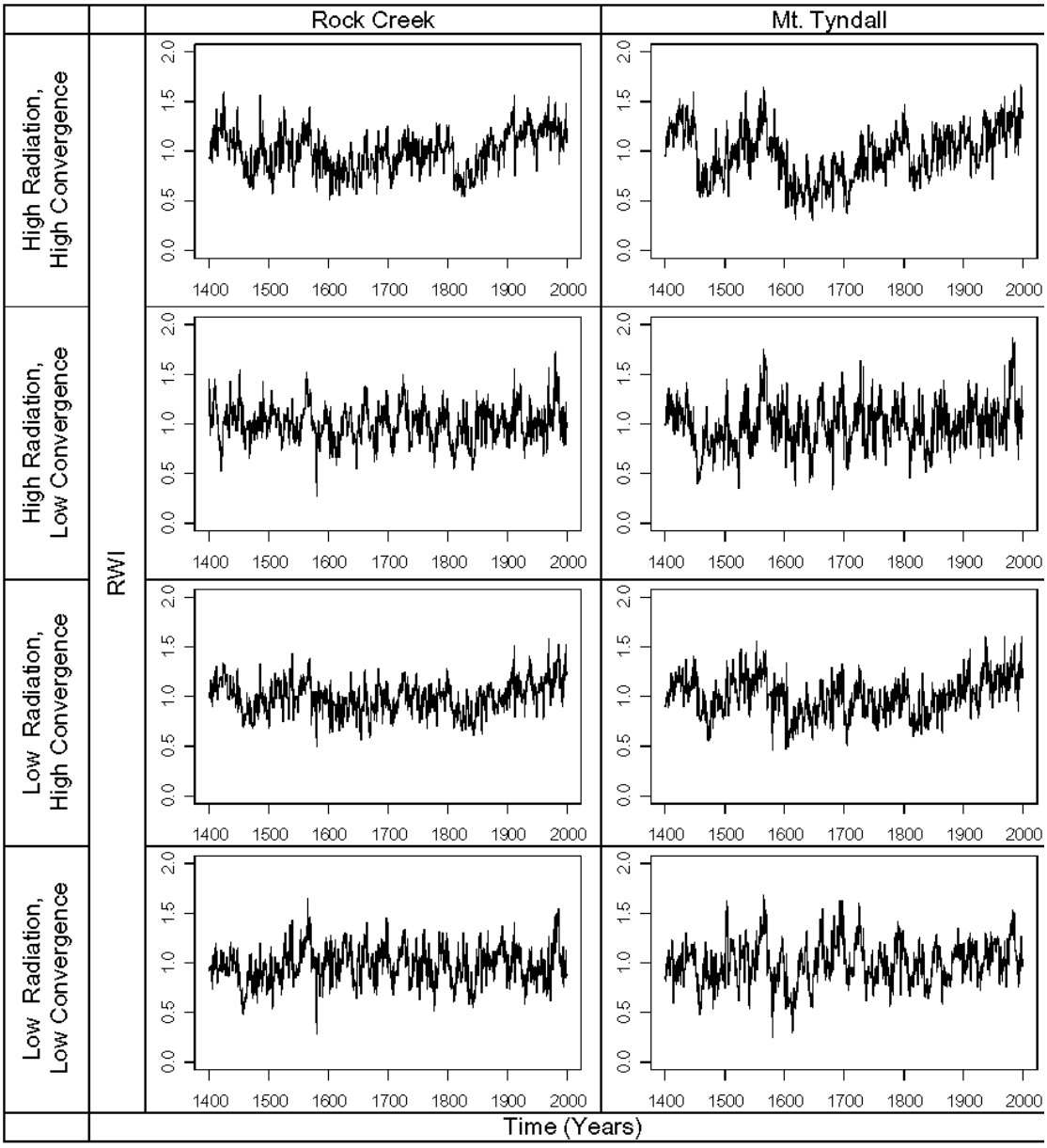

Fig. 4.3. Four tree ring chronologies from different physical settings (rows) are shown for each of two sites (columns). All chronologies run 1400 A.D. to 2000 A.D. Marked differences among the chronologies at each site are clearly visible. For instance, the bright and wet sites (top) have different modes of temporal variation than the dark and dry sites (bottom).

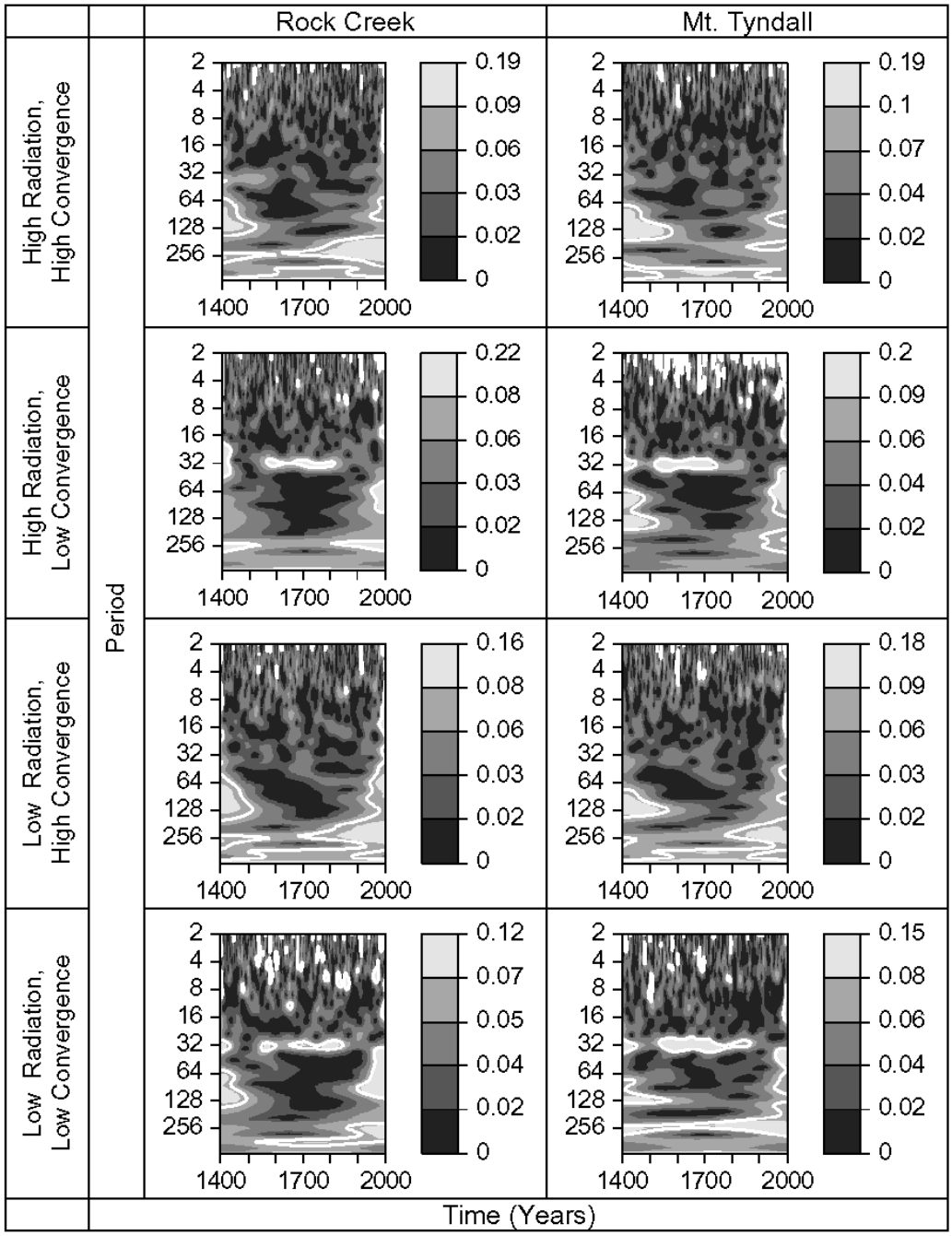

Fig. 4.4. Continuous wavelet power spectra density estimates for each of the eight chronologies are shown. From dark to light the grayscale contour intervals show 0-25%, 25-50%, 50-75%, 75-95%, and 95-100% of the wavelet power. The white contour in the wavelet power spectra shows a 95% confidence interval using a red-noise background spectrum. Important peaks in power occur at similar wavelengths in sites depending on physical setting. Especially interesting are the decadal signals in the low convergence (dry) sites. Also interesting is that the Mt. Tyndall Site shows higher overall power than the Rock Creek site.

The radiation index was expressed more clearly in the age-class structure of the plots, which sorted by topographic positions and was replicated at both sites (Fig. 4.2). The higher proportion of successful recruitment events after 1900 in the high convergence, high radiation sites suggested that the topographic position of these plots has been amenable to tree establishment, as the climate become relatively warmer and wetter after the so-called Little Ice Age (Graumlich, 1991). The opposite might be true of the dark and dry sites, which showed the lowest proportion of successful recruitment events after 1900. Our data cannot speak to whether this pattern is stationary in time, but related work (Lloyd and Graumlich, 1997) has shown the dynamic nature of population processes in these subalpine forests over the last three millennia. The climate niche that allows successful recruitment from immature stem to adult tree is likely matched in the high convergence and high radiation plots, which are likely warmer and wetter than the other plots. This might promote the establishment of the root system, which is deep and spreading in foxtail pine (Arno, 1973) and allows for considerable storage effect (Lloyd, 1996; Chesson and Huntly, 1997). Furthermore, total growing season carbon uptake has been tightly coupled to springtime soil moisture in high mountain systems (Schimel et al., 2002), which can result in higher stand turnover. This observation is possibly exacerbated in the high topographic convergence sites resulting in the observed age-class structure.

Identifying the physical regeneration niches for different life stages is an important challenge in forest ecology and necessary for modeling forests in complex terrain. Given that, it is interesting that immature stem density showed no pattern within or between sites (Table 4.2). This implied that the gradients seen in the age class of the

mature life stages of the trees were not applicable to immature stems at the same scale. This is possible if the abundance of microhabitats available for seedling establishment was not captured by this sampling design, which was based on 10-m cells of a DEM. Patterns of seedling distribution at a finer grain, however, (using a 0.5 m DEM and a 50 m x 50 m plot) have shown seedling presence / absence to be linked to TCI (see chapter five). This implies a classic scaling issue where seedlings clustered in high topographic areas at fine spatial scales, but that pattern was not propagated to the coarser spatial scale addressed in this study (Wiens 1989). Further speculation as to the scale of tree growth and establishment is difficult without research that investigates the establishment niche for different life history stages (seedlings vs. adult trees).

The combination of temperature and precipitation as controls on alpine treeline growth has been successfully exploited in reconstructing climate variability in the Sierra Nevada (Scuderi, 1987; Caprio and Baisan, 1992; Graumlich, 1993; Scuderi, 1993). The ways stands of climate-sensitive trees are selected by analysts, however, have not been physically modeled using the methods above. These results show the importance of multiple limiting factors in a system where tree growth is considered temperature-limited. Our results also showed that landscape position influenced tree-ring width in a manner that corresponds with foxtail pine physiology. Specifically, the high convergence sites keyed more strongly on temperature while the low convergence sites keyed more strongly on precipitation. In addition to a deep root system, foxtail pines are able to maintain photosynthetic activity in an extremely dry environment due to high tracheid density and the retention of needles for several years, which reduces the need for moisture and

nutrients (Mastroguiseppe and Mastroguiseppe, 1980). Given the wide distribution of foxtail pine on the cold and dry, eastern crest of Sequoia National Park, it is interesting that the growth patterns respond to an abiotic proxy for soil moisture. Temperature induced drought stress on tree growth has been shown in boreal Alaska (Barber et al., 2000) and might be reflected in our data where trees in the wetter parts of the landscape show higher relative correlations with temperature. The trees in the drier sites might lose the ability to track warm temperatures if there is insufficient soil water. We are further intrigued by the concept of mountain carbonsheds, where flows of water and air in sloping terrain make it possible to model the accumulation of respired carbon as a function of relief (Schimel et al., 2002). Our results might support the proposal of Schimel et al. (2002) using the coupling of hydrology and carbon exchange to further characterize system respiration and ecological patterns. These correlations represent very simplistic climate-growth models. Better fits between the climate data and the ring widths can be built, for instance, by using multiple predictors across seasons, but for the sake of clarity we have chosen to highlight the simplest results.

The wavelet analysis indicated that topographic factors strongly influence foxtail pine's response to climate variability through time. Further, the wavelet analysis shows the importance of site-to-site differences in determining the way in which climate influenced tree growth at different frequencies. The significant wavelet signals in the tree-ring chronologies were coherent with their instrumental climate correlations and correspond to the current understanding of climate periodicities. Oscillatory and quasi-oscillatory modes of climate have been shown on multiple time scales – from inter-

annual events like El Nino to multidecadal patterns such as the Pacific Decadal and North Atlantic Oscillations (see review by Wang and Schimel, 2003). The concentration of power in the very low frequencies (corresponding to >100 year periods) in the high-convergence, temperature-sensitive settings is consistent with the longer oscillatory mode of temperature variability (Jones et al., 1998; Moore et al., 2002). Similarly, the concentration of power in the frequencies corresponding to multi-decadal periods matches understanding of precipitation variability seen in the low-convergence, precipitation-sensitive sites (e.g., Cayan et al., 1998; McCabe and Dettinger, 1999; Dettinger et al., 2001; Biondi et al., 2001; Gedalof and Smith, 2001). This pattern was displayed between sites comprised of the same species, removing the potential for observed differences to be related to species-specific responses (e.g., as a function of species-specific physiology). The wavelet power spectra are continuous and allowed for examination of various periodicities at specific times. The dry plots show consistent power in the 95% percentile from 1600 to 1800 A.D. at multidecadal periods, implying a strong precipitation signal across sites during that time. This enhances understanding of the 20-year and 50-year positive precipitation anomalies extracted by Graumlich (1993) at various points during that period. Similarly, the dry plots showed a much higher number of long lived El Nino-like events that last from four to eight years as compared to the relatively wetter plots. This adds further support for the low convergence tree-ring chronologies to record the temporal modes of precipitation.

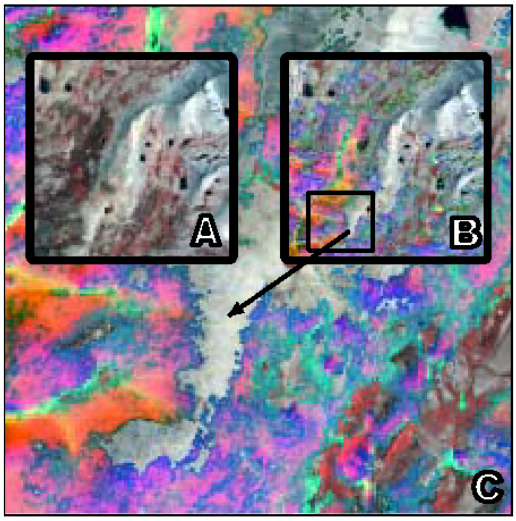

Fig. 4.5. A false-color composite of tree sensitivity for Mt. Tyndall shows some of the implications for process modeling. Red colors are tree density derived from classified IKONOS imagery; green colors are TCI; and blue colors are PRR. For instance, lime green pixels are moderately forested, have high convergence and mid-levels of radiation. Panel A shows the raw imagery in a 7.5 km by 7.5 km area, panel B shows the same extent as a false-color composite, and C shows the false-color composite zoomed in to 2 km by 2 km.

There are at least two implications of these results for process modeling and general understanding of foxtail pine forest dynamics. The first is that a priori modeling of the biotic response to the physical template is both possible and desirable using simple models of tree biology based on the physical template of the landscape. Physical models, such as the one described here, can be used in sampling design and when marshalling

field efforts to improve data collection that is logistically difficult and expensive (Urban, 2000).

The second implication is that the combination of remotely sensed imagery with GIS models can provide greater spatial understanding of biotic indicators of climate variability and stand dynamics over large spatial extents. By classifying IKONOS satellite imagery of the Mt. Tyndall site, for instance, it is possible to locate the lowest relative density foxtail pine forest (Lawrence et al., 2004) where due to low turnover and competition, low-density forests have the strongest climate signal (Fritts, 1976). Mapping relative forest density of foxtail pine together with TCI and PRR allows visualization of covariates potentially important for studying climate change (Fig. 4.5). We propose that in this cold and dry climate, the high convergence and high radiation locales on the landscape are showing the strongest response to 20th century forcings and these locations are where change is rapid, significant, and detectable. We further propose that the low convergence, low radiation sites are the places where precipitation forcing is maximally observable for this ecosystem and that multiple biophysical plots within a site are needed to leverage these complex interactions. A brief analysis of this data shows that <1% of this 7.5 km by 7.5 km landscape is in the bottom quartile of relative tree density, TCI, and PRR. Our results have shown that forest pattern in response to climate processes was not ubiquitous or even, and these are the locations that are likely to be the most sensitive for monitoring precipitation variability. This makes them attractive places, for instance, for instrumentation such as permanent weather stations to help improve understanding of climate-growth relationships.

Conclusion

Long chronologies of tree-ring records are critical climate-change data. We have shown that there are simple techniques that can provide leverage in teasing apart expressed temperature and precipitation variability in subalpine forests. Our results showed the importance of considering the biophysical setting of a forest stand and that biophysical setting affected forest age-class structure, ring-width patterns, and subsequent climatic inference, especially for detection of multidecadal and centennial trends. In this (ostensibly) temperature-limited ecosystem, precipitation was mediating forest patterns at the scale of hectares. This is of utility in looking backward to understand climatic signals in paleoclimatic records. It is also of utility in looking forward in ecological forecasting of when, where and how climatic variability will affect subalpine forests.

References

Arno S.F. (1973) *Discovering Sierra Trees*. Yosemite Association, Yosemite National Park, CA

Bailey D.K. (1970) Phytogeography and taxonomy for *Pinus* subsection *Balfourianae*. *Annals of the Missouri Botanical Garden* 57, 210-249

Barber V.A., Juday G.P. and Finney B.P. (2000) Reduced growth of Alaskan white spruce in the twentieth century from temperature-induced drought stress. *Nature* 405, 668-673

Billings W.D. and Bliss L.C. (1959) An alpine snowbank environemnt and its effects on vegetation, plant development, and productivity. *Ecology* 40, 388-397

Biondi F., Cayan D.R. and Gershunov A. (2001) North pacific decadal climate variability since 1661. *Bulletin of the American Meteorology Society* 14, 5-9

Bond N.A. and Harrison D.E. (2000) The Pacific Decadal Oscillation, air-sea interaction and central north Pacific winter atmospheric regimes. *Geophysical Research Letters* 27, 731-734

Brubaker L.B. (1986) Responses of tree populations to climatic change. *Vegetatio* 67, 119-130

Bunn A.G., Lawrence R.L., Bellante G.J., Waggoner L.A. and Graumlich L.J. (2003) Spatial variation in distribution and growth patterns of old growth strip-bark pines. *Arctic, Antarctic, and Alpine Research* 35, 323-330

Cairns D.M. (1998) Modeling controls on pattern at alpine treeline. *Geographical and Envronmental Modelling* 2, 43-63

Carmona R., Hwang W.L. and Torresani B. (1998) *Practical Time Frequency Analysis: Gabor and Wavelet Transforms with an Implementation in S*. Academic Press, San Diego, CA

Carmona, R. and Whitcher, B. (2002) Rwave version 1.20. R package, http://cran.r-project.org

Cayan D.R., Dettinger M.D., Diaz H.F. and Graham N.E. (1998) Decadal variability of precipitation over western North America. *Jounal of Climate* 11, 3148-3166

Chesson P. and Huntley N. (1997) The roles of harsh and fluctuating conditions in the dynamics of ecological communities. *American Naturalist* 150, 519-553

Crowley T.J. (2000) Causes of climate change over the past 1,000 years. *Science* 289, 270-277

Delcourt P.A. and Delcourt H.R. (1987) Late-Quaternary dyunamics of temperate forests: applications of paleoecology to issues of global environmental change. *Quaternary Science Reviews* 6, 129-146

ESRI (2002) ArcGIS™ version 8.3. Redlands, CA

Fritts H.C. (1976) *Tree Rings and Climate*. Academic Press, New York City, NY

Graumlich L.J. (1991) Subalpine tree growth, climate, and increasing CO_2: An assessment of recent growth trends. *Ecology* 72, 1-11

Graumlich L.J. (1993) A 1000-year record of temperature and precipitation in the Sierra Nevada. *Quaternary Research* 39, 249-255

Graumlich L.J., Waggoner L.A. and Bunn A.G. (2004) Detecting global change at alpine treeline: coupling paleoecology with contemporary studies. In: *Global Change and Mountain Regions: a State of Knowledge Overview* (eds Huber U., Bugmann H. and Reasoner M.), pp. 1-13. Kluwer Academic Publishers, The Netherlands

Gray S.T., Betancourt J.L., Fastie C.L. and Jackson S.T. (2003) Patterns and sources of multidecadal oscillations in drought-senitive tree-ring records from the central and southern Rocky Mountains. *Geophysical Research Letters* 30, 1316

Henry G.H.R. and Molau U. (1997) Tundra plants and climate change: the International Tundra Experiment (ITEX). *Global Change Biology* 3 (Supplement 1), 1-10

Holmes R.L. (1983) Computer-assisted quality control in tree-ring dating and measurement. *Tree-Ring Bulletin* 43, 69-78

Ihaka R. and Gentleman R. (1996) R: A language for data analysis and graphics. *Journal of Computational and Graphical Statistics* 5, 299-314

IPCC (2001) Contribution of working group I to the third assessment report of the intergovernmental panel on climate change. In: *Climate Change 2001: The Scientific Basis* (eds Houghton J.T., Ding Y., Griggs D.J., Noguer M., van der Linden P.J. and Xiaosu D.) Cambridge University Press, Cambridge, UK

Jenson S.K. and Dominique J.O. (1988) Extracting topographic structure from digital elevation data for geographic information analyses. *Photogrammetric Engineering and Remote Sensing* 54, 1593-1600

Jones P.D., Briffa K.R., Barnett T.P. and Tett S.F.B. (1998) High-resolution palaeoclmatic records for the last millennium: interprettion, integration and

comparison with General Circulation Model control-run temperatures. *The Holocene* 8, 455-471

Latif M. and Barnett T.P. (1994) Causes of decadal climate variability over the north Pacific and North America. *Science* 266, 634-637

Lawrence R.L., Bunn A.G., Powell S. and Zambon M. (2004) Classification of remotely sensed imagery using stochastic gradient boosting as a refinement of classification tree analysis. *Remote Sensing of Environment* 90, 331-336

Levin S.A. (1992) The problem of pattern and scale in ecology: the Robert H. MacArthur award lecture. *Ecology* 73, 1943-1967

Lloyd, A.H. (1996) *Patterns and processes of treeline forest response to late Holocene climate in the Sierra Nevada, California*. Doctoral Dissertation, University of Arizona, Tucson, AZ

Lloyd A.H. and Fastie C.L. (2002) Spatial and temporal variability in the growth and climate response of treeline trees in Alaska. *Climatic Change* 52, 481-509

Lloyd A.H. and Graumlich L.J. (1997) Holocene dynamics of treeline forests in the Sierra Nevada. *Ecology* 78, 1199-1210

Lookingbill, T. (2003) *Communities in transition: a multi-phased study of the Tsuga heterophylla/Abies amabilis ecotone in the Oregon Cascades*. Doctoral Dissertation, Duke University, Durham, NC

Lookingbill T. and Urban D.L. (2003) Spatial estimation of air temperature differences for landscape-scale studies in montane environments. *Agricultural and Forest Meteorology* 114, 141-151

Lookingbill T. and Urban D.L. (2004) An empirical approach towards improved spatial estimates of soil moisture for vegetation analysis. *Landscape Ecology*

Mann M.E., Bradley R.S. and Hughes M.K. (1999) Northern hemisphere temperatures during the past millennium: inferences, uncertainties, and limitations. *Geophysical Research Letters* 26, 759-762

Mann M.E., Bradley R.S. and Hughes M.K. (1998) Global-scale temperature patterns and climate forcing over the past six centuries. *Nature* 392, 779-787

Mantua N.J., Hare S.R., Zhang Y., Wallace J.M. and Fancis R.C. (1997) A Pacific interdecadal climate oscillation with impacts on salmon production. *Bulletin of the American Meteorological Society* 78, 1069-1079

Mastroguiseppe R. J. and Mastroguiseppe J.D. (1980) A study of *Pinus balfouriana* Grev et Balf (*Pinaceae*). *Systematic Botany* 5, 86-104

McCabe G.J. and Dettinger M.D. (1999) Decadal variations in the strength of ENSO teleconnections with precipitation in the western United States. *International Journal of Climatology* 19, 1399-1410

Minobe S. (1999) Resonance in bidecadal and pentadecadal climate oscillations over the North Pacific: Role in climatic regime shifts. *Geophysical Research Letters* 26, 855-858

Minobe S. (1997) A 50-70 year climatic oscillation over the North Pacific and North America. *Geophysical Research Letters* 24, 683-686

Moore G.W.K., Holdsworth G. and Alverson K. (2002) Climate change in the North Pacific region over the past three centruies. *Nature* 420, 401-403

Moore I.D., Grayson R.B. and Ladson A.R. (1991) Digital terrain modelling: A review of hydrological, geomorphological, and biological applications. *Hydrological Processes* 5, 3-30

Peet R.K. (1978) Latitudinal variation in southern Rocky Mountain forests. *Journal of Biogeography* 5, 275-289

Schimel D., Kittel T.G.F., Running S., Monson R., Turnipseed A. and Anderson D. (2002) Carbon sequestration studied in western U.S. mountains. *EOS, Transactions, American Geophysical Union* 83, 445-456

Scuderi L.A. (1993) A 2000-year tree ring record of annual temperatures in the Sierra Nevada Mountains. *Science* 259, 1433-1436

Scuderi L.A. (1987) Late-Holocene upper timberline variation in the southern Sierra Nevada. *Nature* 325, 242-244

Stephenson N.L. (1990) Climatic control of vegetation distribution: The role of the water balance. *The American Naturalist* 135, 649-670

Stokes M.A. and Smiley T.L. (1968) *An Introduction to Tree Ring Dating*. The University of Chicago Press, Chicago, IL

Torrence C. and Compo G.P. (1998) A practical guide to wavelet analysis. *Bulletin of the American Meteorological Society* 79, 61-78

Turner M.G., Gardner R.H. and O'Neil R.V. (2001) *Landscape Ecology in Theory and Practice: Pattern and Process*. Springer-Verlag, New York, City, NY

Urban D.L., Goslee S., Pierce K. and Lookingbill T. (2002) Extending community ecology to landscapes. *Ecoscience* 9, 200-212

Urban D.L., Miller C., Halpin P.N. and Stephenson N.L. (2000) Forest gradient response in Sierran landscapes: the physical template. *Landscape Ecology* 15, 603-620

Urban D.L., O'Neill R.V. and Shugart H.H. (1987) Landscape ecology. *Bioscience* 37, 119-127

Urban D.L. (2000) Using model analysis to design monitoring programs for landscape management and impact assessment. *Ecological Applications* 10, 1820-1832

Vale T.R. (1987) Vegetation change and park purposes in the high elevations of Yosemite National Park, California. *Annals of the Association of American Geographers* 77, 1-18

Villalba R. and Veblen T.T. (1994) Climatic influences on the growth of subalpine trees in the Colorado Front Range. *Ecology* 75, 1450-1462

Walker D.A., Halfpenny J.C., Walker M.D. and Wessman C.A. (1993) Long-term studies of snow-vegetation interactions. *BioScience* 43, 287-301

Walker M.D., Webber P.J., Arnold E.H. and Ebert-May D. (1994) Effects of interannual climate variation on aboveground phytomass in apline vegetation. *Ecology* 75, 393-408

Wardle P. (1971) An explanation for alpine timberline. *New Zealand Journal of Botany* 9, 371-402

Wardle P. (1974) Alpine timberlines. In: *Arctic and Alpine Environments* (eds Ives J.D. and Barry R.G.), pp. 371-402. Methuen, London, UK

Whittaker R.H. (1956) Vegetation of the Great Smoky Mountains. *Ecological Monographs* 26, 1-80

Whittaker R.H. (1967) Gradient analysis of vegetation. *Biological Review* 49, 207-264

Wiens J.A. (1989) Spatial scaling in ecology. *Functional Ecology* 3, 385-397

Zhang Y., Wallace J.M. and Battisti D.S. (1997) ENSO-like interdecadal variability: 1900-1993. *Journal of Climate* 10, 1004-1020

CHAPTER 5

THE ROLE OF GROWTH FORM IN MEDIATING ALPINE TREELINE DYNAMICS, SIERRA NEVADA USA

Introduction

Alpine treelines are the transition from subalpine forest to grassland or tundra and are generally considered dynamic ecotones sensitive to climate variability (Brubaker 1986; Kullman 1991; Hansen and di Castri 1992; Graumlich et al. 2004). Growing seasons at alpine treeline tend to be shorter than lower elevation forests due to lower air and soil temperatures characteristic of high elevations. The limitation of growing season temperature, lack of liquid water over much of the year, and irregularity of the snowpack are coupled with strong winds that cause mechanical damage to trees from blowing ice and sand and lead to winter desiccation. These factors tend to produce abrupt termination of forests to treeless alpine areas (Smith et al. 2003).

The treeline forests of the Sierra Nevada of California have been the subject of numerous paleoclimatic studies largely focusing on tree growth patterns in response to fluctuations in temperature and precipitation (e.g., Scuderi 1987; Graumlich 1991; Graumlich 1993; Caprio and Baisan 1992; Scuderi 1993; Millar et al. in press; Bunn et al. in review a; b). Sierran treelines are also ecologically dynamic in space and time, moving up and down slope over decades to centuries (Lloyd and Graumlich 1997; Lloyd 1998; Millar et al. in press). The effect of species autecology, however, and the expression of

climate across rugged topography make the dynamics of even relatively simple ecotones like alpine treeline complex.

Two important species at the treeline ecotone in the Sierra are foxtail pine (*Pinus balfouriana* Grev. et Balf.) and whitebark pine (*P. albicaulis* Engelm.). Although both species are extremely hardy, they demonstrate very different growth forms. Foxtail pine does not grow in a dwarfed or distorted form, unlike many other treeline species, and maintains an upright growth form to its elevational limit. Whitebark pine, in contrast, does grow in stunted krummholz mats and produces large skirts of foliage near the ground that are covered by snow in the winter and protected from desiccation (Arno and Hammerly 1984). The krummholz growth form has been exhaustively described and is best understood as structural facilitation where the dense growth form acts to enhance photosynthetic carbon gain and survival of seedlings (Smith et al. 2003 provide a review). The amelioration of microclimates creates a positive feedback loop that increases seedling survival, which is followed by further facilitation as seedlings are recruited into the adult ranks. Krummholz mats also trap snow, efficiently creating cover for needles and shoots during winter, warmer needle temperatures, and greater photosynthesis in spring and summer (Hadley and Smith 1987). Whitebark pine seed crops are also produced at irregular intervals and the large, heavy, and wingless seeds are dispersed primarily by Clark's nutcracker (*Nucifraga columbiana* Wilson) (Tomback et al. 1982).

Here we consider species autecology as it relates to patterns of regeneration and distribution at four plots near treeline dominated by either foxtail or whitebark pine. We

also examine how biophysical factors mediate climate – growth relationships. The objectives of this study are: (i) to describe the point pattern of these two species by age class, and (ii) to quantify the climate – growth associations with abiotic variables across these contrasting ecotones.

Methods

Study Area

The Sierra Nevada rise from near sea level to 4418 m a.s.l. in less than 100 kilometers horizontal distance creating extremely steep gradients in temperature and precipitation. Between 3000-3400 m a.s.l. there tends to be a well-defined treeline as a result (Arno and Hammerly 1984). This study was comprised of four 50 x 50 meter plots approximately 100 m below alpine treeline in the Sierra Nevada (Fig. 5.1). We selected two sites dominated by foxtail pine near Cirque Peak in Sequoia National Park and two sites immediately east of Yosemite National Park near Lee Vining in the Inyo National Forest dominated by whitebark pine. Both Cirque Peak and Lee Vining have been the sites of several paleoclimatic studies (e.g., Lloyd and Graumlich 1997; Millar et al. in press; Bunn et al. in review a; b). All plots were on steep and uniformly forested open-canopy subalpine sites (Table 5.1). The sites were abbreviated as CP1 and CP2 for the Cirque Peak plots and LV1 and LV2 for the Lee Vining plots.

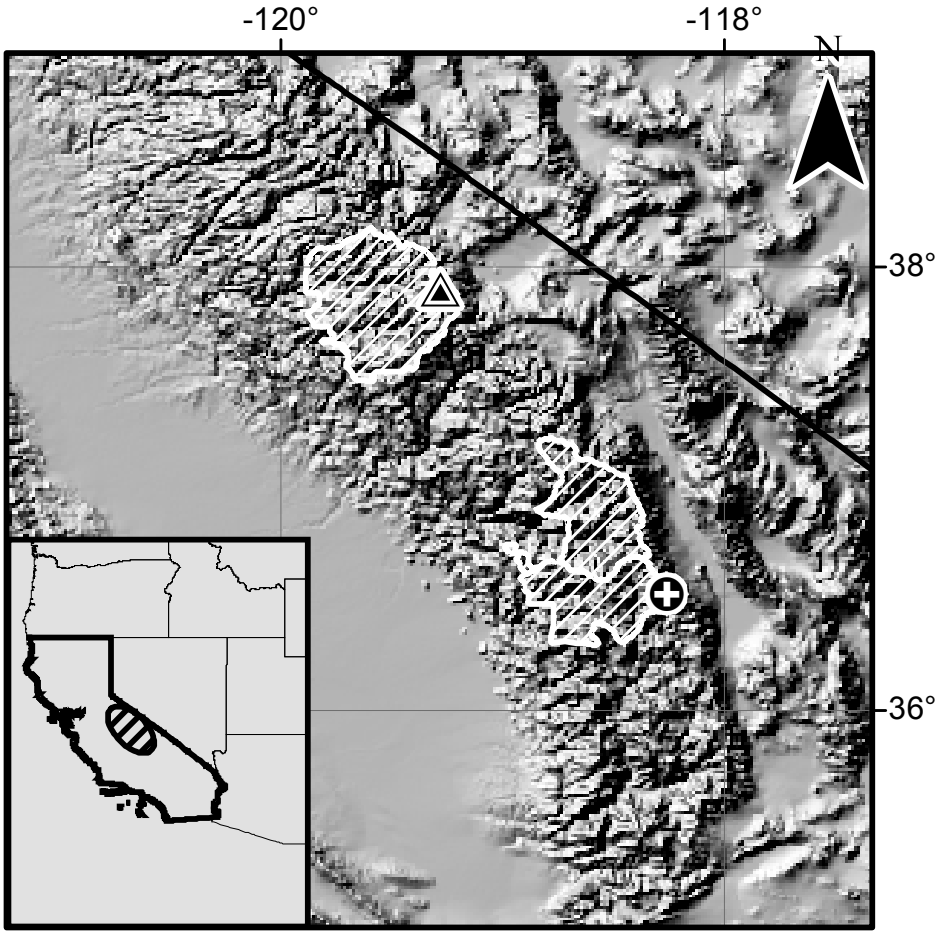

Figure 5.1. The study sites are shown in an overview map of the Sierra Nevada. The circle with the plus sign marks the locations of the foxtail pine dominated Cirque Peak sites in Sequoia National Park the outline of which is shown in white. The triangle marks the whitebark pine dominated sites at Lee Vining near Yosemite National Park the outline of which is also shown in white.

Increment cores were taken at breast height (1.37 m) from all the trees in the study with diameters greater than 2 cm at breast height. Cores were taken parallel to the slope contour to minimize the effects of slope pressure on wood formation. All of the cores were prepared and measured using standard methods in dendrochronology (Stokes

and Smiley 1968; Fritts 1976). Raw ring widths were used, as opposed to normalized widths, to highlight absolute changes in growth rates within and between trees.

Table 5.1. Mean elevation, aspect, and slope are shown for the four sites. The Cirque Peak sites are dominated by foxtail pine (PIBA) and have fewer stems than the Lee Vining sites which are dominated by whitebark pine (PIAL) which grows in a dwarf krummholz form. The number of seedlings is variable.

Site	Elevation (m)	Aspect°	Slope°	Species	Num. of Seedlings	Num. of Vertical Stems	Num. of Krummholz Patches
CP 1	3496	249	21	PIBA	40	26	0
CP 2	3501	212	24	PIBA	27	22	0
LV 1	3306	186	17	PIAL	10	118	18
LV 2	3296	232	21	PIAL	78	96	12

Previous research has demonstrated that precipitation variability plays a key role in controlling growth patterns of Sierran treeline, even though these trees are ultimately limited by temperature (Graumlich 1993; Bunn et al. in review a). Radial growth in this Mediterranean climate is correlated with the amount of winter precipitation falling as snow some of which is subsequently released in the spring as plant available soil moisture. For this study we calculated separate measures of tree vigor during two three-year periods (one during an anomalously wet period from 1996-1998 and one during a dry period from 1986-1989) using high-resolution interpolated climate data from the DayMet model at each plot (Thornton et al. 1997). We used a simple measure of tree vigor calculated as the average of the radial growth during each of these three-year time periods using the winter precipitation from the winter preceding the growing season (total accumulation in December, January, and February).

Environmental Data

At both sites we used a laser surveying system to map the location of every tree and seedling on the plot and at least 1000 additional points between vegetation to develop a fine-scale digital elevation model (DEM). We used the IMPULSE® laser and the MapStar Angle Encoder® from Laser Technology in conjunction with a Global Positioning System receiver. We collected data using an Allegro field computer from Juniper Systems with the Solofield® surveying software package from Tripod Data Systems. We exported data to ArcGIS® (ESRI 2002). We performed frequent checks of the accuracy of surveyed positions throughout the surveying.

A 0.5 m DEM was created from the survey data using inverse distance weighting (IDW) to interpolate between survey points using optimized coefficients and search radii (Johnston et al. 2001). IDW estimates the elevation values between points by averaging the values of the sample data points in the vicinity of each cell. The closer a point is to the center of the cell being estimated, the more influence, or weight, it has in the averaging process. Weights decrease with the inverse of distance from the cell being estimated. Because of the very high number of surveyed points in this study, we were able to test the DEM interpolation by randomly withholding 25% of the collected points and calculating the root mean squared (RMS) difference in the predicted versus withheld points. In all four of the plots the RMS error was less than 0.1 m.

We used the elevation models to construct environmental variables important to tree growth: slope, topographic convergence, and transformed aspect. A topographic convergence index (TCI) measured the tendency of water to collect on the landscape

(Moore et al. 1991; Urban et al. 2000; Bunn et al. 2003). The index takes on high values in gullies or rivulets and low values on rocks and other drained areas. TCI has been shown to be a strong proxy for plant available soil moisture in mountain ecosystems in the west (Lookingbill and Urban 2004; Lookingbill et al. in press). A visual inspection of the TCI surface and its histogram suggested that this surface resembles TCI data from other sources despite the fact that these models were located mid-slope. Evaporative demand varies with aspect and is an important variable in mediating plant growth. But because aspect is a circular variable (i.e., 0° is equal to 360°), it must be transformed before use. We used the transformation of Beers et al. (1966): transformed aspect as a function of *cos (45° - aspect)*, which aligned the values from 1 to -1 along a SW-NE axis with the maximum radiation effect on temperature for SW slopes. Transformed aspect (TASP) and TCI are reviewed by Moore et al. (1991). We assessed the correlation between each tree's vigor during the wet and dry period for all the environmental variables using Pearson Product Moment Correlations.

Point Pattern

The distribution pattern of the trees was described using Ripley's K function to assess the potential for biotic facilitation between species and age classes (Ripley 1976; Ripley 1981). Ripley's K describes the cumulative frequency distribution at a given point-to-point distance for each observation. Ripley's K patterns were compared to simulation envelopes of complete spatial randomness (CSR) using 1000 Monte Carlo simulations ($\alpha = 0.001$) of a Poisson process (Manly 1997). A buffer was invoked to

restrict the analysis to distances up to 25 meters, half the smallest dimension of the study area, to avoid edge effects (Cressie 1993). The expected value of the K-function (transformed as $\hat{L}$) under CSR is a flat line. Values greater than zero indicate clumps and values less than zero indicate regularity (Ripley 1976).

We examined the bivariate spatial interactions using $K_{12}(t)$, a generalization of the K function for a bivariate point process, and determined the spatial relationships between adult trees and seedlings (Diggle 1983; Upton and Fingleton 1985). High values of $K_{12}(t)$ indicate positive association while low values indicate negative association (regularity) between the trees and seedlings (Duncan 1991; Duncan and Stewart 1991). We calculated simulation envelopes from 1000 toroidal shifts of tree classes with respect to the other (i.e., trees and seedlings) (Camarero et al. 2000). All point pattern analyses was conducted using the Splancs contributed package (Rowlingson et al. 2003) to the R statistical programming environment (Ihaka and Gentleman 1996).

Mantel's Test

Using correlograms of Moran's I (Cliff and Ord 1981) we inspected the residuals of a multiple regression of the environmental variables on tree vigor, which indicated significant spatial autocorrelation (p-value ≤ 0.001; not shown). Results from ordinary least squares regressions with non-independent residuals are not reliable, and we therefore chose an alternative analytic framework robust to spatial structure. We identified variables that had the highest degree of correlation with the tree vigor using a series of Mantel's tests. The Mantel's test assessed the degree of correlation between

individual tree vigor during the wet and dry periods and the underlying environmental variables (slope, TASP, and TCI), while taking into account the relative spatial location of each observation and the intercorrelation among other variables. Variables are dissimilarity matrices in a Mantel's test, and the test measures the degree of pairwise similarity between samples (Mantel 1967; Legendre and Fortin 1989; Leduc et al. 1992). Here this measured whether trees that were similar in environmental variables also were similar in terms of vigor. Mantel's test considers geographic location as a predictor variable, indicating whether trees that are close together in space are similar in other variables.

A powerful form of Mantel's test is a partial regression using vigor dissimilarity, environmental dissimilarity, and geographic dissimilarity (distance) (Smouse et al. 1986; Legendre and Fortin 1989; Fortin and Gurevitch 1993). This form indicated how much variability in vigor was explained by abiotic factors. It also indicated spatially structured residual variability in vigor after removing the effects of the environmental variables. Distance matrices were constructed for geographic distance, slope, TASP, TCI, and vigor during the wet and dry periods using Euclidean distance. A test of significance was evaluated via permutation because the elements of a distance matrix are not independent (Legendre and Fortin 1989; Manly 1997). The Mantel's tests were conducted using Ecodist-R (Goslee and Urban 2003), an as of yet uncontributed package to the R statistical programming environment (see Acknowledgements).

Results

Point Pattern

Adult foxtail pine patterns were not strongly clustered or regular at either of the Cirque Peak sites (Fig. 5.2). Foxtail pine seedlings were more clustered than random at both sites, although CP1 showed clustering at more distances than CP2. Adult whitebark pine patterns were strongly clustered at distances up to 15 meters at LV1 and LV2 (Fig. 5.3). Adult trees at LV2 began to show regularity at distances greater than 20 meters. Whitebark pine seedlings were more clustered than random at both sites, although LV1 showed clustering at more distances than LV2. Spatial interactions using the bivariate Ripley's K, between adults and seedlings for foxtail and whitebark pines were not seen any of the sites (not shown).

Tree Vigor and Environment Associations

Tree vigor was associated with TCI, but slope and TASP were not strongly correlated with vigor (Table 5.2). The association between TCI and foxtail pine was positive for foxtail pines and negative for whitebark pines. Correlations were stronger for foxtail pine vigor during the dry period and stronger for whitebark pine vigor during the wet period. The regression of slope, TASP, and TCI on vigor reinforced the correlations for TCI seen above (Tables 5.3 and 5.4). TCI was a significant predictor for foxtail pine vigor during the dry period only (Table 5.3; Fig. 5.4). TCI was a significant predictor for whitebark pine vigor during both dry and wet periods but the relationship was stronger during the wet period (Table 5.4; Fig. 5.5). At LV1 there was also a significant spatial residual that was smaller during the wet period.

Discussion

This data provides a glimpse into some of the patterns and processes at the dynamic alpine treeline ecotone in the Sierra Nevada. Our focus on fine-scale patterns has important consequences for understanding treeline ecology and has the potential to be useful in developing global change monitoring schemes. Our most important result was that we found strong associations in the spatial and growth patterns of whitebark and foxtail pines that correspond to species autecology as it relates to soil moisture and snow distribution.

The nature of the krummholz mat is to facilitate growth by ameliorating the harsh climate at treeline (Arno and Hammerly 1984; Smith et al. 2003). We attribute the difference in the spatial point pattern between species to the distorted growth form of whitebark pine, where stems emerge from foliage mats that create cover for needles and shoots during winter and warmer needle temperatures in spring and summer (Hadley and Smith 1987). This is combined with the caching of seeds by nutcrackers and asexual regeneration that allows multiple genetic individuals of whitebark pine to germinate at the same location. We are not suggesting that each whitebark pine stem on our plots is a genetic individual however. Previous research with krummholz whitebark pines shows that while many genetic individuals can exist in a krummholz mat, separate stems of the same individual can grow independently due to the ability of whitebark pine to regenerate asexually by layering when late lying snow bends low branches onto soil (Arno and Hoff 1990).

Because foxtail pine does not exhibit a stunted growth form we were not surprised to find largely random spatial point pattern in the adult trees. The foxtail pines at CP1 and CP2 do not have the potential to show the same ability for self-structured facilitation as do the whitebark pines at Lee Vining. Foxtail pines have high tracheid density and a root system that is deep and spreading (Mastroguiseppe and Mastroguiseppe 1980). This is combined with long needle retention and individual tree life spans exceeding 1000 years. This allows foxtail pine to grow in cold and dry environments due to strong storage effect in the species (Lloyd 1996; Chesson and Huntley 1997).

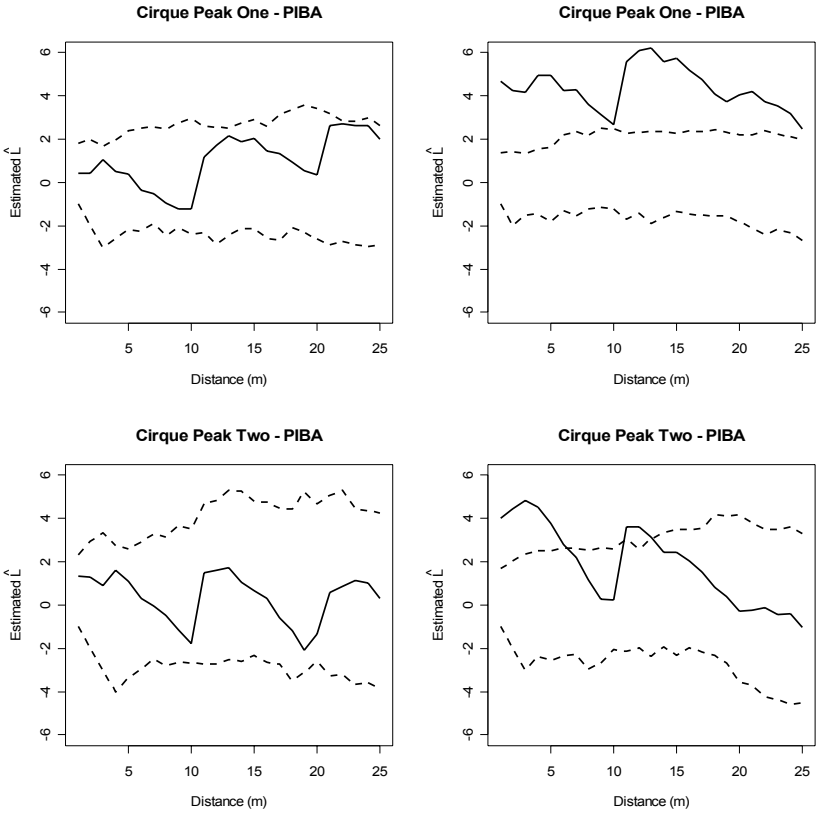

Figure 5.2. Distribution patterns using Ripley's K functions are marked as solid line and show clustering for trees (left) and seedlings (right) for the foxtail pine sites at Cirque Peak. The dotted lines are simulation envelopes that are the result of 1000 Monte Carlo simulations of complete spatial randomness.

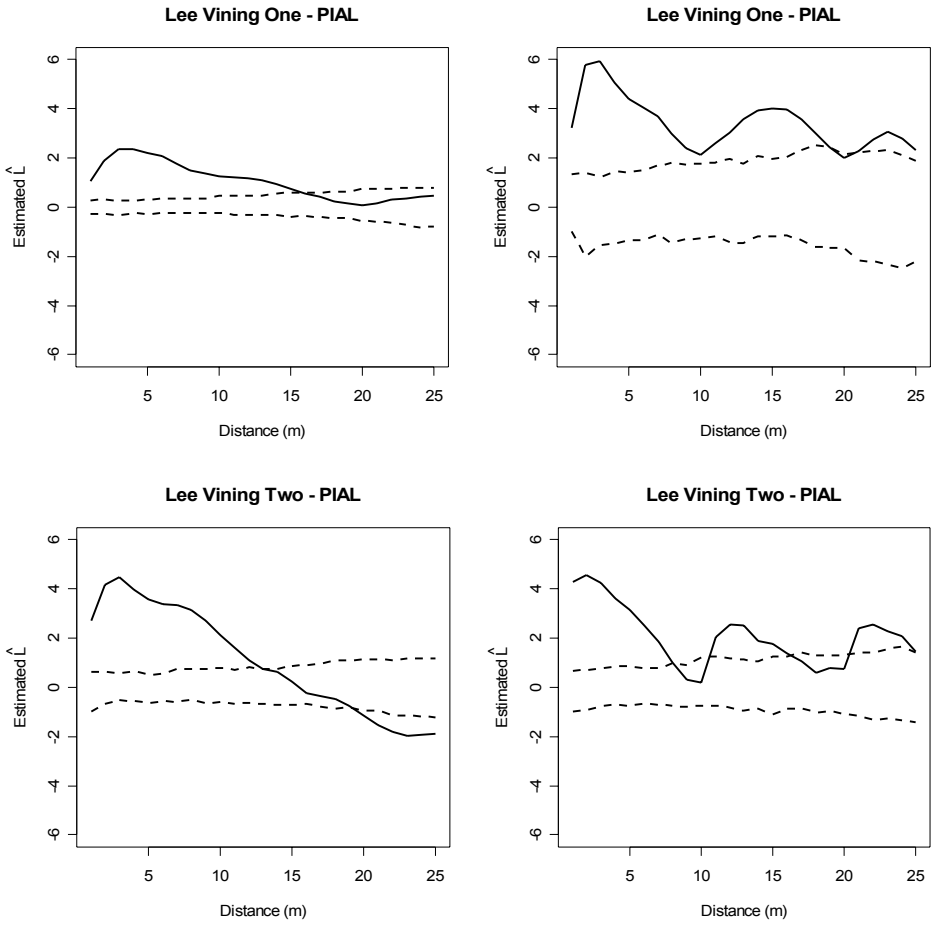

Figure 5.3. Distribution patterns using Ripley's K functions are marked as solid line and show clustering for trees (left) and seedlings (right) for the whitebark pine sites at Lee Vining. The dotted lines are simulation envelopes that are the result of 1000 Monte Carlo simulations of complete spatial randomness.

Both species show significant clustering of seedlings and do not show spatial interaction between the location of seedlings and adult trees at distances up to 25 m. We attribute these clustering patterns to germination of seeds in favorable microsites. For both species we speculate that the high inter-annual mortality of seedlings means that the spatial pattern seen does not propagate to the spatial patterns seen in the adults. That is, even though seedlings are clustered, the pattern becomes thinned over time and is not

expressed the same way in the adults, perhaps due to competitive exclusion of the constant flux of newly germinated seedlings by established seedlings. We further speculate that the clustering seen in the adult whitebark pines arises from the self-structuring process described above (asexual regeneration, seed caching, and amelioration by low growing foliage) and is independent of the process that creates clustering in the seedlings. We did not find seed caches of whitebark pine seedlings at the Lee Vining sites for instance, although we have seen them off the plots in the area.

Table 5.2. The correlations between tree vigor and TCI change sign between the foxtail dominated Cirque Peak and the whitebark dominated Lee Vining sites. The Cirque Peak sites show stronger correlations during the dry period while the Lee Vining Sites are stronger during the wet periods. Slope and TASP show weak correlations that are not consistent between plots or within species.

	Pearson correlations with vigor		
Site and Period	Slope	TASP	TCI
CP 1 Dry Period	-0.078	-0.044	0.257
CP 1 Wet Period	-0.058	0.110	0.209
CP 2 Dry Period	-0.079	0.076	0.594
CP 2 Wet Period	-0.039	0.055	0.404
LV 1 Dry Period	-0.027	0.130	-0.566
LV 1 Wet Period	-0.056	0.029	-0.636
LV 2 Dry Period	0.026	-0.066	-0.714
LV 2 Wet Period	0.046	0.133	-0.844

Table 5.3. Results of simple and partial Mantel's tests for foxtail pine vigor at Cirque Peak [a]. TCI was the most important variable once spatial autocorrelation was taken into account.

[a] The column entries are as follows: Mantel r Coefficient, and P-values.

[b] The notation implies a regression of an environmental variable B (e.g., slope, TASP, TCI) on tree vigor A. The second column implies a regression of either tree presence A or an environmental variable B on space. The third column represents a regression of an environmental variable on tree vigor, controlling for spatial autocorrelation. The fourth column extends the regression to control for both spatial autocorrelation and the correlation with the other variables B'.

[c] The first entry in this column is the effect of space on tree presence, controlling for all environmental variables—a pure partial spatial residual.

CP1 Dry	A~B[b]	A or B ~ space	A ~ B + space	A ~ B + B' + space [c]
Vigor		NS		NS
Slope	NS	NS	NS	NS
TASP	NS	NS	NS	NS
TCI	0.184 (p = 0.042)	NS	0.184 (p = 0.040)	0.191 (p = 0.032)
CP1 Wet	A~B[b]	A or B ~ space	A ~ B + space	A ~ B + B' + space [c]
Vigor		NS		NS
Slope	NS	NS	NS	NS
TASP	NS	NS	NS	NS
TCI	NS	NS	NS	NS
CP2 Dry	A~B[b]	A or B ~ space	A ~ B + space	A ~ B + B' + space [c]
Vigor		NS		NS
Slope	NS	0.192 (p = 0.046)	NS	NS
TASP	NS	NS	NS	NS
TCI	0.272 (p = 0.0280)	NS	0.280 (p = 0.031)	0.278 (p = 0.039)
CP2 Wet	A~B[b]	A or B ~ space	A ~ B + space	A ~ B + B' + space [c]
Vigor		NS		NS
Slope	NS	0.192 (p = 0.046)	NS	NS
TASP	NS	NS	NS	NS
TCI	NS	NS	NS	NS

Table 5.4. Results of simple and partial Mantel's tests for whitebark pine vigor at Lee Vining [a]. TCI was the most important variable once spatial autocorrelation was taken into account.

[a] The column entries are as follows: Mantel r Coefficient, and P-values.

[b] The notation implies a regression of an environmental variable B (e.g., slope, TASP, TCI) on tree vigor A. The second column implies a regression of either tree presence A or an environmental variable B on space. The third column represents a regression of an environmental variable on tree vigor, controlling for spatial autocorrelation. The fourth column extends the regression to control for both spatial autocorrelation and the correlation with the other variables B'.

[c] The first entry in this column is the effect of space on tree presence, controlling for all environmental variables—a pure partial spatial residual.

LV1 Dry	A~B[b]	A or B ~ space	A ~ B + space	A ~ B + B' + space [c]
Vigor		0.475		0.425
		(p < 0.003)		(p < 0.001)
Slope	NS	NS	NS	NS
TASP	NS	NS	NS	NS
TCI	0.477	0.205	0.445	0.314
	(p = 0.006)	(p = 0.048)	(p = 0.029)	(p = 0.022)
LV1 Wet	A~B[b]	A or B ~ space	A ~ B + space	A ~ B + B' + space [c]
Vigor		0.307		0.273
		(p = 0.024)		(p = 0.024)
Slope	NS	NS	NS	NS
TASP	NS	NS	NS	NS
TCI	0.376	0.205	0.323	0.368
	(p = 0.010)	(p = 0.045)	(p = 0.022)	(p = 0.007)
LV2 Dry	A~B[b]	A or B ~ space	A ~ B + space	A ~ B + B' + space [c]
Vigor		NS		NS
Slope	NS	0.414	NS	NS
		(p = 0.019)		
TASP	NS	NS	NS	NS
TCI	0.334	NS	0.357	0.360
	(p = 0.050)		(p = 0.036)	(p = 0.037)
LV2 Wet	A~B[b]	A or B ~ space	A ~ B + space	A ~ B + B' + space
Vigor		NS		NS
Slope	NS	0.414	NS	NS
		(p = 0.019)		
TASP	NS	NS	NS	NS
TCI	0.624	NS	0.634	0.626
	(p = 0.003)		(p = 0.003)	(p = 0.003)

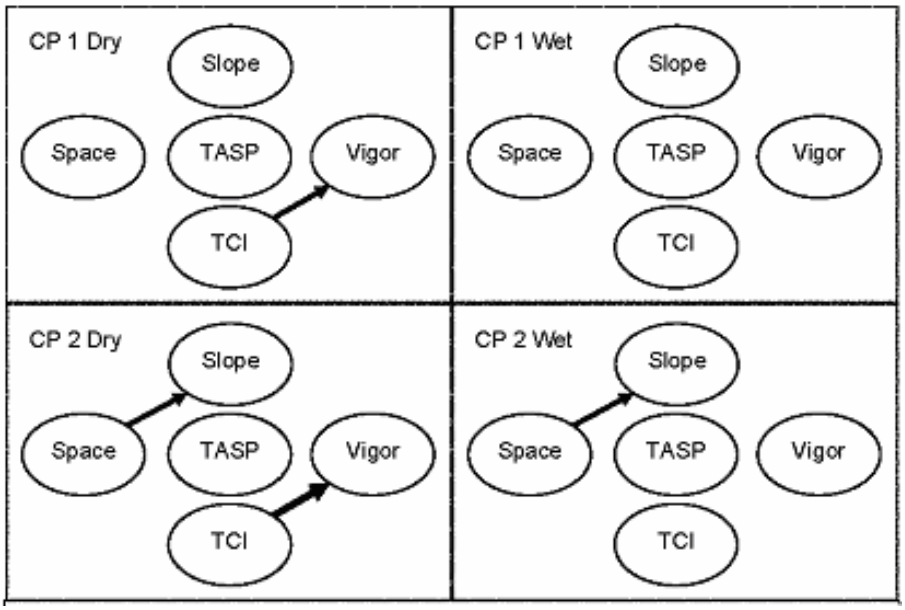

Figure 5.4. Results from Mantel's test for foxtail pine vigor for Cirque Peak are presented as a path diagram. Arrows indicate a significant effect. Magnitude of arrow represents strength of Mantel coefficient. The arrows to the left of the ecological variables indicate simple correlations, while the arrows to the right indicate partial correlations (compare to Table 5.3).

TCI has the strongest association with tree vigor for both species for the suite of environmental correlates we examined in this study. What is most interesting about this alliance is that the sign of the correlation between TCI and vigor changes by species. The correlation also changes in strength between vigor calculated in the wet versus the dry period. Foxtail pine shows stronger correlation for vigor calculated for the dry period. In fact, the correlation is significant in the spatially explicit framework shown in the Mantel's test for the dry period only. The association for whitebark pine is significant during the dry and wet periods but stronger during the wet period. It should be noted here that the sign of the Mantel's correlation is positive for both foxtail and whitebark pine even though relationship between TCI and whitebark pine vigor is negative. This results

from the structure of Mantel's test, which works on dissimilarity and shows positive dissimilarity as the distance between matrices increases whether or not the numerical relationship is positive or negative.

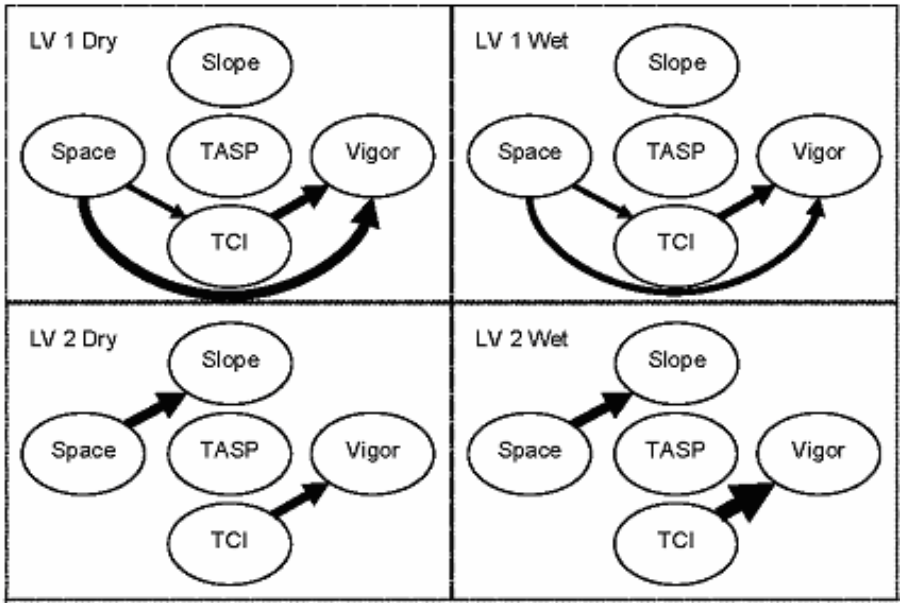

Figure 5.5. Results from Mantel's test for foxtail pine vigor for Lee Vining are presented as a path diagram. Arrows indicate a significant effect. Magnitude of arrow represents strength of Mantel coefficient. The arrows to the left of the ecological variables indicate simple correlations, while the arrows to the right indicate partial correlations (compare to Table 5.4).

We interpret these results as further expression of the difference in growth form between the species. Foxtail pine, with an upright structure and lack of low growing foliage, shows increased vigor in high TCI locations. The increase that foxtail pine experiences in high TCI microsites is more extreme (and in fact significant) only during the dry periods. That the opposite is true for whitebark pine is an especially appealing aspect of this study. White bark pine with low growing foliage in skirts or in dense

krummholz mats shows decreased vigor in high TCI locations. That decrease is magnified during the wet periods in the exact opposite association as compared to foxtail pine. We speculate that whitebark pines in the high TCI areas trap snow that lingers through the beginning of the growing season or covers foliage more effectively during periods in the winter when the tree might be able to respire. Although this missed opportunities for growth exists during both wet and dry periods it is exacerbated during times of strong winter precipitation from the pervious year, which is expressed on the landscape as blowing and drifting snow. That whitebark pine exists ubiquitously on the high elevation mountain landscape throughout much of the North American West demonstrates the broad niche of this species as compared to foxtail pine. The negative correlation of the abiotic proxy for soil moisture on radial growth does not suggest that this species is limited by mesic sites however. Rather, it shows the success of the adaptation of the stunted growth form in allowing these trees to maintain growth on the driest microsites.

Foxtail pine in the Sierra is known to move up and down slope in concert with variations in climate. Detailed population reconstructions of foxtail pine have been possible due to extensive stands of dead wood rooted above current treeline, and analysis of this data has demonstrated that the ecotone can shift hundreds of meters on century time scales (Lloyd and Graumlich 1997). Similar evidence of past whitebark pine movement in the Sierra has not been demonstrated despite extensive reconnaissance for dead wood above treeline (Graumlich unpublished data; C. Millar pers. comm.), although such evidence is available in the Rocky Mountains (Graumlich et al. 2004). The

contemporary evidence of change complicates the picture further. Whitebark pine stands at treeline, which are often mixed with limber pine (*Pinus flexilis* James), are currently expanding into snowfields and wet meadows (Millar et al. in press). There is ample evidence of foxtail pine seedling establishment above current treeline (Lloyd 1998). Evidence for the successful recruitment of foxtail pine seedlings into more mature age classes and the contemporary invasion of foxtail pine into tundra has not been systematically demonstrated unlike recent trends with whitebark pine (Millar et al. in press).

The foxtail pine treeline in the Sierra was higher over much of the last 3500 years than it is at present (Lloyd and Graumlich 1997). The adult populations experienced mortality during periods of prolonged drought and recruitment increased during periods that were relatively cold and wet. These patterns are consistent with our observations that strong foxtail pine vigor is associated with high TCI microsites. The physiological mechanisms for tree mortality are often poorly known, but ring widths are associated with mortality since tree rings are integrators of biotic and abiotic influences that reflect tree fitness (Fritts 1976; Waring and Pitman 1985; Biggler and Bugmann 2003). Low growth rates for multiple years (i.e., low vigor in our study) are predicted for dying trees under the low-growth hypothesis (Manion 1981) and have been used successfully as an index of mortality risk (Wyckoff and Clark 2000). The complex growth form of whitebark pine might make the treelines at Lee Vining more robust to long-term drought and explain the lack of obvious treeline migration over the last millennia that are seen in the foxtail pine.

Conclusions

This research illuminates striking differences in the spatial pattern for two contrasting pine species growing in similarly harsh environments. It emphasizes that differences in plant growth form can influence mechanisms for plant survival and that growth-form plasticity can influence spatial pattern and ecological processes. Careful attention will have to be paid to species biology when monitoring the alpine treeline ecotone for structural changes in response to predicted global warming.

References

Arno S.F. and Hammerly R.P. (1984) *Timberline: Mountain and Arctic Forest Frontiers*. The Mountaineers, Seattle, WA

Arno, S.F. and Hoff, R.J. (1989) Silvics of whitebark pine (*Pinus albicaulis*). General Technical Report INT-253. Denver, CO: United States Department of Agriculture Forest Service

Beers T.W., Dress P.E. and Wensel L.C. (1966) Aspect transformation in site productivity research. *Journal of Forestry* 64, 691-692

Bigler C. and Bugmann H. (2003) Growth-dependent tree mortality models based on tree rings. *Canadian Journal of Forest Research* 33, 210-221

Brubaker L.B. (1988) Vegetation history and anticipating future vegetation change. In: *Ecosystem Management for Parks and Wilderness* (eds Agee J.K. and Johnson D.R.), pp. 41-61. University of Washington Press, Seattle, WA

Bunn A.G., Graumlich L.G. and Urban D.L. (In review) Interpreting the climatic significance of trends in twentieth-century tree growth at high elevations. *The Holocene*

Bunn A.G., Waggoner L.A. and Graumlich L.G. (In review) Topographic mediation of growth of subalpine trees in the Sierra Nevada, USA . *Global Ecology and Biogeography*

Bunn A.G., Lawrence R.L., Bellante G.J., Waggoner L.A. and Graumlich L.J. (2003) Spatial variation in distribution and growth patterns of old growth strip-bark pines. *Arctic, Antarctic, and Alpine Research* 35, 323-330

Camarero J.J., Gutierrez E. and Fortin M.-J. (2000) Spatial pattern of subalpine forest-alpine grassland ecotones in the Spanish Central Pyrenees. *Forest Ecology and Management* 134, 1-16

Caprio, A.C. and Baisan, C.H. (1992) Multi-millenial tree-ring chronologies from foxtail pine in the southern Sierras of California. Bulletin of the Ecological Society of America, Honolulu, HI

Chesson P. and Huntley N. (1997) The roles of harsh and fluctuating conditions in the dynamics of ecological communities. *American Naturalist* 150, 519-553

Cliff A.D. and Ord J.K. (1981) *Spatial Processes*. Pion Limited, London, UK

Cressie N.A.C. (1991) *Statistics for Spatial Data*. Wiley, New York City, NY

Diggle P.J. (1983) *Statistical Analysis of Spatial Point Patterns*. Academic Press, London, UK

Duncan R.P. (1991) Competition and the coexistence of species in a mixed podocarp stand. *Journal of Ecology* 79, 1073-1084

Duncan R.P. and Stewart G.H. (1991) The temporal and spatial analysis of tree age distributions. *Canadian Journal of Forest Research* 21, 1703-1710

Fortin M.-J. and Gurevitch J. (1993) Mantel tests: spatial structure in field experiments. In: *Design and Analysis of Ecological Experiments* (eds Scheiner S.M. and Gurevitch J.), pp. 342-359. Chapman and Hall, New York City, NY

Fritts H.C. (1976) *Tree Rings and Climate*. Academic Press, New York City, NY

Goslee, S. and Urban, D.L. (2003) Ecodist-R version 0.1. R package, Unreleased

Graumlich L.J. (1991) Subalpine tree growth, climate, and increasing CO_2: An assessment of recent growth trends. *Ecology* 72, 1-11

Graumlich L.J. (1993) A 1000-year record of temperature and precipitation in the Sierra Nevada. *Quaternary Research* 39, 249-255

Graumlich L.J., Waggoner L.A. and Bunn A.G. (2004) Detecting global change at alpine treeline: coupling paleoecology with contemporary studies. In: *Global Change and Mountain Regions: a State of Knowledge Overview* (eds Huber U., Bugmann H. and Reasoner M.), pp. 1-13. Kluwer Academic Publishers, The Netherlands

Hadley J.L. and Smith W.K. (1987) Influence of krummholz mat microclimate on needle physiology and survival. *Oecologia* 73, 82-90

Hansen A.J. and di Castri F. (1992) *Landscape boundaries: consequences for ecological flows*. Springer-Verlag, New York City, NY

Ihaka R. and Gentleman R. (1996) R: A language for data analysis and graphics. *Journal of Computational and Graphical Statistics* 5, 299-314

Johnston K., Ver Hoef J.M., Krivoruchko K. and Lucas N. (2001) *Using ArcGIS Geostatistical Analyst*. ESRI, Redlands, CA

Kullman L. (1991) Pattern and process of present tree-limits in the Tärna region, souther Swedish Lapland. *Fennia* 169, 25-38

Leduc A., Drapeau P., Bergeron Y. and Legendre P. (1992) Study of spatial components of forest cover using partial Mantel's tests and path analysis. *Journal of Vegetation Science* 3, 69-78

Legendre P. and Fortin M.-J. (1989) Spatial pattern and ecological analysis. *Vegetatio* 80, 107-138

Lloyd, A.H. (1996) *Patterns and processes of treeline forest response to late Holocene climate in the Sierra Nevada, California*. Doctoral Dissertation, University of Arizona, Tucson, AZ

Lloyd A.H. (1998) Growth of foxtail pine seedlings at treeline in the southeastern Sierra Nevada, California. *Ecoscience* 5, 250-257

Lloyd A.H. and Graumlich L.J. (1997) Holocene dynamics of treeline forests in the Sierra Nevada. *Ecology* 78, 1199-1210

Lookingbill T., Goldenberg N. and Williams B. (In press) Understory plants as soil moisture indicators in Oregon's western Cascades old-growth forests. *Northwest Science*

Lookingbill T. and Urban D.L. (2004) An empirical approach towards improved spatial estimates of soil moisture for vegetation analysis. *Landscape Ecology*

Manion P. (1981) *Tree disease concepts*. Prentice Hall, Englewood Cliffs, NJ

Manly B.F.J. (1997) *Randomization, Bootstrap and Monte Carlo Methods in Biology*, 2nd edn. Chapman and Hall, London, UK

Mantel N. (1967) The detection of disease clustering and a generalized regression approach. *Cancer Research* 27, 209-220

Mastroguiseppe R. J. and Mastroguiseppe J.D. (1980) A study of *Pinus balfouriana* Grev et Balf (*Pinaceae*). *Systematic Botany* 5, 86-104

Millar C.M., Westfall R.D., Delany D.L., King J.C., and Graumlich L.G.(In press) Response of high elevation conifers to 20th century climate change. *Arctic, Antarctic and Alpine Research*

Moore I.D., Grayson R.B. and Ladson A.R. (1991) Digital terrain modelling: A review of hydrological, geomorphological, and biological applications. *Hydrological Processes* 5, 3-30

Ripley B.D. (1976) The second-order analysis of stationary point processes. *Journal of Applied Probability* 13, 255-266

Ripley B.D. (1981) *Spatial Statistics*, 1st edn. Wiley, New York City, NY

Rowlingson, B., Diggle, P., and Bivand, R. (2003) Splancs version 2.01-13. R package, http://cran.r-project.org

Scuderi L.A. (1993) A 2000-year tree ring record of annual temperatures in the Sierra Nevada Mountains. *Science* 259, 1433-1436

Scuderi L.A. (1987) Late-Holocene upper timberline variation in the southern Sierra Nevada. *Nature* 325, 242-244

Smith W.K., Germino M.J., Hancock T.E. and Johnson D.M. (2003) Another perspective on altitudinal limits of alpine timberlines. *Tree Physiology* 23, 1101-1112

Smouse P.E., Long J.C. and Sokal R.R. (1986) Multiple regression and correlation extensions of the mantel test of matrix correspondence. *Systematic Zoology* 35, 627-632

Stokes M.A. and Smiley T.L. (1968) *An Introduction to Tree Ring Dating*. The University of Chicago Press, Chicago, IL

Thornton P.E., Running S.W. and White M.A. (1997) Generating surfaces of daily meteorological variables over large regions of complex terrain. *Jounral of Hydrology* 190, 241-251

Tomback D.F. (1982) Dispersal of whitebark pine seeds by Clark's nutcracker: A mutualism hypothesis. *Journal of Animal Ecology* 51, 451-467

Upton G.J.G. and Fingleton B. (1985) *Spatial Data Analysis by Example. Volume 1: Point Pattern and Quantitative Data*. Wiley, Chichester, UK

Urban D.L., Miller C., Halpin P.N. and Stephenson N.L. (2000) Forest gradient response in Sierran landscapes: the physical template. *Landscape Ecology* 15, 603-620

Waring R.H. and Pitman G.B. (1985) Modifying lodgepole pine stands to change susceptibility to mountain pine beetle attack. *Ecology* 66, 889-897

Wyckoff P.H. and Clark J.S. (2000) Predicting tree mortality from diameter growth: A comparison of approaches. *Canadian Journal of Forest Research* 30, 156-167

CHAPTER 6

POTENTIAL GLOBAL WARMING IMPACTS AT ALPINE TREELINE IN THE SIERRA NEVADA, CALIFORNIA: AN OPPORTUNITY FOR MONITORING

Introduction

Whether anthropogenic global change will impact terrestrial ecosystems is no longer an academic question. There is growing evidence that warming is already physiology, productivity, and growth of plant species (Cannel 1998; Blaustein et al. 2002) and thereby altering their distributions and ranges (Parmesan 1996; Parmesan et al. 1999; Parmesan and Yohe 2003; Root et al. 2003). Most scientists agree that recent warming trends are partly anthropogenic and will increase dramatically over the next one hundred years (IPCC 2001). The task at hand for land managers is to find ecosystems at risk of undergoing rapid change and devise strategies for quantifying impacts.

The United States National Park Service (NPS) has a mandate to monitor the ecosystems in park units through the Inventory and Monitoring of Park Natural Resources program (NPS 1998). This involves inventories of park resources and monitoring programs that provide an important feedback between park conditions and management objectives. Park managers need to know how and why parks change over time to make sound management decisions. National parks have a tremendous opportunity to provide consistent monitoring of change due to the relative stability of

park administration within and between park units, provided that monitoring guidelines can be flexible and inexpensive to implement.

Parks in the western USA are home to vast extents of alpine ecosystems, which are forecast to change dramatically in coming decades (Vale 1987; Hansen et al. 2001; Seastedt et al. 2004). Alpine (and arctic) ecosystems have long been assumed to be critical ecosystems for detecting and characterizing climate change (Billings and Bliss 1959; Henry and Molau 1997; Walker et al. 1993; Walker et al. 1994; Walker et al. 1995). Alpine treeline, the boundary between forest and tundra on high mountains, is a particularly attractive system in which to investigate forest dynamics due to the abundance of high-resolution paleoecological records of growth from climatically sensitive trees associated with subalpine forest (Graumlich et al. 2004). While tree growth and reproduction at alpine treeline are primarily temperature limited (Wardle 1974), precipitation is also an important factor at alpine treeline (Lloyd and Graumlich 1997). The combination of a rich paleoclimatic record with a dynamic ecosystem has made alpine treeline an attractive system to monitor for assessing the impacts of global climate change and an important area for natural resource management (Vale 1987).

The alpine treelines of the Sierra Nevada in and between Sequoia and Yosemite National Parks have been the subject of numerous paleoecological studies. Past treeline studies in the Sierra Nevada have largely focused on tree growth patterns in response to fluctuations in temperature and precipitation (e.g., Scuderi 1987; Graumlich 1991; Graumlich 1993; Caprio and Baisan 1992; Scuderi 1993; Millar et al. in press; Bunn et al. in review a; b). Sierran treelines are also dynamic in space and move up and down slope

over decades to centuries (Lloyd 1996; Lloyd and Graumlich 1997; Millar et al. in press). The goal of this study was to refine our conceptual models of treeline dynamics in order to highlight ways that Sierran treelines might change in the coming decades.

Changes in treeline structure and position in the Sierra Nevada will probably not be ubiquitous but are likely to be idiosyncratic and species specific (Dullinger et al. 2004; Millar et al. in press). The effect of species autecology, competitive interactions among species, and the expression of climate across complex topography makes the biotic response of even relatively simple ecosystems like alpine treeline potentially complex. This is further compounded with a paucity of spatial data at fine enough scales to be useful to land managers. In this paper, however, we demonstrated a way to further knowledge of potential treeline changes using coarse-scale land cover data that can be used to predict areas likely to change and then refined those predictions with remotely sensed imagery. We used coarse scale land cover data at km resolution to project bioclimatic envelopes for six species of Sierran treeline conifers under climate change scenarios. We then used treeline density data derived from satellite imagery for two areas where bioclimatic envelopes are likely to undergo change in the coming decades. The research described below is general enough to further understanding of basic issues in treeline ecology in ways that can inform monitoring of this system.

Methods

This study encompassed much of the alpine treeline in the southern Sierra Nevada. We used analyzed data at two different spatial scales with different techniques.

The coarser-scale data had one km resolution and used land-cover types and output from a spatially explicit climate simulator. We used constrained ordination and a General Additive Modeling (GAM) approach for understanding treeline at this scale. The finer-scale data had ten m cells and comprised of classified satellite imagery and proxies for soil moisture and radiation derived from an elevation model. We used regression tree analysis to understand treeline at this scale. Due to the complexity of the study, we present the methods by describing the data and analysis at the coarse and finer scales separately after generally describing the study area.

Study Area

This study encompassed the alpine treeline ecotone in the Sierra Nevada from Sequoia National Park to Yosemite National Park (Fig. 6.1). The Sierra Nevada Mountains rise from near sea level to 4,418 m a.s.l. in less than 100 kilometers horizontal distance creating extremely steep gradients in temperature and precipitation. Between 3000-3400 m a.s.l. there tends to be a well-defined treeline (Arno and Hammerly 1984). The Sierra Nevada is also home to a wide variety of long lived and hardy treeline species. Foxtail pine (*Pinus balfouriana* Grev. et Balf.), Jeffery pine (*P. jeffreyi* Grev. et Balf.), lodgepole pine (*P. contorta* var. *murrayana* Dougl. ex Loud.), red fir (*Abies magnifica* A. Murr.), western white pine (*P. monticola* Dougl. ex D. Don), whitebark pine (*P. albicaulis* Engelm.), and limber pine (*P. flexilis* James) grow at near treeline on both sides of the Sierran crest in considerable numbers. Other species, like western juniper (*Juniperus occidentalis Englem.*) also occur at treeline in smaller populations. Although

all species are hardy, species demonstrate different growth forms and niches at treeline (see below).

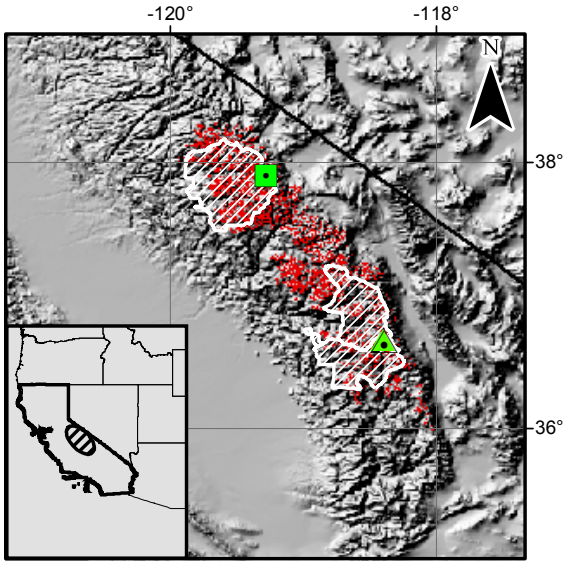

Fig. 6.1. Treeline is shown from Sequoia - Kings Canyon to Yosemite National Park along with the boundaries of those parks. The triangle is the location of an IKONOS image for Upper Wright Lakes while the square is the locations of an IKONOS image for Lee Vining. Both images are 5 km by 5 km.

Coarse Scale Portion of the Study

Coarse Land Cover Data. A digital coverage of the alpine treeline was created in the Geographic Information System ArcGIS (ESRI 2002). Scanned images of the U.S. Geological Survey (USGS) standard series topographic maps were obtained as digital raster graphics at 1:24,000 resolution. A grid of dots was overlaid evenly at 500 m intervals. Alpine treeline was digitized on screen by following the upper extent of vegetation classed as “woods” from the topographic maps using the overlaid 500 m grid

to ensure a consistent mapping unit. This treeline coverage was transformed into a raster with one km cells after being buffered five hundred meters downslope. Finally, a potential treeline habitat map was created by buffering the treeline coverage upslope from the existing treeline up to the highest elevation possible. Because trees are rare on very steep slopes, we omitted all the 1 km cells with an average slope angle greater than 45% as calculated from the 30 m DEM.

A raster land cover dataset with one km cells for the Sierra Nevada was obtained from the Sierra Nevada Ecosystem Project (SNEP) data archive (Davis and Stoms 1998). Grid cells were coded by percentage to primary, secondary, and tertiary land cover using the California Natural Diversity Data Base natural communities classifications based on Holland's (1986) vegetation types. The land cover classes for all the digitized treeline cells were extracted. If the primary cover class was a non-forest class (e.g., montane meadow, dwarf shrub, barren, water) the cell was dropped, leaving 1809 cells classified as foxtail pine, Jeffery pine, lodgepole pine, red fir, western white pine, whitebark pine, and limber pine. Red fir and western white pine were further aggregated into a single class based on their elevational and landscape characteristics in the montane forests on the western slope of the Sierra Nevada. Whitebark pine and limber pine were also collapsed into a single class given the tendency of these species to grow in mixed stands at treeline where they are virtually impossible to distinguish without the cones being present (Arno and Hammerly 1984). The final data matrix used for characterizing treeline communities is summarized in Table 6.1.

Table 6.1. Sierran treeline communities coded by primary cover type (greater than 80% coverage) for the coarse scale data. Percentages sum to 100.

Common Name	Standard Name	Abbreviation	Percentage of Treeline Cells (n = 1809)
Foxtail pine	*Pinus balfouriana*	Piba	4.4
Jeffery iine	*Pinus jeffreyi*	Pije	7.5
Lodgepole iine	*Pinus contorta*	Pico	34.7
Red fir – western white pine	*Abies magnifica – Pinus monticola*	Abma – Pimo	35.9
Whitebark pine – limber pine	*Pinus albicaulis – P. flexilis*	Pial – Pifl	17.5

Climate Data. A climate dataset was developed using the DayMet model (Thornton et al. 1997), which estimates daily meteorological variables from 1980–1997 over the United States using interpolated weather station data with adjustments for topography. These were combined into annual summaries, imported to ArcGIS, and clipped to the study area.

The growth and reproduction of Sierra Nevada conifers at the alpine treeline are known to be related to temperature and precipitation (Graumlich 1993; Lloyd 1996; Lloyd and Graumlich 1997). We limited analysis to two climate variables for this study: total yearly precipitation during the calendar year and average minimum daily temperature. We chose to use minimum daily temperature rather than mean temperature because evidence suggests that growth and reproduction at high elevation is strongly related to minimum temperatures (Allen 2002; Wilson and Luckman 2003; Millar et al. in press). Minimum temperatures have also been changing more rapidly than mean or maximum temperatures at high elevations (Diaz and Bradley 1997). This reduction in the diurnal temperature range could be especially important at treeline (Barry 2001).

Analysis. Previous work by others has given us a wealth of physiological and ecological evidence to support the idea that average minimum temperature and total precipitation strongly pattern treeline forests. To define these relationships with respect to our current data set, we performed a constrained ordination of the community composition by the climate variables in order to characterize treeline forests in the Sierra. We used Canonical Analysis of Principal Coordinates (CAP), where the community composition matrix was summarized using the Bray-Curtis (1957) dissimilarity index, which emphasizes shared abundances in species composition (McCune and Grace 2002), and is generally acknowledged to be a good measure of ecological distance for species abundances (Legendre and Legendre 1998). This family of ordination is growing in popularity in community and landscape ecology and is similar to more popular constrained ordination techniques like Canonical Correspondence Analysis (ter Braak 1986; 1987; Jongman et al. 1995). CAP begins with the calculation of dissimilarities within the vegetation matrix, followed by principal coordinate analysis, followed by redundancy analysis on the climate matrix (Anderson and Willis 2003). The ordination was performed using the Vegan contributed package (Oksanen 2004) to the R statistical programming environment (Ihaka and Gentleman 1996). A permutation test, implemented in Vegan, was used to gauge the effectiveness of the constraints in ordination using the pseudo-F statistic (Legendre and Legendre 1998).

Based on the results of the ordination and ancillary exploratory analysis, we created bioclimatic envelopes for foxtail pine (PIBA), lodgepole pine (PICO), and the whitebark - limber pine complex (PIAL-PIFL) using spatially explicit general additive

models (Lehman et al. 2002) with the contributed GRASP-R package (Fivaz et al. 2003). GRASP-R fits a surface as a function of the predictor variables with GVC-optimized binomial regression and can be used to make predictions in geographic space by using the spatial patterns of the predictor surfaces (Lehman et al. 2002). This has been shown to capture large-scale relationships between biotic characteristics and the environment and to make good spatial predictions using model relationships to interpolate within the predictor space (Lehman et al. 2002).

Climate Change Scenarios. We used climate change predictions from the general circulation models HadCM3 and CCC as implemented in the VEMAP2 program for the simulated period 1993-2100 over the conterminous United States arrayed in topographically-adjusted half degree cells (Schimel et al. 2000). We extracted the layers for average minimum daily temperature and total precipitation and clipped the layers to the study area. We used the DayMet model as the baseline and calculated the median difference in temperature and precipitation estimates for both model scenarios. We used the climate change scenarios and the niche model for each species to predict probability surfaces for the potential treeline habitat map resulting in maps that indicate shifts in the potential niche of these species under climate change.

Fine Scale Portion of the Study

Satellite and Abiotic Proxy Data. We used classified IKONOS imagery from two sites to develop understanding of the alpine treeline ecotone in relation to the abiotic physical template of the landscape, at a finer scale of 10 m cells (Fig. 6.1). We chose two sites at either end of the study area populated with different species. The site at Upper

Wright Lakes in Sequoia National Park is dominated by foxtail pine while the site at Lee Vining near Yosemite National Park is dominated by mixed stands of whitebark and limber pine. Multi-spectral imagery (four m cells) from the IKONOS sensor was combined with a slope layer calculated from a ten m digital elevation model and classified using stochastic gradient boosting, a refinement of classification tree analysis (Lawrence et al. 2004). We chose a simple four-way classification scheme of water, meadow, rock, and tree and performed an accuracy assessment with data independent from the training set (Appendix). We passed a moving window (10,000 m^2) that averaged the pixels classified as tree to obtain a relative measure of tree density [0-100%].

Although foxtail pine does not grow in a dwarfed or stunted form like other treeline species, it does occur with stunted forms of whitebark pine where their ranges overlap. For this study, therefore, we define the treeline as the altitude limit above which trees no longer occur, even in severely distorted forms (Smith et al. in press). Timberline, in contrast, has been defined as the elevation at which trees occur with upright growth form and not in distorted stunted forms, like krummholz (Tranquillini 1979, Arno and Hammerly 1990, Stevens and Fox 1991). The treeline ecotone was digitized with a minimum mapping unit of 10 meters using the one m panchromatic band of the IKONOS imagery. The line coverage was buffered 100 m downslope and used to clip a relative tree density map (RTD). One hundred meters was chosen as a distance to isolate the trees closest to the treeline where the effects of climate are likely the strongest force on regeneration as compared to, for instance, stand dynamics (Lloyd and Fastie 2002).

We described treeline density with respect to proxies for soil moisture and radiation. Topographic convergence and potential relative radiation were calculated from a 10 m digital elevation model (DEM) with spurious sinks filled to remove data anomalies according to standard procedures (Jenson and Domingue 1988). Topographic convergence index (TCI) is a function of upslope contributing area and slope and describes how water collects on landscapes (Moore et al. 1991; Urban et al. 2000; Bunn et al. 2003). The index has high values in coves or streambeds, has lower values on drained areas such as ridge tops, and is a good predictor for soil moisture (Lookingbill 2003; Lookingbill and Urban in press). The potential relative radiation (PRR) index utilizes measurements of sun location over the course of a year and a shading function common to most GIS packages to measure the relative amount of sunlight that a particular raster element receives given the shading that the local neighborhood provides (Bunn et al. 2003). This index is a good predictor for air temperature (Lookingbill and Urban 2003).

Analysis. We used regression tree analysis to describe relative treeline density. Regression trees devise a step by step scheme that partitions the dependent variable (i.e., relative treeline density) on the independent variables (i.e., PRR and TCI) recursively into subsets that are increasingly homogeneous (McCune and Grace 2002). This system is similar to classification trees used in taxonomy. Regression trees are robust to spatial dependence and nonlinearities in data and provide highly interpretable results. We used the Rpart contributed package in R to implement the trees (Therneau and Atkinson 2002).

The trees were grown until they reached a split that did not increase the model fit by 0.01 at each step.

Results

Coarse Scale

The five classes of Sierran treeline forest were unevenly distributed by dominant species and showed variability in community composition (Tables 6.1 and 6.2). The species dominant in each cell occupied different distributions of minimum temperature and precipitation at treeline through their range in the Sierra and between species (Fig. 6.2). Jeffery pine cells at treeline, for instance, were considerably colder than cells throughout the rest of the range. In contrast, foxtail pine, which had similar distributions at treeline and within its range but was on considerably colder cells than Jeffery pine. The CAP ordination supported this exploratory data and showed the species sorting distinctly in the ordination space according to the biplot vectors for minimum temperature and precipitation (Fig. 6.3). The correlation between average minimum daily temperature and axis one was 0.97. The correlation between average minimum daily temperature and axis two was -0.26. The correlation between total precipitation and axis one was 0.46 while the correlation between total precipitation and axis two was 0.85. Axis one of the CAP ordination explained 51% of the variance in the original ordination space and axis two explained 27%. A permutation test of the significance of the constrained eigenvalues yielded a pseudo-F of 0.34396 (p-value < 0.0001 with ten thousand permutations)

indicating a good fit of composition by minimum daily temperature and total precipitation.

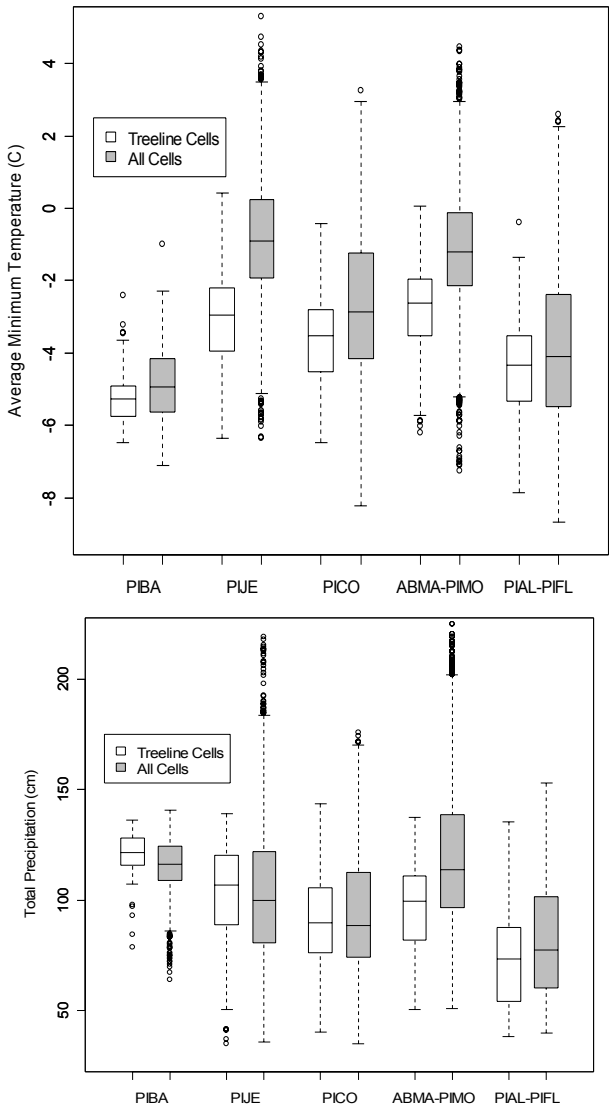

Fig. 6.2. Box plots for the historical climate range for annual average minimum daily temperature and for total annual precipitation are shown at treeline (white) and through their range in the Sierra (gray). The boxes range from the 25^{th} – 75^{th} quantile and the lines extend from the 5^{th} – 95^{th} quantile. The center line is the median and the dots are outliers.

Table 6.2. Summary of the community matrix used in the ordination of the coarse scale data.

	Number of Cells in Each Category				
% Cover	Piba	Pije	Pico	Abma-Pimo	Pial-Pifl
90-100%	50	76	271	377	146
80-90%	29	40	253	109	61
70-80%	-	12	69	60	44
60-70%	-	-	2	-	-
50-60%	-	-	3	-	-
40-50%	-	-	-	-	6
30-40%	-	4	-	1	1
20-30%	-	12	48	38	89
10-20%	5	30	60	194	29
0-10%	1725	1635	1103	1030	1433

The GAM models converged with good generalized cross validation statistics for all species (Table 6.3). The percent deviance explained by the models was relatively low for all the species except foxtail pine. Using the model fits to predict over the range of observed climate allowed a graphical representation of the realized niches for the species (Fig. 6.4). The climate change models predicted an increase of 27 cm in total annual precipitation under the HAD model and 80 cm under the CCC model for the study area. Temperatures predictions were more coherent between scenarios with the HAD model estimating a degree rise in average daily minimum temperature and the CCC model estimating two degrees (Fig. 6.5). The extrapolation of the GAM models using the predicted climate and the potential treeline habitat map allowed visualization of the potential range shifts (Figs. 6.6-6.9).

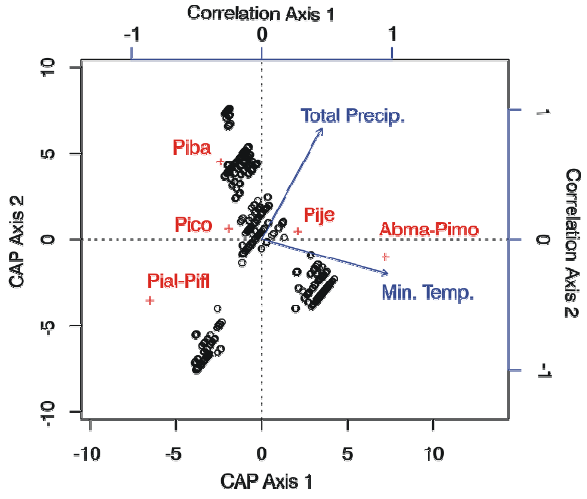

Fig. 6.3. A Canonical Analysis of Principal Coordinates of treeline community composition is shown as a triplot. Sites are shown with circles and community types (species) are shown with plus signs. Correlations with the predictor variables are shown as vectors.

Fine Scale

The median relative density of foxtail pine was 37% at the ten m scale. This was lower than the median density of whitebark pine, which was 62% (Fig. 6.10). The calculation of the TCI and PRR indices produced similar distributions to those seem in other studies (Fig. 6.11; Bunn et al. 2003; Lookingbill and Urban 2003). The regression tree analysis of relative density on TCI and PRR yielded two very different trees (Fig. 6.12). The tree for the foxtail-pine dominated forests at Upper Wright Lakes explained 44% of the variance of relative treeline density while the whitebark / limber pine complex dominated site at Lee Vining explained 48% of the variance in relative treeline density.

Both trees used the explanatory variables PRR and TCI but in different ways as discussed below.

Discussion

The composition of species at treeline in the Sierra Nevada was tied to the climate patterns seen in the instrumental climate record. Furthermore, the distributions of species across the study area and the climate window occupied by each species at treeline were coherent with our understanding of species autecology. Foxtail pine, for instance, is considered a true treeline species, which does not tend to grow well below treeline (Arno and Hammerly 1984). The range of precipitation and temperature values occupied by the treeline cells is similar to the range of values occupied by the species throughout the Sierra Nevada (Fig. 6.2). The same is true for the whitebark / limber pine complex, which are the other true treeline species in the study. Lodgepole pine showed similar response but with tails of the distribution that were more similar to conditions downslope. These relationships contrasted strongly with the red fir / white pine complex, which typically grow at the higher end of the mixed conifer zone in the Sierra Nevada but still well below treeline (Urban et al. 2000). These species, along with Jeffery pine, are less well suited to the severe conditions at treeline and lack certain adaptations for succeeding in such harsh environments such as needle retention over many years, the ability to grow in dwarfed form (although see discussion of foxtail pine below), and extreme longevity. The red fir / white pine complex at treeline were growing in locations that were colder and drier than through the rest of the range. This corresponds with classic notions of species

distributions, environmental gradients, and ecological tolerance (Whittaker 1956; 1960). Seen in that light, red fir and white pine are growing in the tail of the suitability envelope at treeline while foxtail pine at treeline is situated in the heart of its, albeit narrow, niche.

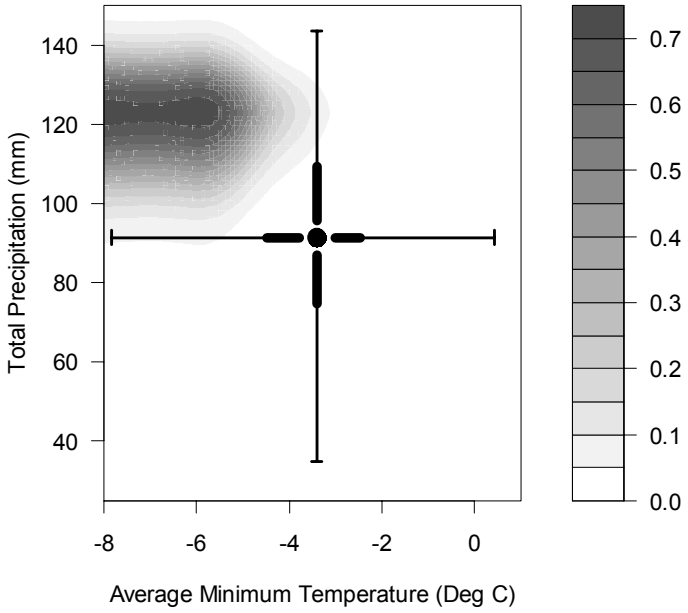

Fig. 6.4. A probability surface for foxtail pine occurrence as a function of annual average minimum daily temperature and total annual precipitation is shown. Note the correspondence with figures two and three. The range of the historical observed climate range is also shown. The circle at the center is the 50th quantile, the boxes range from the 25th – 75th quantile and the lines extend from the 5th – 95th quantile for each variable.

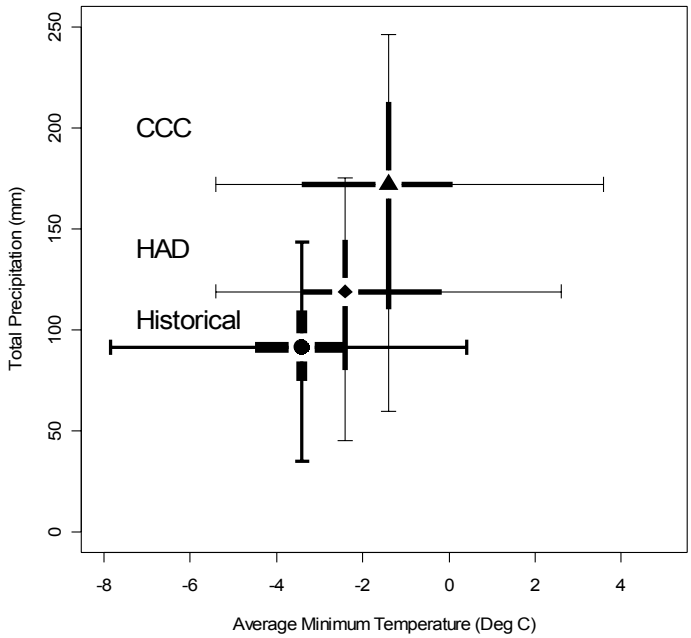

Fig. 6.5. Two climate change scenarios at current treeline in the Sierra are shown with the historical climate range for annual average minimum daily temperature and for total annual precipitation. The center of each plots is the 50th quantile, the boxes range from the 25th – 75th quantile and the lines extend from the 5th – 95th quantile.

The exploratory analysis of treeline distributions versus regional distributions was complemented by the ordination of treeline species composition (Fig. 6.3). The constrained ordination space explained 78% of the variance in the species composition matrix supporting our decision to limit the analysis to the climate variables we believed to be proximate controls at treeline. The sorting of species in the ordination also supported our understanding of each species' distribution and autecology. The radial growth, reproduction, and population ecology of foxtail pine, for instance, has been strongly tied to variability in temperature and precipitation over the past three millennia

(Lloyd and Graumlich 1997). No such linkage has been made in the red fir / western white pine stands at treeline in Sequoia National Park despite repeated efforts (Graumlich unpublished data). This analysis showed red fir / western white pine stands occupying the warmest areas of treeline forest in the Sierra. As such, the lack of strong paleoecological inference in these species is not surprising as classic notions of the alpine treeline ecotone suggest that the best locations for such inference would be trees in the coldest environments (e.g., Fritts 1976). This is further coupled with other aspects of the ecology of these species, which are not extremely long-lived. The maximum ages observed in the Sierra Nevada are about 500 years but usually less than 100 years (e.g., King and Graumlich 1991; Graumlich unpublished data). Although not quantified, at some of the red fir / western white pine dominated stands at treeline we have observed extremely steep topography immediately upslope that would preclude tree establishment and remove the potential for hardier species to establish in adjacent colder environments upslope.

Table 6.3. The GAM models for species presence / absence converged to small gradients with positive definite Hessian matrices

	Number of Iterations	RMS error at convergence	Deviance explained	GCV Score
PIBA	4	2e-07	55.2%	0.69
PIJE	5	2e-06	9.8%	0.96
PICO	7	9e-07	17.7%	1.00
ABMA-PIMO	8	1e-05	18.7%	0.95

The sorting of foxtail pine, lodgepole pine, and the whitebark / limber pines in the ordination space also corresponds with species biology. Those species show more classic

adaptations to cold conditions, including the ability to grow in dwarf forms (whitebark, limber, and lodgepole pine) or in massive strip-bark forms (foxtail pine). The sorting of foxtail pine and whitebark / limber pine slightly further out on the minimum temperature vector than lodgepole pine also reinforces the observation that these species usually occur at the absolute treeline, with lodgepole pine tending to mix in the stands a few hundred meters below treeline. The sorting of foxtail pine, lodgepole pine, and whitebark / limber pine along the precipitation vector is also interesting. The radial growth of foxtail pine correlates extremely well with the instrumental precipitation record (Graumlich 1991; Graumlich 1993; Lloyd and Graumlich 1997) and lodgepole pine less so (Graumlich 1991). The relationship between treeline whitebark pine growth and precipitation is not as well defined but not nearly as robust as with foxtail pine (Graumlich unpublished data).

Regional species occurrence was also well modeled statistically using the GAM approach (Wood 2000). That the models explained a relatively low amount of deviance in the presence / absence data should not be surprising given the lack of balance in the observed data (Table 6.2) and difficulties associated with presence / absence data. The occurrence of so many zeros (absences) in abundance data are well recognized in ecology (Beals 1984). It is impossible to ultimately know why a species does not occur on a site, and inferring reasons for a species absence are difficult (McCune and Grace 2002). The remainder of the variation in the model could be accounted for by competitive interactions among species that share these environmental niches for example. Similarly, local effects associated with the distributions of some species distributions are likely to

be heterogeneous at scales too fine for these models to captured (McKenzie et al. 2003). This is likely the case for Jeffery pine, which is especially common on local rock outcroppings and other xeric, infertile sites (Waring and Major 1964; Urban et al. 2000).

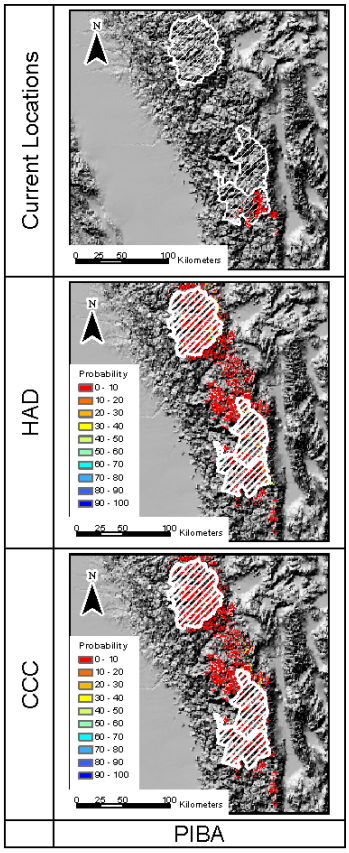

Fig. 6.6. The current locations of foxtail pine in the Sierra Nevada from Sequoia to Yosemite National Parks are shown in the top row. Bioclimatic envelopes have been projected in areas that are at or above current treeline using projected climate change 1993-2100 from the HAD and CCC GCMs.

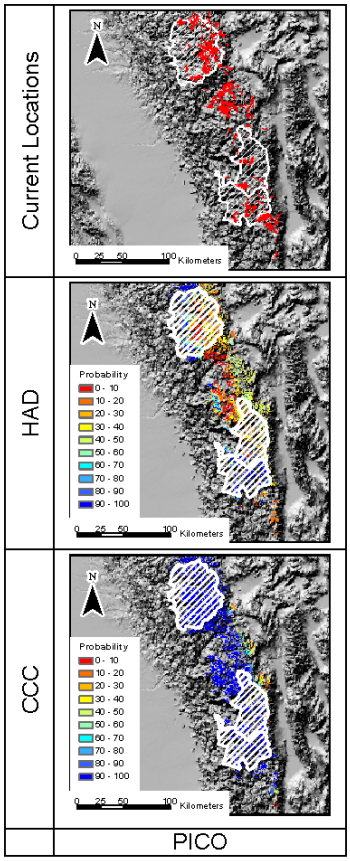

Fig. 6.7. The current locations of lodgepole pine in the Sierra Nevada from Sequoia to Yosemite National Parks are shown in the top row. Bioclimatic envelopes have been projected in areas that are at or above current treeline using projected climate change 1993-2100 from the HAD and CCC GCMs.

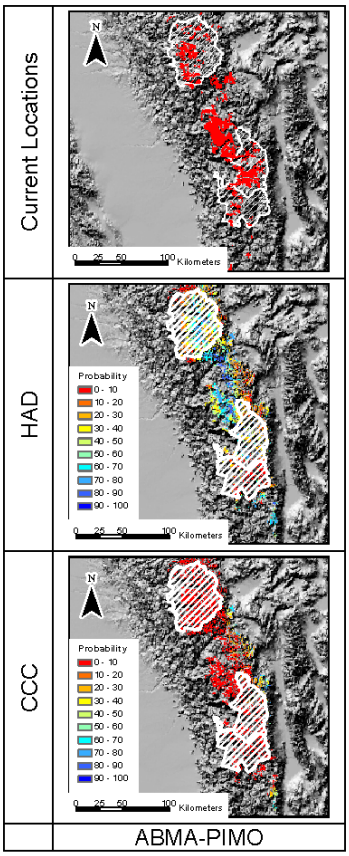

Fig. 6.8. The current locations of red fir and western white pine in the Sierra Nevada from Sequoia to Yosemite National Parks are shown in the top row. Bioclimatic envelopes have been projected in areas that are at or above current treeline using projected climate change 1993-2100 from the HAD and CCC GCMs.

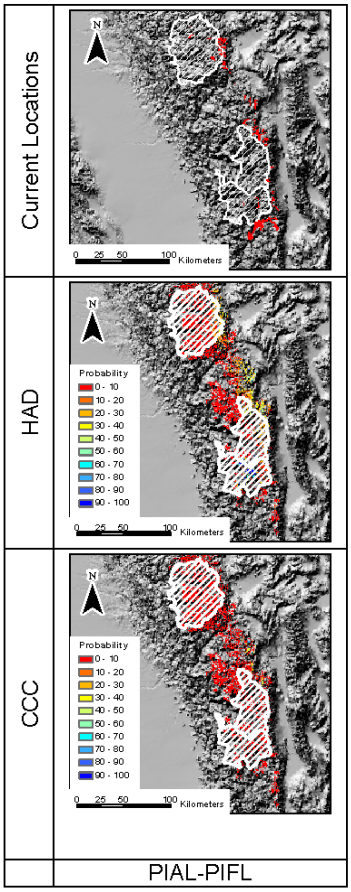

Fig. 6.9. The current locations of high elevation whitebark pine and limber pine in the Sierra Nevada from Sequoia to Yosemite National Parks are shown in the top row. Bioclimatic envelopes have been projected in areas that are at or above current treeline using projected climate change 1993-2100 from the HAD and CCC GCMs.

The chief benefits of these models are to quantify the probability of species presence in the historical climate space and make spatial predictions on the landscape. We can also see the correspondence between the GAM model predictions and the ordination. The foxtail pine probability surface, for instance, showed high occurrence at low temperatures and high precipitation (Fig. 6.4), which matches the location of foxtail

pine relative to the vectors in the ordination space. Most importantly, these models allowed us to develop change scenarios.

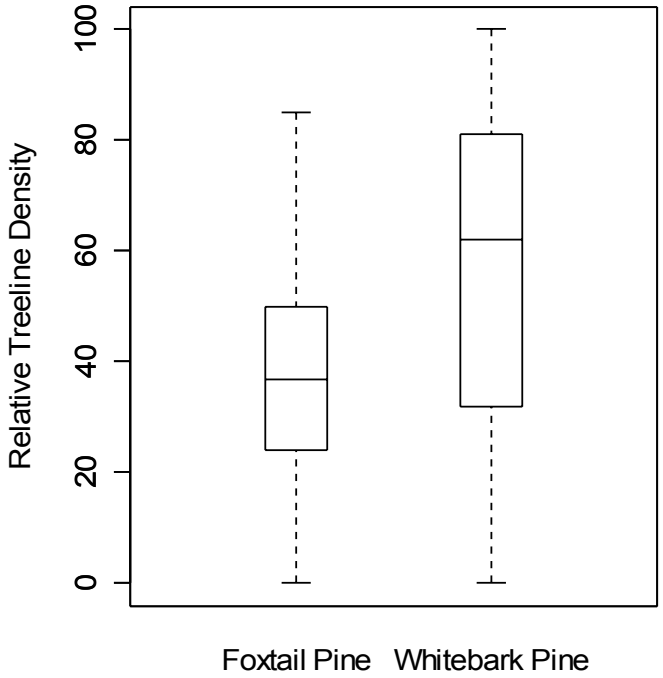

Fig. 6.10. The distributions for relative treeline density are shown for foxtail and whitebark pine in the IKONOS image for Upper Wright Lakes and Lee Vining respectively. The center of each plots is the 50th quantile, the boxes range from the 25th – 75th quantile and the lines extend from the 5th – 95th quantile.

Across the globe, climate change predictions are particularly severe at high elevation (IPCC 2001), and the change predictions in the Sierra Nevada extracted from the VEMAP data are no exception. The median difference between the half degree cells from VEMAP and the one km cells from DayMet under the HAD scenario pushed the treeline environment into the 75% quantile of historical climate and the CCC scenario reached an analog not seen in the historical record (Fig. 6.5). When these climate

scenarios were used to make predictions about the potential for treeline expansion the results were striking. Under both change scenarios, for example, the narrow climate envelope inhabited by foxtail pine virtually disappeared from treeline and alpine habitats in the Sierra Nevada (Fig. 6.6). The climate envelope for lodgepole pine, in contrast, was predicted to greatly expand but was highly dependent on the scenario (Fig. 6.7). A similar difference in scenarios was seen for the envelope for red fir / western white pine, which existed in abundance under the HAD scenario but not the CCC scenario (Fig. 6.8).

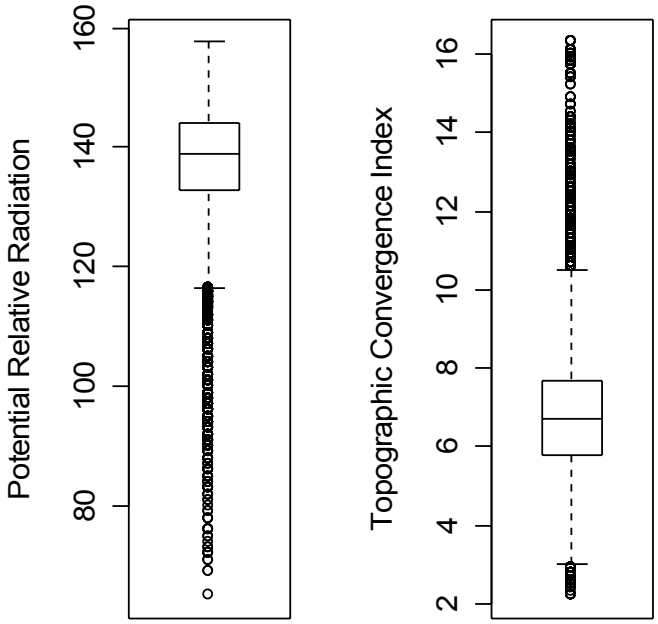

Fig. 6.11. The distributions for Potential Relative Radiation and Topographic Convergence Index are shown. The center of each plots is the 50th quantile, the boxes range from the 25th – 75th quantile and the lines extend from the 5th – 95th quantile.

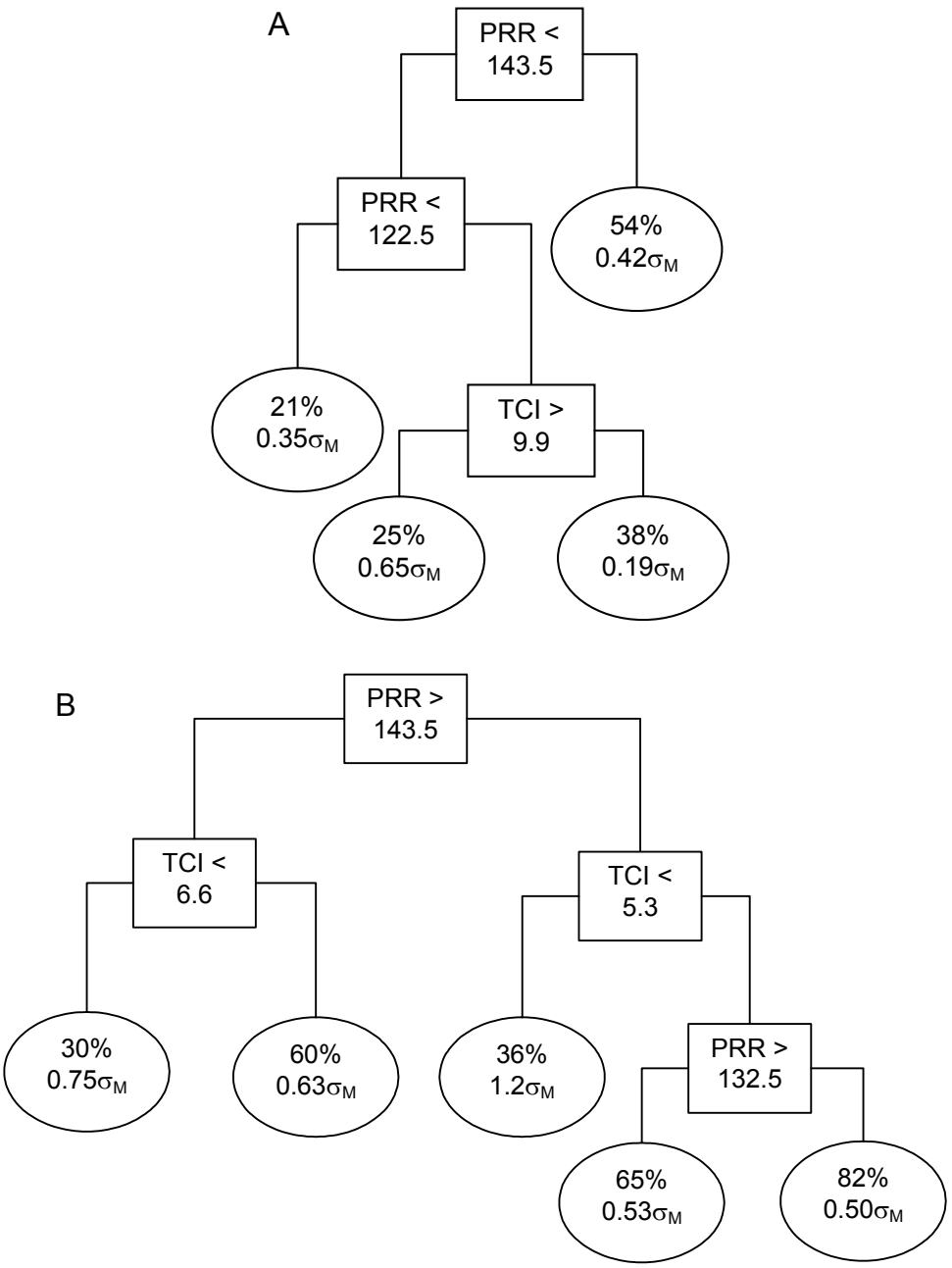

Fig. 6.12. Regression trees for relative treeline forest density are shown for two plots. Upper Wright Lakes (A) is dominated by foxtail pine and Lee Vining (B) is dominated by mixed whitebark and limber pine. The regression trees are read with the signs of the variables indicating a split to the left and the percentages shown at the bottom are relative density with the standard error of the mean shown at the bottom.

We do not suggest that these envelopes be considered as maps of future species compositions, but rather used as a guide to think about potential biotic changes in ecologically realistic ways. Many of the whitebark and foxtail pines found at treeline, for instance, are many hundreds of years old. The inertia of these mature individuals, which were recruited during past climate regimes, is likely sufficient to remain on a site long after these models would predict their absence (e.g., Dunwiddie 1986; McKenzie et al. 2003). Predictions of climate change, however, in the coming century are of a magnitude and rate not seen in at least the last millennium (IPCC 2001). The expansion of lower elevation species like lodgepole pine, western white pine and red fir are therefore of concern because of the changes they will make to the successional cycle and the potential for increased disturbance (fire and pathogens), largely through densification of the sparse treeline forests. Lodgepole pine in the Sierra Nevada is fire sensitive and expansion in the Sierra Nevada is particularly interesting in this light. When fires occur in Sierra Nevada lodgepole stands, they are usually intense and extensive (Rundel et al. 1977). This is very much unlike the fire pattern in high elevation foxtail pine sites where surface fires are extremely infrequent and low intensity (Mastroguiseppe and Mastroguiseppe 1980).

The models above were likely too coarse spatially to look for the “fingerprint” of change by themselves (Root et al. 2003) anticipated at treelines in the Sierra. They also did not take into account the plasticity of individual species in their response to the bioclimatic effects of complex topography at treeline. The use of moderately high-resolution satellite imagery partially filled that gap by informing our conceptions of how foxtail and whitebark pine adapt to microclimates at the scale of meters. The regression

tree analysis for each species captured much of the variability and used the physical proxies related to temperature and soil moisture in different ways that corresponded to species autecology.

Foxtail pine has a deep spreading root system much like a desert shrub (Arno 1973) and allows for considerable storage effect (Lloyd 1996; and see Chesson and Huntly 1997). Foxtail pines are also able to maintain photosynthetic activity in extremely cold environments due to high tracheid density and the retention of needles for up to a decade, which reduces the need for nutrients (Mastroguiseppe and Mastroguiseppe 1980). Unlike most other treeline species, foxtail pine does not grow in a dwarfed krummholz form and maintains an upright growth form to its elevational limit. Whitebark pine, in contrast, does grow in krummholz mats and produces large skirts of foliage near the ground that are covered by snow in the winter and protected from desiccation (Arno and Hammerly 1984). The krummholz growth form has been exhaustively described and is best conceived of as structural facilitation where the dense growth form acts to enhance photosynthetic carbon gain and survival of seedlings (Smith et al. 2003 provide a review). The amelioration of microclimates creates a positive feedback loop that increases seedling abundance, which is followed by further facilitation. Krummholz mats also trap snow, efficiently creating cover for needles and shoots during winter and warmer needle temperatures and greater photosynthesis in spring and summer (Hadley and Smith 1987). The difference in growth form might account for the lower relative density at treeline at Upper Wright Lakes, which is typical of the open park-like stands that occur in foxtail pine stands near the ecotone (Mastroguiseppe and Mastroguiseppe

1980). Whitebark pine tends to grow in denser stands immediately below treeline in large krummholz mats that transition into denser forests comprised of trees with skirted bases (Arno and Hammerly 1984).

Growth form is not a passive trait in these trees but an active mediator of the environment. The difference in the way the regression trees used the proxies for soil moisture (TCI) and temperature (PRR) might be related to the differences in growth forms for these two species. Foxtail pine density was low at sites with radiation values below the median of the distribution and lowest in the low radiation sites (Figs. 6.11 and 6.12). Sites that were dark and wet also had very low density. The highest density sites were located in the brightest spots. We interpret the tendency for foxtail pine to grow densely in the warmest microsites to its ability to utilize water efficiently and take advantage of early season growing conditions. The lack of traditional self-structuring facilitation in foxtail pine dictated by its upright growth form might help high radiation sites melt earlier as sub-canopy long-wave radiation can be a significant component of melt energy under conditions of strong insolation (Pomeroy et al. 2003). Other possibilities exist, however, and the higher density could be related to processes leading to decreased mortality (e.g., as shelter from damaging wind) or increased seed rain (e.g., by trapping windborne seed). Determining a precise mechanism would require an extensive study and might or might not increase the success of future monitoring efforts.

The whitebark pine treeline at Lee Vining made more complex use of PRR and TCI with the lowest density cells occurring in the dry microsites (especially if those sites were also bright) and the highest density cells occurring in the dark and wet sites. The

ability for whitebark pine to grow densely in dark and wet microsites that are cold and where snow remains late into the spring can be explained by the formation of dense krummholz, which can increase local needle temperature and trap snow to provide soil water for much of the growing season (Smith et al. 2003). That low density whitebark was found in low TCI sites (30% and 36%,) regardless of the first split of the regression tree on PRR indicates the potential importance of drifting snow for this species. The same elasticity of whitebark pine might explain the lower densities seen in the brighter and drier sites where the trees are growing upright in stands that more closely resemble the park-like stands seen in foxtail pine forests.

Conclusions and Prospectus – a Call for Monitoring

Our models indicate the potential for tremendous change in the bioclimatic envelopes of treeline species in the coming decades. Empirical models, such as the ones presented above, are data-driven and self-calibrating (McKenzie et al. 2003). Although empirical models have inherent uncertainty (Elith et al. 2002), they also have tremendous potential to predict species distributions under climate change, particularly when coupled to sensitivity analysis of climate scenarios (Hannah et al. 2002). Establishing inventory and monitoring protocols are a major lacuna in global change research in general and in protected areas management in particular. However, there are fundamental discrepancies in the resolution of reliable climate data and the complexity of species response at scales useful for *in situ* field work.

Our bioclimatic models indicate that montane tree species like lodgepole pine, red fir, and western white pine will be able, in the coming decades, to invade treeline habitats

currently occupied by foxtail, limber, and whitebark pine. Recent research near Yosemite National Park indicates that these invasions are happening already and are more complicated than the simple iconography of treeline creeping upslope (Millar et al. in press). Our regression tree models indicate that there is substantial mediation of forest structure in relation to the abiotic template of the landscape. Related research shows that stand age-class structure and ring width patterns of foxtail pine are linked to the same proxies for soil moisture and radiation (Bunn et al. in review b). There has not been a systematic effort to locate places on the landscape where change in species composition is most likely to take place, and predicted changes in species composition at the scale of kilometers are still too coarse to be useful in a monitoring protocol. The interaction of coarse-scale changes in distribution and finer-scale mediation of forest structure with complex topography provides opportunities. The prediction of distribution changes can be further refined using terrain modeling with finer scale elevation models to partition the landscape into manageable plots for on-the-ground investigation (e.g., Urban 2000).

The alpine treeline ecotone in the Sierra Nevada is poised to experience massive changes in species composition and structure. Changes in subalpine forests need to be quantified for myriad of management reasons at global scales (furthering understanding of carbon sequestration in mountain systems – e.g., Schimel et al. 2002), regional scales (changes in snow pack density and extent for water planning – e.g., Dettinger and Cayan 1995), and local scales (the loss of rare habitat types like wet subalpine meadows – e.g., Vale 1987). There are multiple management agencies in the Sierra Nevada that have a stake in understanding global change impacts over the coming decades. Together, they

have the potential to establish a robust and flexible monitoring program that can disentangle regional climate change impacts on a complex landscape and address the pressing management challenges of the day.

References

Allen K.J. (2002) The temperature response in the ring widths of *Phyllocladus asplenifolius* (celery-top pine) along an altitudinal gradient in the Warra LTER area, Tasmania. *Australian Geographical Studies* 40, 287-299

Anderson M.J. and Willis. T.J. (2003) Canonical analysis of principal coordinates: a useful method of constrained ordination for ecology. *Ecology* 84, 511-525

Arno S.F. (1973) *Discovering Sierra Trees*. Yosemite Association, Yosemite National Park, CA

Arno S.F. and Hammerly R.P. (1984) *Timberline: Mountain and Arctic Forest Frontiers*. The Mountaineers, Seattle, WA

Barry, R.G. (2001) Mountain climate change and cryospheric responses: a review. Proceedings of the World Mountain Symposium, Interlaken, Switzerland

Beals E.W. (1984) Bray-Curtis ordination: an effective strategy for analysis of multivariate ecological data. *Advances in Ecological Research* 14, 1-55

Billings W.D. and Bliss L.C. (1959) An alpine snowbank environemnt and its effects on vegetation, plant development, and productivity. *Ecology* 40, 388-397

Blaustein A.R., Root T.L., Kiesecker J.M., Belden L.K., Olson D.H. and Green D.M. (2002) Amphibian phenology and climate change. *Conservation Biology* 16, 1454-1455

Bray J.R. and Curtis J.T. (1957) An ordination of upland forest communities of southern Wisconsin. *Ecological Monographs* 27, 325-349

Bunn A.G., Graumlich L.G. and Urban D.L. (In review) Interpreting the climatic significance of trends in twentieth-century tree growth at high elevations. *The Holocene*

Bunn A.G., Waggoner L.A. and Graumlich L.G. (In review) Topographic mediation of growth of subalpine trees in the Sierra Nevada, USA . *Global Ecology and Biogeography*

Bunn A.G., Lawrence R.L., Bellante G.J., Waggoner L.A. and Graumlich L.J. (2003) Spatial variation in distribution and growth patterns of old growth strip-bark pines. *Arctic, Antarctic, and Alpine Research* 35, 323-330

Cannel M.G.R. (1998) UK conifer forests may be growing faster in response to increased N deposition, atmospheric CO_2 and temperature. *Forestry* 71, 277-296

Caprio, A.C. and Baisan, C.H. (1992) Multi-millenial tree-ring chronologies from foxtail pine in the southern Sierras of California. Bulletin of the Ecological Society of America, Honolulu, HI

Chesson P. and Huntley N. (1997) The roles of harsh and fluctuating conditions in the dynamics of ecological communities. *American Naturalist* 150, 519-553

Davis, F.W. and Stoms, D.M. (1996) Sierra Nevada Ecosystem Project: Final Report to Congress. Davis, CA: University of California, Centers for Water and Wildlands Resources

Dettinger M.D. and Cayan D.R. (1995) Large-scale atmospheric forcing of recent trends toward early snowmelt runoff in California. *Journal of Climate* 8, 606-623

Diaz H.F. and Bradley R.S. (1997) Temperature variations during the last century at high elevation sites. *Climatic Change* 36, 253-279

Dullinger S., Dirnbock T. and Grabherr G. (2004) Modelling climate-driven treeline shifts: relative effects of temperature increase, dispersal and invisibility. *Journal of Ecology* 92, 241-252

Dunwiddie P.W. (1986) A 6000-year record of forest history on Mount Rainer, Washington . *Ecology* 67, 58-68

Elith J., Burgman M.A. and Regan H.M. (2002) Mapping epistemic uncertainties and vague concepts in predictions of species distribution. *Ecological Modelling* 157, 313-329

ESRI (2002) ArcGIS™ version 8.3. Redlands, CA

Fivaz, F., Lehmann, A., Leathwick, J.R., and McOverton, J. (2003) Grasper version 0.4-2. R package, http://cran.r-project.org

Graumlich L.J. (1991) Subalpine tree growth, climate, and increasing CO_2: An assessment of recent growth trends. *Ecology* 72, 1-11

Graumlich L.J. (1993) A 1000-year record of temperature and precipitation in the Sierra Nevada. *Quaternary Research* 39, 249-255

Graumlich L.J., Waggoner L.A. and Bunn A.G. (2004) Detecting global change at alpine treeline: coupling paleoecology with contemporary studies. In: *Global Change and Mountain Regions: a State of Knowledge Overview* (eds Huber U., Bugmann H. and Reasoner M.), pp. 1-13. Kluwer Academic Publishers, The Netherlands

Hadley J.L. and Smith W.K. (1987) Influence of krummholz mat microclimate on needle physiology and survival. *Oecologia* 73, 82-90

Hannah L., Midgley G.F. and Millar D. (2002) Climate change-integrated conservation strategies. *Global Ecology and Biogeography* 11, 485-495

Hansen A.J., Neilson R.R., Dale V.H., Flather C.H., Iverson L.R., Currie D.J., Shafer S., Cook R. and Bartlein P.J. (2001) Global change in forests: Responses of species, communities, and biomes. *Bioscience* 51, 765-779

Holland, R.F. (1986) Preliminary Descriptions of the Terrestrial Natural Communities of California. Sacramento, CA: State of California, The Resources Agency, Nongame Heritage Program, Deptartment of Fish and Game

IPCC (2001) Contribution of working group I to the third assessment report of the intergovernmental panel on climate change. In: *Climate Change 2001: The Scientific Basis* (eds Houghton J.T., Ding Y., Griggs D.J., Noguer M., van der Linden P.J. and Xiaosu D.) Cambridge University Press, Cambridge, UK

Jenson S.K. and Dominique J.O. (1988) Extracting topographic structure from digital elevation data for geographic information analyses. *Photogrammetric Engineering and Remote Sensing* 54, 1593-1600

Jongman R.H.G., ter Braak C.J.F. and van Tongeren O.F.R. (1995) *Data Analysis in Community and Landscape Ecology*. Cambridge University Press, Cambridge, UK

King, J.C. and Graumlich, L.J. (1991) Gin flat tree-ring chronology, data contribution series CA574. Holdings of the International Tree-Ring Data Bank. IGBP

PAGES/World Data Center for Paleoclimatology, NOAA/NGDC Paleoclimatology Program, Boulder, CO

Lawrence R.L., Bunn A.G., Powell S. and Zambon M. (2004) Classification of remotely sensed imagery using stochastic gradient boosting as a refinement of classification tree analysis. *Remote Sensing of Environment* 90, 331-336

Legendre P. and Legendre L. (1998) *Numerical Ecology*, 2nd edn. Elsevier, New York City, NY

Lehmann A., Overton J.M. and Leathwick J.R. (2002) GRASP: generalized regression analysis and spatial prediction. *Ecological Modelling* 157, 189-207

Lloyd, A.H. (1996) *Patterns and processes of treeline forest response to late Holocene climate in the Sierra Nevada, California*. Doctoral Dissertation, University of Arizona, Tucson, AZ

Lloyd A.H. and Fastie C.L. (2002) Spatial and temporal variability in the growth and climate response of treeline trees in Alaska. *Climatic Change* 52, 481-509

Lloyd A.H. and Graumlich L.J. (1997) Holocene dynamics of treeline forests in the Sierra Nevada. *Ecology* 78, 1199-1210

Lookingbill, T. (2003) *Communities in transition: a multi-phased study of the Tsuga heterophylla/Abies amabilis ecotone in the Oregon Cascades*. Doctoral Dissertation, Duke University, Durham, NC

Lookingbill T. and Urban D.L. (2003) Spatial estimation of air temperature differences for landscape-scale studies in montane environments. *Agricultural and Forest Meteorology* 114, 141-151

Lookingbill T. and Urban D.L. (2004) An empirical approach towards improved spatial estimates of soil moisture for vegetation analysis. *Landscape Ecology*

Mastroguiseppe R. J. and Mastroguiseppe J.D. (1980) A study of *Pinus balfouriana* Grev et Balf (*Pinaceae*). *Systematic Botany* 5, 86-104

McCune B. and Grace J.B. (2002) *Analysis of Ecological Communities*. MjM Software Deisgn, Gleneden Beach, OR

McKenzie D., Peterson D.W., Peterson D.L. and Thornton P.E. (2003) Climatic and biophysical controls on conifer species distributions in mountain forests of Washington State, USA. *Journal of Biogeography* 30, 1093-1108

McKenzie D., Peterson D.W. and Peterson D.L. (2003) Modelling conifer species distributions in mountain forests of Washington State, USA. *The Forestry Chronicle* 79, 253-258

Millar C.M., Westfall R.D., Delany D.L., King J.C., and Graumlich L.G.(In press) Response of high elevation conifers to 20th century climate change. *Arctic, Antarctic and Alpine Research*

Moore I.D., Grayson R.B. and Ladson A.R. (1991) Digital terrain modelling: A review of hydrological, geomorphological, and biological applications. *Hydrological Processes* 5, 3-30

National Park Service (1998) Inventory and Monitoring Program Annual Report, http://www.nature.nps.gov/publications/

Oksanen, J. (2004) Vegan version 1.72. R package, http://cran.r-project.org

Parmesan C. (1996) Climate and species' range. *Nature* 382, 765-766

Parmesan C., Ryrholm N., Stefanescu C., Hill J.K., Thomas C.D., Descimon H., Huntley B., Kaila L., Kullberg J., Tammaru T., Tennet W.J., Thomas J.A. and Warren M. (1999) Poleward shifts in geographical ranges of butterfly species associated with global warming. *Nature* 399, 579-583

Parmesan C. and Yohe G. (2003) A globally coherent fingerprint of climate change impacts across natural systems. *Nature* 421, 37-42

Pomeroy J., Essery R., Hardy J., Rowlands A. and Marks D. (2003) Uncertainty in estimating longwave fluxes to snow under forest canopies. *Geophysical Research Abstracts* 5, 12810-12811

Root T.L., Price J.T., Hall K.R., Schnieder S.H., Rosenweig C. and Pounds J.A. (2003) Fingerprints of global warming on wild animals and plants. *Nature* 421, 57-60

Rundel P.W., Parsons D.J. and Gordon D.T. (1977) Montane and subalpine vegetation of the Sierra Nevada and Cascade Ranges. In: *Terrestrial Vegetation of California* (eds Barbour M.G. and Major J.), pp. 559-599. John Wiley and Sons, New York City, NY

Schimel D., Melillo J.M., Hanqin T., McGuire D.A., Kicklighter D., Kittel T., Rosenbloom N., Running S., Thornton P., Ojima D., Parton W., Kelly R., Sykes M., Neilson R. and Rizzo B. (2000) Contribution of increasing CO_2 and climate to carbon storage by ecosystems in the United States. *Science* 287,

Scuderi L.A. (1993) A 2000-year tree ring record of annual temperatures in the Sierra Nevada Mountains. *Science* 259, 1433-1436

Scuderi L.A. (1987) Glacier variations in the Sierra Nevada, California, as related to a 1200-year tree-ring chronology. *Quaternary Research* 27, 220-231

Scuderi L.A. (1987) Late-Holocene upper timberline variation in the southern Sierra Nevada. *Nature* 325, 242-244

Seastedt T.R., Bowman W.D., Caine T.N., Mcknight D., Townsend A. and Williams M.W. (2004) The landscape continuum: a model for high-elevation ecosystems. *Bioscience* 54, 111-121

Smith W.K., Germino M.J., Hancock T.E. and Johnson D.M. (2003) Another perspective on altitudinal limits of alpine timberlines. *Tree Physiology* 23, 1101-1112

Stevens G.C. and Fox J.F. (1991) The causes of treeline. *Annual Review of Ecology and Systematics* 22, 177-191

ter Braak C.J.F. (1986) Canonical correspondence analysis: a new eigenvector technique for multivariate direct gradient analysis. *Ecology* 67, 1167-1179

ter Braak C.J.F. (1987) The analysis of vegetation-environment relationships by canonical correspondence analysis. *Vegetatio* 69, 69-77

Therneau, T.M. and Atkinson, B. (2002) Rpart version 3.1-13. R package, http://cran.r-project.org

Thornton P.E., Running S.W. and White M.A. (1997) Generating surfaces of daily meteorological variables over large regions of complex terrain. *Jounral of Hydrology* 190, 241-251

Tranquillini W. (1979) *Physiological Ecology of the Alpine Timberline*. Springer-Verlag, New York City, NY

Urban D.L., Miller C., Halpin P.N. and Stephenson N.L. (2000) Forest gradient response in Sierran landscapes: the physical template. *Landscape Ecology* 15, 603-620

Urban D.L. (2000) Using model analysis to design monitoring programs for landscape management and impact assessment. *Ecological Applications* 10, 1820-1832

Vale T.R. (1987) Vegetation change and park purposes in the high elevations of Yosemite National Park, California. *Annals of the Association of American Geographers* 77, 1-18

Wardle P. (1974) Alpine timberlines. In: *Arctic and Alpine Environments* (eds Ives J.D. and Barry R.G.), pp. 371-402. Methuen, London, UK

Waring R.H. and Major J. (1964) Some vegetation of the California coastal redwood region in relation to gradients of moisture, nutrients, light, and temperature. *Ecological Monographs* 34, 167-215

Whittaker R.H. (1956) Vegetation of the Great Smoky Mountains. *Ecological Monographs* 26, 1-80

Whittaker R.H. (1967) Gradient analysis of vegetation. *Biological Review* 49, 207-264

Wilson R.J.S. and Luckman B.H. (2003) Dendroclimatic reconstruction of maximum summer temperatures from upper treeline sites in Interior British Columbia, Canada. *The Holocene* 13, 851-861

Wood S.N. (2000) Modelling and Smoothing Parameter Estimation with Multiple Quadratic Penalties. *Journal of the Royal Statistical Society* 62, 413-428

CHAPTER 7

DISSERTATION CONCLUSIONS

Introduction

Throughout this work I have contributed to understanding of the role of climate variability in shaping alpine treeline landscapes from our ability to extract tree-growth signals at centennial frequencies to understanding the impact of microsite variation in tree growth / climate relationships. This research shows that using changes in treeline growth, structure, and position as direct indicator of global warming is naïve: the relationships between treeline forests and climate are complex. Establishing Sierran treelines as a robust indicator of global warming will involve a substantial monitoring effort that incorporates analyses of treeline growth patterns and spatial composition at the level of the region (10^9 m^2), stand (10^3 m^2), and organism (10^{-1} m^2). These analyses will need to include the interactions of autecology, biophysical setting, and climate variability in shaping these subalpine forests.

Research Chapter Summaries

Chapter Two: Tree-Ring Detrending Methods and Low Frequency Signals

A looming issue in dendroclimatology is whether tree-ring data can provide information on centennial changes in climate. This question has important implications for the robustness of climate reconstructions relating to the natural range of climate

variability. We used a simulation model to generate tree-ring like data with systematic growth forcings and subject it to two methods of standardization: Regional Curve Standardization (RCS) and Negative Exponential Curve Standardization (NECS). The coherency between very low frequency forcings (hundreds of years) and the chronologies was slightly higher when RCS was used to detrend the component series. We found that the detectability of systematic forcings was heavily dependent on amplitude and wavelength of the input signal as well as the number of trees simulated. These results imply that for very long tree-ring chronologies where the analyst is interested in low-frequency variability, RCS is a better method for detrending series if the requirements for that method can be met. In the majority of situations, however, NECS is an acceptable detrending method. Most critically, we found that multi-centennial signals can be recovered using both methods.

Chapter Three: Trends in twentieth-century tree growth at treeline

Networks of long, annually-resolved proxies of past climate derived from tree rings, ice cores, and historical records play a pivotal role in assessing the degree of greenhouse warming in current Northern Hemisphere climate trends. We analyzed a multi-species tree-ring database to assess the degree to which twentieth century growth trends reflect tree growth of the last millennium. We examined ~1000-year chronologies for five species of high-elevation conifers at 13 sites in western North America. We decomposed the variability at annual to decadal time scales into two dimensions, both of which were significantly correlated to temperature and precipitation variation, using non-parametric ordination and cluster analysis. Tree-ring sites mapped onto the ordination

axes according to species and relative position on the landscape. A spectral analysis of the ordination axes indicated a secular trend and significant quasi-periodic variation on scales of years to decades. Further, we found that the pattern of high-elevation conifer growth rates during the last half of the twentieth century are different than any time in the past 1000 years, indicating a distinct biological signature of global climate change.

Chapter Four: Topographic mediation of growth at treeline

Climate variability is an important mediator of ecosystem dynamics in cold, semi-arid regions such as the mountains of western North America. Climatically sensitive tree-ring chronologies offer a means of assessing the impact of climate variability on tree growth across temporal scales of years to centuries and spatial scales of meters to subcontinents. Our goal was to bring the practices of landscape ecology to bear on a dendroclimatic study and show that the biophysical setting of target tress greatly mediates ring-width patterns. This study was conducted at two sites near alpine treeline in Sequoia National Park. We collected stand information and increment cores from foxtail pines for eight tree-ring chronologies in four extreme biophysical settings at two sites using proxies for soil moisture and radiation derived from a digital elevation model. Forest age-class structure varied with biophysical setting with wet and bright sites showing high recruitment after 1900 A.D. but had no obvious effect on immature stem density. Biophysical setting strongly affected ring-width patterns and subsequent climatic correlations with wet sites having higher correlation with instrumental temperature records while dry sites correlated better with instrumental precipitation. Wet sites showed strong variability on centennial scales while dry sites showed strong variability on the

scale of multiple decades. The physical template of the landscape, especially as it relates to soil moisture, created strong patterns for foxtail pine stands in terms of forest age-class structure and mediating the expression of synoptic-scale climate. When combined with remotely sensed imagery, this type of approach offers a viable means to devise first-order predictions of climatic impacts in subalpine forest dynamics and to develop flexible and powerful monitoring schemes.

Chapter Five: The role of growth form in mediating treeline dynamics

Past research near or at treeline in the Sierra Nevada has greatly contributed to understanding of late Holocene climate variability and shown the treeline ecotone to be dynamic, moving up and down slope over decades to centuries. This research has shown that the effect of species autecology and the expression of climate across rugged topography make treeline dynamics complex. We considered species autecology, at the scale of the organism, as it relates to patterns of regeneration and distribution at four plots near treeline dominated by either foxtail or whitebark pine. We also examined how biophysical factors mediated climate / growth associations. The objectives of this study were to describe the patterns of these species by age class and quantify the climate / growth associations with abiotic variables. Important results from this study were that strong associations in the spatial and growth patterns of whitebark and foxtail pines corresponded to species autecology as it relates to soil moisture and snow distribution. This research illuminated differences in the spatial pattern for two pine species growing in similarly harsh environments. It emphasized that differences in plant growth form influence mechanisms for plant survival and that growth-form plasticity can influence

spatial pattern and ecological processes. This research suggests that careful attention will have to be paid to species biology in terms of monitoring the alpine treeline ecotone for structural changes in response to predicted global warming.

Chapter Six: An opportunity for monitoring treeline in the Sierra Nevada

Alpine ecosystems in general, and treelines in particular, are forecast to change dramatically in coming decades and have long been assumed to be critical ecosystems for detecting and characterizing climate change. Previous studies, as well the work in this dissertation, are largely supportive of treeline as a conceptual ecosystem for climate change monitoring while showing some of the complexities of treeline growth and structure. The goal of this study was to refine our conceptual models of treeline composition and position and highlight ways that treelines in the Sierra Nevada might change in the coming decades. Our results showed that changes in treeline structure and position in the Sierra Nevada will probably not be ubiquitous but are likely to be idiosyncratic and species specific and include effects of species autecology, competitive interactions among species, and the expression of climate across complex topography. We demonstrated a way to further knowledge of potential treeline changes using coarse-scale land cover data to predict areas likely to change and then refined those predictions with remotely sensed imagery. These models might be combined with fine-scale plot studies (e.g., chapter four) to arrive at flexible and powerful monitoring schemas for the alpine treeline forests of the Sierra Nevada.

Prospectus

Mountain ecosystems provide unique opportunities to detect and understand global change impacts due to strong altitudinal gradients and the presence of nature reserves in many mountain areas. Many of these systems are replete with large extents of alpine treeline which can appear to be a simple temperature limited ecotone and, therefore, a ready indicator of changing temperatures. This work, and a rich history of other research, has revealed that treelines are complex. Findings from this research on treeline support results from other fields in ecology in emphasizing the importance of scale in detecting pattern. There is a general consensus that the position of alpine treeline is ultimately controlled by climate but proximately subject to a variety of biotic and abiotic processes at finer spatial scales. An important implication of this research is that changes in treeline position are an important, although not simple, indicator of climate change.

The melding of paleoecological approaches with spatial analysis tools, including remote sensing, is a key to refining the role of alpine treeline as an indicator of global change at scales conducive to establishing monitoring schemes. Concrete products from such an approach would be maps of change potential for subalpine forests along major mountain chains of the world. These maps would identify sites best suited as indicators of a specific aspect of global change (e.g., change in growing season degree days). The development of a network of strategically placed sites where *in situ*, remotely sensed, and model data can be gathered to monitor and gauge the effects of change that would complement other observing systems (e.g., glacial monitoring network).

Beyond its role as an indicator of change, the alpine treeline ecotone has long fascinated researchers as a landscape where pattern and process are tightly linked. Changes from tundra or meadows to forested landscapes entrain a host of feedbacks, involving ecology, hydrology and biogeochemistry. Of critical importance in all these fields is the continued effort to integrate our understanding of high-elevation landscapes as systems in which pattern and process interact at a variety of temporal and spatial scales.

APPENDIX A

METADATA AND ACCURACY OF SATELLITE IMAGERY

Lee Vining

The IKONOS satellite image for Lee Vining was obtained from the Space Imaging Corporation in Thornton, Colorado. The image was obtained on July 19, 2001 at 18:58 GMT and delivered as orthorectified tagged image files (TIFFs). The collection azimuth was 247.51°; the collection elevation was 70.67°; the sun angle azimuth was 135.92°; and the sun angle elevation was 67.89°. The scan azimuth was 180.04°.

The multispectral bands from the image were resampled to 10 m using cubic convolution and merged with a slope gradient layer from a digital elevation model obtained from the USGS at the same resolution. The image was classified into land cover classes of tree, meadow, rock, and water using stochastic gradient boosting (Lawrence et al. 2004). An independent accuracy assessment was performed using 100 randomly selected classified pixels for each class using standard error matrix procedures (Tables A.1 and A.2; Lillesand and Kiefer 2000). The overall accuracy of the classification was 95% and kappa analysis indicated that the classification was 93% better than a random four scheme classification (Congalton and Green 1999).

Table A.1. Error matrix and of the classification map derived from the IKONOS image of Lee Vining

		Reference Data				
		Tree	Meadow	Rock	Water	Row Total
Classification Data	Tree	99	0	1	0	100
	Meadow	6	94	0	0	100
	Rock	13	1	86	0	100
	Water	0	0	0	100	100
	Column Total	118	95	87	100	400

Table A.2. Accuracies of the classification map derived from the IKONOS image of Lee Vining

Producer's Accuracy (errors of omission)		
Tree	99/118	84%
Meadow	94/95	99%
Rock	86/87	99%
Water	100/100	100%
User's Accuracy (errors of commission)		
Tree	99/100	99%
Meadow	94/100	94%
Rock	86/100	86%
Water	100/100	100%
Overall	379/400	95%
$\hat{K}$	0.93	

Upper Wright Lakes

The IKONOS satellite image for Upper Wright Lakes was obtained from the Space Imaging Corporation in Thornton, Colorado. The image was obtained on July 19, 2001 at 18:58 GMT and delivered as orthorectified tagged image files (TIFFs). The collection azimuth was 252.63°; the collection elevation was 61.67°; the sun angle

azimuth was 135.37°; and the sun angle elevation was 69.34°. The scan azimuth was 359.96°.

The multispectral bands from the image were resampled to 10 m using cubic convolution and merged with a slope gradient layer from a digital elevation model obtained from the USGS at the same resolution. The image was classified into land cover classes of tree, meadow, rock, and water using stochastic gradient boosting (Lawrence et al. 2004). An independent accuracy assessment was performed using 100 randomly selected classified pixels for each class using standard error matrix procedures (Tables A.3 and A.4; Lillesand and Kiefer 2000). The overall accuracy of the classification was 96% and kappa analysis indicated that the classification was 94% better than a random four scheme classification (Congalton and Green 1999).

Table A.3. Error matrix and of the classification map derived from the IKONOS image of Upper Wright Lakes

		Reference Data				
		Tree	Meadow	Rock	Water	Row Total
Classification Data	Tree	99	1	0	0	100
	Meadow	9	91	0	0	100
	Rock	1	1	98	0	100
	Water	1	5	0	94	100
	Column Total	110	98	98	94	400

Table A.4. Accuracies of the classification map derived from the IKONOS image of Upper Wright Lakes

Producer's Accuracy (errors of omission)		
Tree	99/110	90%
Meadow	91/98	93%
Rock	98/98	100%
Water	94/94	100%
User's Accuracy (errors of commission)		
Tree	99/100	99%
Meadow	91/100	91%
Rock	98/100	98%
Water	94/100	94%
Overall	382/400	96%
$\hat{K}$	0.94	

References

Congalton R.G. and Green K. (1999) Assessing the Accuracy of Remotely Sensed Data: Principles and Practices. CRC Press, Boca Raton, FL

Lawrence R.L., Bunn A.G., Powell S. and Zambon M. (2004) Classification of remotely sensed imagery using stochastic gradient boosting as a refinement of classification tree analysis. Remote Sensing of Environment 90, 331-336

Lillesand T.M. and Kiefer R.W. (2000) Remote Sensing and Image Interpretation. John Wiley and Sons Inc., New York City, NY